TECHNISCHE UNIVERSITÄT MÜNCHEN

Lehrstuhl für Entwicklungsgenetik

Selective interference with HDAC2 induces multiple effects on cell death signaling in colon cancer cells

Mariana Claudia Constantin

Vollständiger Abdruck der von der Fakultät Wissenschaftszentrum Weihenstephan für Ernährung, Landnutzung und Umwelt der Technischen Universität München zur Erlangung des akademischen Grades eines

Doktors der Naturwissenschaften

genehmigten Dissertation.

Vorsitzender:	Univ.-Prof. Dr. M. Schemann
Prüfer der Dissertation:	1. Univ.-Prof. Dr. W. Wurst
	2. Priv.-Doz. Dr. K.P. Janssen
	3. Univ.-Prof. Dr. M. Göttlicher

Die Dissertation wurde am 16.12.2010 bei der Technischen Universität München eingereicht und durch die Fakultät Wissenschaftszentrum Weihenstephan für Ernährung, Landnutzung und Umwelt am 06.12.2011 angenommen.

TABLE OF CONTENT

1 INTRODUCTION

1.1 The programmed cell death / Apoptosis

Current cancer therapies, like chemotherapy, γ-irradiation, immunotherapy or suicide gene therapy exert their antitumor effect by triggering apoptosis in cancer cells [1-4]. Apoptosis or programmed cell death, first described by Kerr et al. in 1972 [5] is an evolutionary conserved mechanism of cellular suicide. A tightly regulated programmed sequence of events leads to selective elimination of unnecessary or unhealthy cells, maintaining the sensitive balance between cell proliferation and cell death [3, 6]. Programmed cell death is characterized by typical morphological and biochemical hallmarks, including cell shrinkage, nuclear DNA fragmentation, specific protein cleavage, membrane blebbing and clearance of apoptotic cells by phagocytes. Not surprisingly, deregulation of apoptosis results in pathological conditions ranging from cancer and neurodegeneration to autoimmune diseases [3, 7-9].

1.1.1 Apoptosis cell pathways

Apoptosis is a proteolytic pathway. Its objective is to activate signaling effector proteases, which cleave specific cellular proteins to drive forward the biochemical events that result in cell death. The death proteases that transmit the apoptotic signal are members of a large protein family known as the caspase family. The name *caspase* is derived from *C*ysteine-dependent *A*spartate-specific *p*rote*ase*. The catalytic activity of caspases is governed by a conserved Cystein side chain and by a stringent specificity for cleaving substrates at Asp-XXX bonds. Caspase-mediated cleavage of specific substrates induces most of the characteristic features of the apoptotic cell death e.g. nuclear shrinking is a result of the nuclear laminins cleavage, nucleosomal DNA fragmentation is induced by cleavage of ICAD (inhibitor of caspase activated DNase) and loss of cell shape is caused by cleavage of cytoskeletal proteins like gelsolin and fodrin [1, 7, 10]. Caspases are synthesized as enzymatically inert zymogenes, which consist of three domains: an N-prodomain, the p20 (large subunit) and p10 (small subunit) domains. The zymogenes are constitutively dimers which are activated by proteolytic cleavage at the intersubunit linker. This leads to the rearrangement of the subunits, so that the mature active caspase is a dimer of catalytic units, each containing one small and one large subunit. Interestingly, the cleavage occurs at Asp-X sites, which are caspases specific substrate sites. Therefore, the cells use a ‘cascade caspase’ strategy for caspase activation [7, 10].

Two pathways of apoptosis can be distinguished by whether they do or do not require the Bcl-2 family proteins [10, 11] (**Figure 1**). Which of these two pathways is selected in the cell depends on the nature of the death signal, but they also partially overlap to control initiation of apoptosis [12-14].

Figure 1. Apoptosis cell pathways.

Apoptosis can be induced by cell surface receptors, such as CD95/Fas (death receptor pathway, left) or by cytotoxic signals, such as DNA damage (mitochondrial pathway, right). The death receptor pathway leads to activation of caspase 8, while the mitochondrial pathway activates caspase 9. The initiator caspases 8 and 9 cause activation of downstream effector caspases, like caspase 3. Subsequently, the effector caspases cleave specific substrates and induce most of the characteristic features of the apoptotic cell death (from Hengartner, 2000 ([7]).

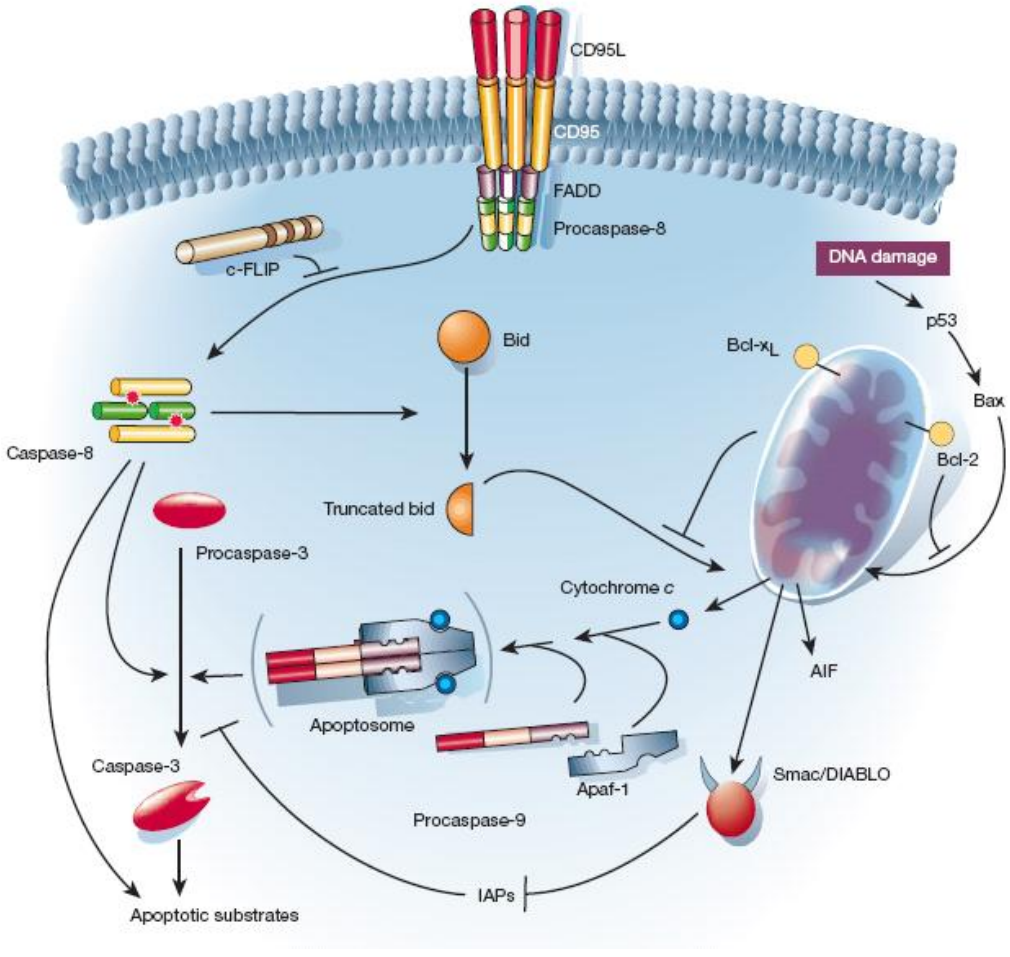

1.1.1.1 The death receptor pathway of apoptosis

The extrinsic pathway or death receptor pathway of apoptosis is triggered by extracellular ligands, such as FasL (CD95L), TNF (tumor necrosis factor) or TRAIL (TNF-related apoptosis-inducing ligand). They bind to the extracellular domains of the transmembrane death receptors, such as Fas (CD95/APO1), TNFR1 (tumor necrosis factor

receptor 1), TRAILR1 (TRAIL receptor 1/DR1) or TRAILR2 (DR2). The death signal is transmitted to the cytosol by receptor clustering and by formation of a death-inducing signaling complex (DISC), which recruits multiple molecules of the initiator caspase of the extrinsic pathway, caspase 8, to the intracellular death domain. This leads to caspase 8 activation through the adaptor protein Fas-associated death domain (FADD/MORT1). Further on, the activated caspase 8 cleaves and activates effector caspases, such as caspase 3, 6 or 7, without any involvement of the Bcl-2 family. Activation of the effector caspases results in a proteolytic cascade leading to cell death [1, 3, 10, 11] (**Figure 1**).

The death receptor pathway can activate the mitochondrial pathway through caspase 8-mediated cleavage of Bid, a Bcl-2 family-member protein. The C-terminally truncated form of Bid (tBid) translocates to the mitochondria, where it promotes the activation of the initiator caspase of the intrinsic pathway, caspase 9 [2, 7, 15, 16]. Similar, caspase 6 activated through the mitochondrial pathway can activate the receptor pathway by cleaving caspase 8 [17] (**Figure 1**).

1.1.1.2 The mitochondrial pathway of apoptosis

The intrinsic pathway or mitochondrial pathway of apoptosis is activated by cytotoxic stimuli and is highly controlled by the Bcl-2 family of proteins [7, 11]. The complex interplay between the members of Bcl-2 family proteins either promotes or prevents apoptosis, providing a mitochondrial checkpoint for the release into the cytosol of the mitochondrial proapoptogenic molecules responsible for downstream apoptotic events, e.g cytochrom c, Smac/DIABLO (second mitochondria-derived activator of caspase/direct inhibitor of apoptosis protein (IAP)-binding protein with low PI), AIF (apoptosis-induction factor) or endonuclease G [4, 18-21] (**Figure 1**).

The receptor of the mitochondrial pathway is the cytosolic protein Apaf-1, which is a multidomain protein with three functional domains: the N-terminal caspase-recruitment domain (CARD), the nucleotide-binding and oligomerization domain (NOD) and the WD40 repeats in the C-terminal. In the absence of apoptotic signals, Apaf-1 is located in cytosol in a monomeric form. Upon the mitochondrial pathway activation, the cytocrom c is released into the cytoplasm, where it binds to the WD40 region of the Apaf-1 inducing a conformational change, which allows association of dATP (2'-deoxyadenosine 5'-triphosphate) with Apaf-1. This results in the exposure of the CARD domain, which induces oligomerization of Apaf-1 into a multimeric complex, the heptameric protein ring called the apoptosome. The apoptosome recruits and activates caspase 9, which is the initiator caspase of the intrinsic

apoptotic pathway. Caspase 9 activates the downstream effectors caspases 3, 6 and 7 by cleavage [7, 10] (**Figure 1**).

Nevertheless, certain cell types (neurons and cardiomyocytes) can survive the cytochrome c release step, at least for a limited amount of time. In these cells, caspases are stringently regulated by caspase-inhibiting IAPs (inhibitory apoptosis proteins) and inducement of apoptosis requires the release of Smac/DIABLO from mitochondria to neutralize inhibitors of caspases like XIAP, cIAP1, cIAP2 and survivin [22-24].

1.1.2 The role of the Bcl-2 family of proteins in apoptosis

Numerous cytotoxic stimuli converge on mitochondria to induce outer mitochondrial membrane (OMM) permeabilization. The permeabilization of the OMM is tightly regulated by the proteins from the Bcl-2 (B-cell lymphoma-2) family. They insert into the OMM, where they form channels, either alone or by interaction with components of the mitochondrial permeability transition pore (PTP) like VDAC (voltage-dependent anion channel). Therefore, the proteins from the Bcl-2 family regulate the bioenergetic metabolite flux and channel activity of PTP [1, 7, 25, 26]. As a result of the opening of pores, the membrane potential is lost, the OMM is disrupted and the proteins from mitochondrial intermembrane space, e.g. cytochrom c and Smac/DIABLO are released into the cytosol. These apoptogenic proteins trigger the execution of cell death by promoting the activation of the caspase cascade [12, 24].

The Bcl-2 gene was discovered at the t(14;18) chromosome translocation breakpoint in B-cell follicular lymphomas, where its transcription is excessively driven by the immunoglobulin heavy chain promoter and enhancer on chromosome 14 [27-29]. One crucial early discovery that introduced a new paradigm for carcinogenesis was that overexpression of Bcl-2 does not promote cell proliferation, as the previous discovered oncogenes do, rather, overexpression of Bcl-2 inhibits cell death [11, 30].

1.1.2.1 The different classes of the Bcl-2 family of proteins

In mammals there are at least 12 members of the Bcl-2 family that exhibit highly similar tertiary structures. They are able to form functional homo- and heterodimers and can be divided into three different subclasses based on the conservation of Bcl-2 homology domains (BH1-BH4) [11]. Interestingly, while some of these proteins promote cell survival, the others promote cell death [11, 31, 32]. The antiapoptotic Bcl-2 family proteins (e.g. Bcl-2,Bcl-XL, Bcl-w, Mcl-1, Bfl-1/A-1) have four BH domains (BH1-BH4), with the exception of Mcl-1 that contains only three BH domains [4, 18, 19, 32-34]. These proteins are crucial for cell survival, as the loss of any of them causes cell death [4]. They function by

counteracting the effects of the proapoptotic Bcl-2 family members, which are divided in two subgroups: the BH3-domain only proteins (e.g. Bim, Bid, Bad, Bik, Bmf, Hrk, Noxa, Puma/BBC3) and the BH1-BH3-multidomain proteins (e.g. Bak, Bax and Bok) (**Figure 2**). The BH-3 domain proteins Bim and Bid act as "activators". In the presence of distinct apoptotic stimuli, they translocate to mitochondria, directly activating Bak and Bax. The other BH3-only proteins act as "sensitizers or derepressors", binding via their BH3 domain to antiapoptotic proteins and neutralizing their prosurvival function. The antiapoptotic proteins prevent Bak and Bax activation by sequestering "activator" BH-3 only proteins or directly binding to Bak and Bax at the mitochondrial membrane [11, 19, 26, 35-37]. The multidomain proteins Bak and Bax are essential for commitment to apoptosis. Upon activation, they oligomerize and form pores in the OMM [19, 25]. This leads to the release of proapoptogenic factors (e.g. cytochrome c) into the cytosol, where they induce caspase 9 activation (**Figure 2**). Further on, the activated caspase 9 activates by cleavage the downstream effector caspases [11, 25, 34].

Figure 2. The role and regulation of the Bcl-2 family proteins in apoptosis signaling.

The BH3-only members function as sensors of the apoptotic stimuli and act at the mitochondria, activating the proapoptotic proteins Bak and Bax or neutralizing the antiapoptotic proteins Bcl-2 and Bcl-XL. Bak and Bax form oligomers, inducing the permeabilization of the OMM and the release of apoptogenic factors (cytochrom c, AIF, Smac/DIABLO). These factors are involved in cell death execution through caspase-dependent or independent mechanisms (from Chan and Yu, 2004 [6])

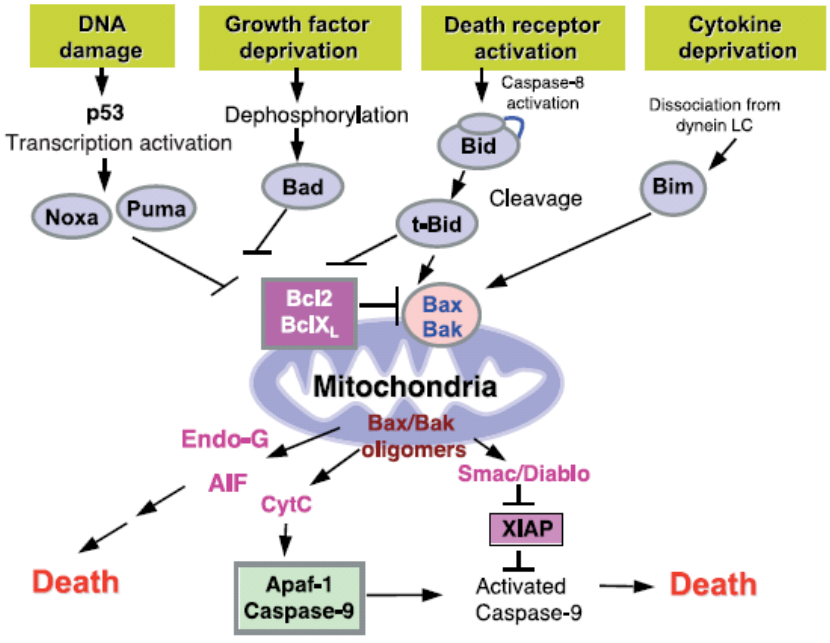

1.1.2.2 The subcellular localization and regulation of activation of the Bcl-2 family

Bcl-2 and **Bcl-XL** proteins are embedded in the mitochondrial membrane with their hydrophobic C-terminal domain. They reside also at the endoplasmic reticulum (ER) membranes, where are involved in ER Ca^{2+} dependent apoptosis [26, 38-40]. **Bcl-XL** is one of the alternative splicing variants of bcl-x gene. Its expression is controlled from distinct promoters of bcl-x gene in response to specific stimuli by several transcription factors as STAT, NF-KB or Ets2 [41].

Bim isoforms (Bim-EL, Bim-L and Bim-S) are generated by alternative splicing. In healthy cells, Bim-EL and Bim-L are maintained in an inactive conformation through binding to the microtubule-associated dynein complex**. Bim-L** and **Bim-EL** act like sensors of cytoskeletal integrity and are involved in mediating apoptosis induced by microtubules stabilizing drugs [42]. Certain apoptotic stimuli, such taxol, that perturbs the microtubules, induce the release of Bim from dynein and its translocation to the mitochondria, where it associates with Bcl-2 and Bcl-XL [43, 44]. **Bim-S**, the most potent Bim isoform in inducing apoptosis is not sequestered by microtubules and is not normally found in healthy cells [45, 46].

Bid is localized in the cytoplasm in non-apoptotic cells. Upon apoptosis induction, cytosolic p22 Bid is cleaved by caspase 8. Then the p15 active tBid fragment translocates to mitochondria where it binds to proapoptotic Bak or Bax, as well as to antiapoptotic Bcl-2 [16]. **Bad** is kept in the cytoplasm in a phosphorylated inactive form bound to 14-3-3 protein. In the presence of a death stimulus Bad is dephosphorylated. Then, it translocates to the mitochondria, where it interacts with the antiapoptotic Bcl-XL protein [26]. **Bik** is integrated almost exclusively in the membrane of the endoplasmic reticulum [47]. **Puma** and **Noxa** are transcription targets of p53 and their expression is induced as a result of DNA-damage apoptosis [48, 49].

In physiological conditions **Bax** is a cytosolic protein. Upon apoptosis induction, Bax changes its conformation, translocates to the mitochondria. There it inserts into the OMM with its C-terminal membrane anchor [11, 31, 36].

Bak resides in complexes on the OMM and on the ER in healthy cells [11, 19, 26, 50, 51]. The regulation of the expression level of Bak is not known and the protein appears to be posttranscriptionally regulated by other members of Bcl-2 family [11]. Bak is subjected to negative regulation at the mitochondrial site by Mcl-1 and Bcl-XL, which sequester Bak, by binding to its BH3 domain. This prevents its oligomerization [11]. Contrary to expectation, Bcl-2 does not bind Bak, but interacts with Bid, the open conformer of Bak, indirectly inhibiting Bak oligomerization [33, 52]. Upon apoptosis induction by death stimuli, Mcl-1 is

degraded by the ubiquitin-proteasome pathway [53, 54] or the concentration of the BH3-only proteins rises to a level which is higer than the one of the antiapoptotic proteins. The Mcl-1/Bak and Bcl-XL/Bak interactions are disrupted by the BH3-only proteins (e.g. Bim, tBid). This allows the pore forming Bak to change its conformation (exposure of NH2-terminal domain), oligomerize and trigger apoptosis [3, 4, 11, 16, 26, 35, 55].

Similar to the wild-type cells, cells deficient for either Bax or Bak still release mitochondrial proteins and undergo apoptosis in response to cytotoxic agents and death receptor signaling. The cells deficient for both Bax and Bak are profoundly defective and form highly invasive carcinomas [56, 57]. Bax- and Bak-deficient cells are resistant to death signaling by overexpression of BH3-only proteins, indicating that Bak and Bax are required downsteam components of cell death pathways [58, 59]. Thus, Bax and Bak function in a redundant fashion to facilitate the release of mitochondrial proteins such as cytochrome c and Smac/DIABLO from the intermembrane space [56, 57].

Confocal and electron microscopic analysis showed that Bak and Bax were found to be concentrated on the mitochondrial membrane at small focal regions, which develop into mitochondrial fission sites. This finding supports the hypothesis that Bak and Bax are involved in the promotion of the mitochondrial fragmentation process that occurs simultaneously with the release of cytochrome c [60, 61]. Brooks et al. [62] reported that mitochondrial fragmentation is attenuated in Bak-deficient cells, while Bax-deficiency did not prevent mitochondrial fragmentation. It has been reported that the function of Bak is independent of Bid and Bax [63].

The step of apoptosis regulation that is controlled by Bak, Bcl-2 and Bcl-XL appears to be the most general final commitment step for the decision between life and death of a cell and regulates survival of a cell beyond the Apaf 1-caspase 9 axis. The disruption of mitochondria by Bak may be one cause of cell death in the absence of the apoptosome activation [11].

1.1.2.3 Bcl-2 family members as therapeutic targets in cancer

Alterations in the expression of genes encoding key apoptotic proteins or their mutation are characteristic features of tumorigenesis, providing cancer cells with a survival advantage. Members of the Bcl-2 family are important regulators of apoptotic signaling through mitochondria. Their deregulation is associated with disease, particularly with cancer and drug resistance to cancer therapies [1, 37, 40, 64].

One mechanism of resistance to apoptosis involves the increase in expression of the antiapoptotic proteins Bcl-2 and Bcl-XL. For many types of cancers, the overexpression of

Bcl-2 and Bcl-XL correlates with poor survival and the progression of the disease [3]. In addition to follicular lymphomas, where the expression of Bcl-2 is highly upregulated as a result of a chromosomal translocation, increased expression of Bcl-2 and of its homologue Bcl-XL is also observed in solid tumors, including prostate, breast and colorectal tumors [65]. Moreover, overexpression of Bcl-2 and Bcl-XL is associated with resistance to various chemotherapeutic agents and radiotherapy, making these members of the Bcl-2 family promising drug targets for anticancer therapy [3, 65-67].

It has been observed that critical Bcl-2 family proteins, like Bak and Bax are lost during tumor development [68]. Loss-of-function Bax mutations have been reported to be selected during progression of colorectal tumors [69]. Mutations in the Bak gene were observed in gastric and colorectal tumors [70]. It has been reported that colorectal carcinomas have reduced Bak protein expression compared with normal mucosal epithelial cells [71]. Therefore, overcoming the loss of Bak and Bax function in tumors or drug-based upregulation of Bak and Bax expression in tumor cells could be an effective approach of cancer treatment.

1.2. The histone deacetylase family (HDACs)

1.2.1 The regulation of histone acetylation

Aberrant transcriptional repression of the genes involved in the cell cycle and in apoptosis is a hallmark of cancer. The expression of such genes is epigenetically regulated by chromatin remodelling and posttranslational histone modifications such as acetylation [72-75]. The level of acetylation of the histones is controlled by two opposing families of enzymes: histone acetyltransferases (HAT) and histone deacetylases (HDAC), which catalyse acetylation or the removal of acetyl groups on lysine residues of the nucleosomal histones (**Figure 3A**) [76-78]. Transcriptional activators can bind and recruit HATs at specific gene promoters. Therefore, histone acetylation induced by HATs correlates with a relaxed chromatin state and gene-transcription activation. Histone hypoacetylation, as a result of HDACs activity is associated with a condensed chromatin structure and gene silencing, as HDACs form multiprotein complexes with transcriptional repressors and corepressors, e.g. mSin3, N-CoR, SMRT. These complexes are recruited to target genes by interactions with cell cycle regulators such as Rb protein, nuclear receptors such as ER (estrogen receptor) and RAR (retinoic acid receptor) or other epigenetic modifiers such as DNMT and DNA methyl binding proteins [73-75, 79].

The histones are not the only targets of HDACs, also non-histone proteins have been found to be modified by acetylation and to be substrates of HDACs. These include

transcription factors (p53 and E2F), signaling mediators (STAT 3), DNA repair enzymes (Ku 70) and structural proteins (α-tubulin). The acetylation level influences the stability, activity and localization of these HDAC-substrate proteins, which are involved in the regulation of proliferation, differentiation and cell death pathways [74, 77, 80, 81].

Figure 3. The regulation of histone acetylation and the effects of HDAC inhibition on gene expression. (**A**) Acetylation of histones is mediated by HAT enzymes, while HDACs catalyze the removal of acetyl groups from histones. HDACs are recruited to target genes in complexes with transcriptional repressors. Therefore, they are primarily involved in gene repression of cell cycle inhibitors and apoptosis inducers. (**B**) Inhibition of HDACs results in histone hyperacetylation, which is associated with gene activation, but also leads to hyperacetylation of non-histone substrates of HDACs, such as transcriptional factors (TF) and proteins with diverse biological functions. The hyperacetylation of TF increases their gene regulatory activity. The hyperacetylation of proteins mediates the effects of HDAC inhibitors on the induction of apoptosis and cell cycle arrest (adaptation from Bolden et al., 2006, [72]).

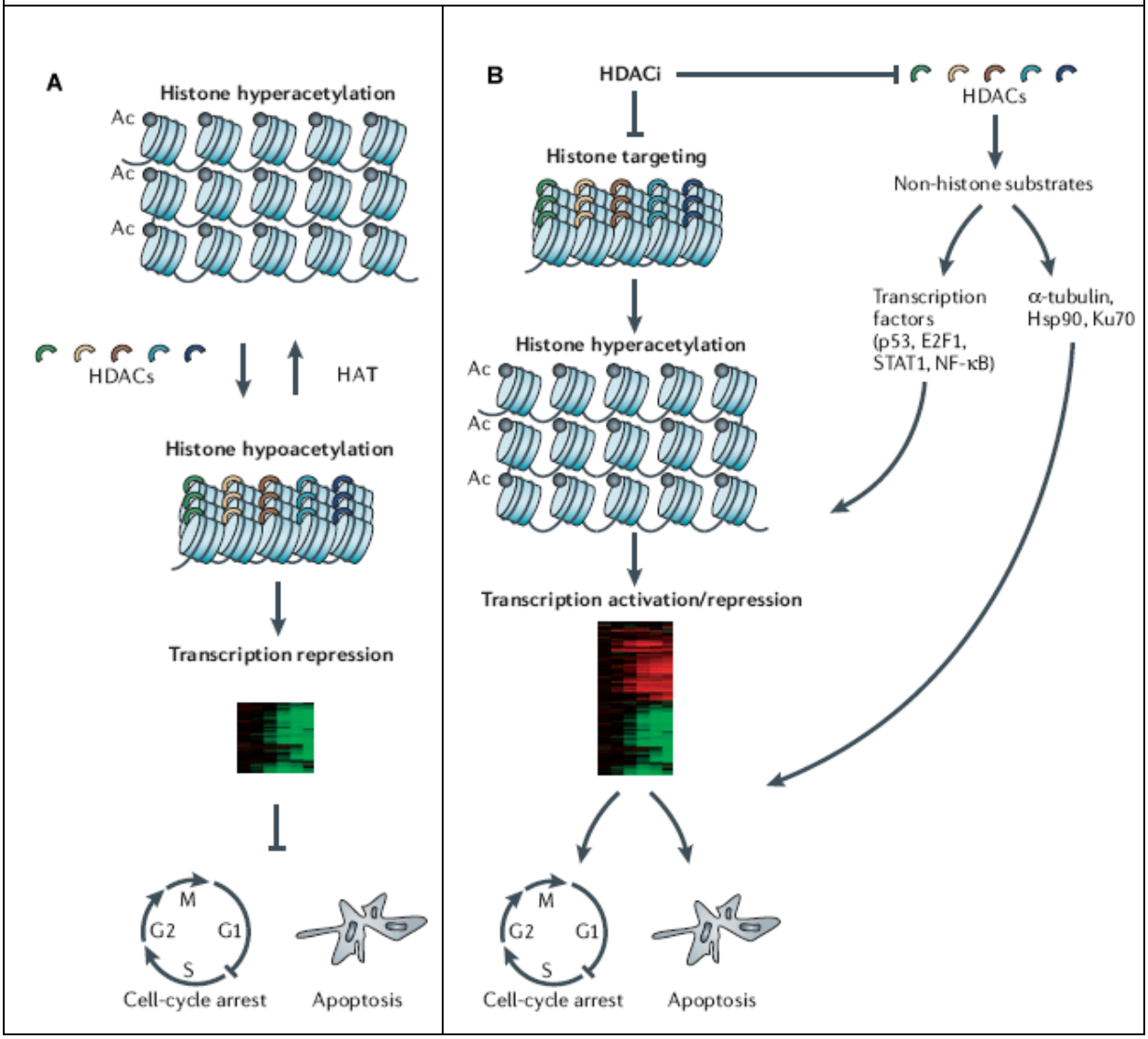

1.2.2 Classification of HDACs

Eighteen human HDACs have been identified and they are divided into four classes based on their homology to yeast HDACs, their subcellular localization and their enzymatic activity [72, 80, 82]. Class I HDACs include HDAC1, 2, 3, and 8, which are related to yeast RPD 3 deacetylase and have a high homology in their catalytic domain. Further phylogenetic analysis subdivided class I HDACs in Ia (HDAC1 and 2), Ib (HDAC3) and Ic (HDAC8) [83]. Class II HDACs have a sequence homology in the catalytic domain with yeast Hda 1 and include HDAC4-7 and HDAC9-10. This class is divided into class IIa (HDAC4, 5, 7 and 9) and class IIb (HDAC6 and 10), which contain two deacetylase domains [84]. All class I and class II HDACs are Zn-dependent enzymes. Class III HDACs or sirtuins (Sirt 1-7) are homologs of yeast Sir 2 and require NAD^+ for their enzymatic activity [85]. Class IV HDACs is represented by HDAC11, which share homology with catalytic regions of both class I and II HDACs [86]. Class I HDACs are generally detected in the nucleus and have a ubiquitous expression, while class II HDACs are tissue restricted and shuttle between the nucleus and the cytoplasm [82, 87].

1.2.3 The role of HDACs in cancer

Altered expression of individual HDACs, abnormal recruitment of HDACs to promoter regions or overexpression of transcription repressors lead to gene transcription deregulation and have been involved in the pathogenesis of leukemia, lymphomas, as well as of solid tumors [72, 75, 81, 87]. Acute promyelocytic leukemia (APL) and acute myeloid leukemia (AML) are induced by abnormal recruitment of HDAC-containing repressor complexes to promoters of specific target genes, through their interaction with oncogenic DNA binding proteins like PML-RARα or AML1-ETO, which result from chromosomal translocations [88-90]. In non-Hodkin's lymphoma, the overexpression of the transcriptional repressor Bcl-6 (B cell lymphoma 6) is associated with the aberrant repression of growth-regulatory target genes such as p21 (CDKN1A) through the recruitment of HDAC2 [91].

In addition to aberrant recruitment of HDACs to specific target genes in leukaemia and lymphomas, a number of studies showed an altered expression of HDACs in different solid tumors in comparison to normal tissue [92, 93] (see **Table 1**). For example, HDAC2 is overexpressed in colon carcinomas. In colon cancer cells, the RNAi-mediated knockdown of HDAC2 resulted in cell death, indicating a role of HDAC2 in protecting cancer cells against apoptosis [94]. Recently, Zimmermann et al., 2007 [95] showed that HDAC2 is not only increased in tumors of the gut, but plays an important role for tumor development *in vivo*,

since the number of the intestinal tumors is significantly reduced in HDAC2-deficient APC^{min} mice compared with HDAC2 wild-type APC^{min} mice.

Table 1. The altered expression of HDACs in different solid tumors.

HDAC class	**HDACs upregulated in tumor vs. normal cells**	**Tumor**
HDAC class I	HDAC1	gastric cancer [96, 97], prostate carcinomas [98], colorectal cancer ([99])
	HDAC2	colon cancer [94], prostate carcinomas [98], cervical carcinoma [100]
	HDAC3	colon cancer [99], prostate carcinomas [98]
	HDAC8	neuroblastoma [101]
HDAC class II	HDAC4	breast cancer [102]
	HDAC5	hepatocellular carcinomas [103]
	HDAC6	oral squamous cell carcinomas [104]
	HDAC7	colorectal cancer; hepatocellular carcinomas [102, 103]

Taken together, these data show that transcriptional repression by aberrant expression or recruitment of HDACs to target genes is involved in the tumor onset and progression. This highlights that HDACs are attractive targets for therapeutic interventions [74, 87, 92, 105, 106]. For example, inhibition of HDAC2 is thought to be a promising chemotherapeutic approach for colon cancer therapy.

1.2.4 The histone deacetylase inhibitors

A relatively wide range of natural and synthetic compounds able to inhibit the activity of HDACs have been identified. However, most of these compounds act unselectively against several HDAC family members. Only few of them are preferential inhibitors of class I vs. class II of HDACs and even fewer are able to discriminate efficiently among HDACs belonging to the same class [93]. SAHA (Virinostat) inhibits many isoforms from class I and II HDACs [72]. MS-275 is more active against HDAC1 and HDAC9, than against HDAC3, while it has no significant effect against HDAC6 and HDAC8 [93, 107]. Depsipeptide (FK228) has stronger activity against HDAC1 and 2, than against HDAC4 and 6 [108]. Tubacin selectively inhibits HDAC6 activity, but does not inhibit cell cycle progression [109]. Some HDAC inhibitors such as butyrate and phenylbutyrate are rapidly degraded and have a low specificity. Other HDAC inhibitors, such as trichostatin A (TSA) have a poor bioavailability and toxic side effects at high doses [81, 110, 111].

Induction of apoptosis in tumor cells is one of the prominent goals in cancer therapy [112, 113]. The potential significance as anticancer agents of several HDAC inhibitors

(e.g. SAHA, FK-228, MS-275) has been supported by many *in vitro* experiments, studies in animal models and ongoing clinical trials of phase I-III in hematological disorders and several solid tumors. SAHA (Virinostat) is the first HDAC inhibitor approved in 2006 by the US Food and Drug Administration for the treatment of cutaneous T-cell lymphoma. However, the clinical trials with unselective HDAC inhibitors document a wide range of side effects and many questions are currently poorly solved. Therefore, the current challenges in the field are: i) to define the cancer relevant HDAC isoenzymes that have to be inhibited in a given tumor type; ii) to estabilish if the expression of key mediators of cell death is dependent on specific HDAC isoforms; iii) to identify the predictive markers for a successfull therapy with HDAC inhibitors and iv) to estabilish if HDAC inhibitors synergize with other chemotherapeutic drugs to induce the death of tumor cells (for a review see [72, 75, 80, 81, 87, 93, 106, 114]).

The response to the HDAC inhibition depends on the cell type and on the nature of the HDAC inhibitors. In general, HDAC inhibitors induce cell cycle arrest, differentiation and apoptosis in tumor cells. Normal cells are relatively resistant to HDAC inhibitors-induced cell death, making HDAC inhibitors well suited for cancer therapy (**Figure 3B**) [115-117]. Nevertheless, how HDAC inhibitors trigger the activation of the apoptotic cascade in tumor cells is a major question that remains to be fully answered [72]. At the moment, there is available data from a number of studies, showing that HDAC inhibitors alter the expression of several factors that mediate or regulate the apoptotic pathway. HDAC inhibitors like SBHA, SAHA, TSA, FK228, MS-275 and CBHA alone or in combination with TRAIL upregulated the expression of the proapoptotic proteins Bak, Bmf, Bax and Bik [118-123]. The mechanism of this effect is not understood yet [80]. It has been shown that SAHA and TSA increase Bim transcription by the activation of the E2F1 transcription factor [124]. Bmf is transcriptionally activated by FK228 and CBHA [125]. Bid is cleaved and activated in response to HDAC inhibitors such as SAHA and MS-275 [126, 127]. HDAC inhibitors like VPA, TSA, MS-275, CBHA and SBHA alone or in combination with TRAIL decrease the expression of the antiapoptotic proteins Bcl-2, Bcl-XL and Mcl-1 [118, 121, 122, 128-130]. Overexpression of Bcl-2 or Bcl-XL, which block the intrinsic apoptotic pathway, inhibits HDAC inhibitors-induced apoptosis [80, 119, 127, 128]. However, the effects of HDAC inhibition on the expression of proapoptotic and antiapoptotic proteins are cell context dependent. The basal levels of these proteins vary dramatically in different tumor cells, as do the expression changes of these proteins induced by different HDAC inhibitors [80].

One interesting HDAC inhibitor is valproic acid (VPA, 2-propylpentanoic acid), a drug with tolerable side effects and favourable pharmacokinetic properties, which has been clinically used for over two decades to treat epilepsy and bipolar disorders. It has been shown

that VPA inhibits HDAC catalytic activity at therapeutically useful concentrations and that VPA inhibits preferentially class I HDACs. In comparison with other HDAC inhibitors, VPA reduces the half-life of HDAC2 protein due to proteasomal degradation mediated by ubiquitination [110, 111, 131, 132]. VPA has been reported to induce cell cycle arrest, cell differentiation and apoptosis in hepatoma cells, but not in primary healthy hepatocytes [133], in melanoma [134, 135], thyroid cancer cells [136], prostate cancer cells [137], breast cancer cells [138], human leukaemia cell lines [139], chronic lymphocytic leukaemia [129], acute myeloid leukaemia cells [140], endometrial cancer cells [141] and cervical epithelial cells [142] (**Table 2**). Göttlicher et al., 2001 [110] showed that tumor growth and metastasis formation are significantly reduced by VPA in animal experiments. VPA induced tumor growth inhibition and survival advantage in treated mice bearing human multiple myeloma xenografts vs. controls. Although VPA may be less potent than the newer generation of HDAC inhibitors, there are several arguments that supported the evaluation of VPA as anticancer agent in clinical trials: the well known toxicity profile, long term safety data and cost-effectiveness [143]. Clinical trials with VPA (alone or in combination with retinoic acid) have been mainly focused on acute myeloid leukaemia and the myelodysplastic syndromes [111, 144, 145]. Clinical trials with VPA have been recently performed in cervical cancer [146] and several progressing solid tumors [147]. The treatment with VPA and retinoic acid resulted in the reduction of myeloid blast cells counting values and in transient disease control of a subset of patients with AML [111, 144]. The VPA treatment induced stable disease in one patient with metastatic non-small cell lung cancer and one patient with metastatic colorectal cancer. These patients have had rapid disease progression prior to VPA therapy [147].

However, the critical molecular mechanism underlying the biological effects of VPA treatment remains to be fully elucidated. Currently it is unclear i) which are the key targets specifically required for the VPA-induced tumor cell death in a given tumor and ii) which is the molecular event that leads to the effect of VPA treatment on cell death associated proteins from Bcl-2 family. Detection of critical HDAC2-dependent alterations in the regulation of apoptosis that permit survival of HDAC2 overexpressing cells and mediate initiation of cell death upon HDAC2 inhibition is essential for understanding the VPA effects on apoptosis. Identifying markers that can predict the response to VPA treatment is required for the selection of patients who are potential candidates for a successful therapy with VPA, but also for the design of combination therapies of VPA with other anticancer drugs.

Table 2. The mediators of VPA-induced cell cycle block and cell death		
Effects of VPA treatment	**Tissue/Cells**	**Ref.**
Upregulation of p16 and p21 proteins	M14 human melanoma cell line	[134]
Increase of survivin in VPA resistant cells, decrease of survivin in VPA-sensitive cells, no change in Bcl-2, Bcl-XL, Mcl-1 and Noxa expression	human melanoma cell lines WM115, Sk-Mel28, WM266, A375	[135]
Activation of caspase 3 and 9, upregulation of cyclin A and p21	thyroid carcinoma cell lines N-Pa, BHT-101	[136]
Downregulation of PCNA, upregulation of p21	prostate cancer cell lines DU-145, PC-3PCa	[137]
Upregulation of Bak and p21, downregulation of Bcl-2, activation of caspase 8 and 9	breast cancer cell lines MCF-7, MDA-MB-231,-435, ZR-75-1	[138]
Activation of caspase 3, 8 and 9, cytochrom c release	human leukaemia cell lines RS4-11, MV4-11, THP-1, MOLT-4, Jurkat, KG-1, KOCL-33 and -44	[139]
Activation of caspase 8 and 9, cleavage of BID, downregulation of Bcl-2	primary B-chronic lymphocytic leukaemia cells	[129]
Downregulation of FLICE, overexpression of Bcl-2 and absence of Bax inhibited VPA-induced apoptosis	acute myeloid leukemia cells K562 and HL60	[140]
Upregulation of p21 and p27, downregulation of Bcl-2 and cyclin D1, D2	endometrial tumor cell lines HEC-1B, RL95-2, KLE, AN3CA, HEC59	[141]
Activation of caspase 3, 6 and 8; inhibition of prosurvival Akt.	HeLa human cervical tumor cells	[142]

1.3 Resistance of colon tumors to chemotherapy

Colorectal cancer is the third most common cancer and the second leading cause of cancer-related death in the Western world [148]. One of the most widely used drugs in chemotherapy of colon cancer is 5-fluorouracil (5-FU), but drug resistance is the major obstacle to a successful therapy with 5-FU [149].

5-FU is a fluoropyrimidine that inhibits cell growth and induces apoptosis by inhibiting thymidylate synthase (TS), a key enzyme in DNA synthesis and by incorporation of its metabolites into RNA and DNA [149, 150] (**Figure 4**). 5-FU is converted intracellularly to three main active metabolites: FdUMP (fluorodeoxyuridine monophosphate), FdUTP (fluorodeoxyuridine triphosphate) and FUTP (fluorouridine triphosphate). TS is a dimeric cytosolic protein that catalyzes the synthesis of dTMP (deoxythymidine monophosphate) from dUMP (deoxyuridine monophosphate), this reaction being the sole *de novo* source of

dTMP (deoxythymidine triphosphate). Further on, the dTMP is metabolized to dTTP, an essential precursor of DNA biosynthesis. Therefore, TS is required for proliferation and DNA repair [149, 151-153]. The 5-FU metabolite, FdUMP binds to the catalytic site of TS, blocking access of dUMP and inhibiting dTMP synthesis. This results in dNTP pool imbalances, depletion of dTTP and increase in dUTP. Subsequently, dUTP and the 5-FU metabolite FdUTP are misincorporated into the DNA, which causes DNA single/double-strand breaks and induces cell death of tumor cells. Moreover, the 5-FU metabolite, FUTP is misincorporated into RNA, which distrupts RNA processing, leading to critical effects on cellular viability [149, 152] (**Figure 4**). However, tumor cells develop strategies to evade the cytotoxic effect of 5-FU, which allows them to acquire resistance to the 5-FU therapy.

Figure 4. The mechanism of 5-FU action.

5-FU induces apoptosis and inhibits cell growth by its active metabolites FUTP, FdUTP and FdUMP. FUTP is misincorporated into RNA, which disrupts RNA processing. FdUTP incorporates into DNA, which induces DNA strand breaks. FdUMP binds to the catalytic site of TS, which results in the inhibition of DNA replication and repair (adaptation from Longley et al., 2003 [149]).

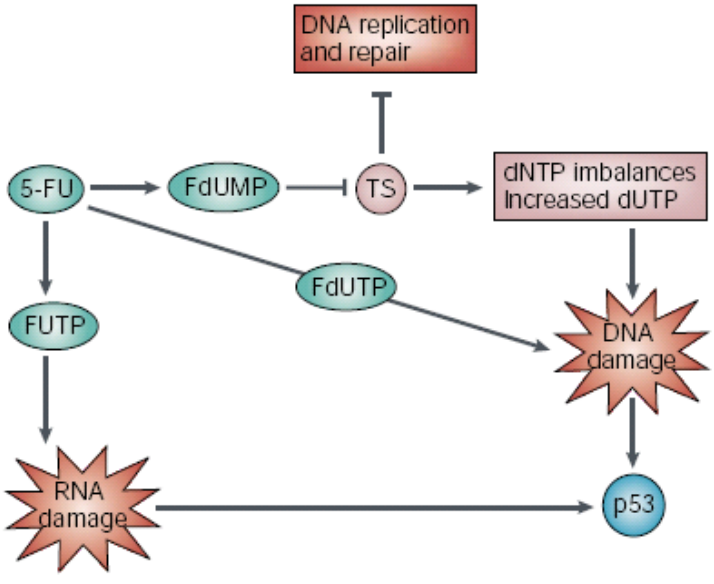

Over the recent years, molecular and biochemical markers specifically associated with resistance and response to 5-FU have been identified. This highlights the development of 5-FU resistance as a result of the deregulation of proliferation, apoptosis, DNA repair and metastasis pathways [154-158]. For example, TS expression is a key determinant of 5-FU

resistance and high TS levels of expression have been shown to be a negative prognostic and predictive factor of poor response to 5-FU treatment in primary and metastatic colorectal cancer [153, 158-160,161]. Elevated TS expression does not account for all 5-FU non-responding tumors in colon cancer patients. Sensitivity to 5-FU is also influenced by expression levels of apoptotic-regulatory proteins. Low levels of proapoptotic protein Bax are correlated with a high resistance of cells to 5-FU. Overexpression of apoptotic inhibitory genes Bcl-XL and Bcl-2 has been shown to be associated with the resistance to 5-FU treatment in colon cancer [67, 154, 162, 163].

New therapeutic valuable strategies are required to improve the response rate in colon cancer [164]. It has been reported that knockdown of Bcl-XL protein levels by small interfering RNA (siRNA) inhibited the proliferation of 5-FU resistant cells. Thus, down-regulation of Bcl-XL protein expression might be an effective therapy for 5-FU resistant colon tumors [162, 165]. The ability of HDAC inhibitors to synergize with other anti-cancer agents to potently kill tumor cells has been recently evaluated in various tumors [166]. The potential efficacy of a combined therapy with 5-FU and several HDAC inhibitors in different tumors, including colon tumors has been reported in several publications [167-170]. Potential mechanisms of the enhanced tumor cell death following treatment with HDAC inhibitors in combination with DNA damaging agents are: i) the HDAC inhibitors-mediated hyperacetylation of core histones may increase accessibility of DNA damaging agents to their targets and enhance their cytotoxic effects and ii) the HDAC inhibitors may increase the apoptotic effects of cytotoxic drugs through an increase in the overall apoptotic response as a result of altered expression of key apoptotic regulators e.g. decreasing the levels of antiapoptotic proteins [166, 171]. Taken together this data suggests that a combined VPA and 5-FU chemotherapy might also lead to antisurvival responses in colon cancer cells.

1.4 The aim of the study

Altered expression of individual histone deacetylases (HDACs) or abnormal recruitment of HDACs to promoter regions of genes regulating cell cycle and apoptosis are involved in the pathogenesis of cancer. Therefore, inhibition of HDACs is thought to be a promising approach in cancer therapy. Previous studies and ongoing clinical trials of phase I to III showed that HDAC inhibition results in cell cycle arrest and cell death. However, several questions are currently poorly solved: i) which HDAC isoforms have to be inhibited, ii) is the expression of key mediators of cell death dependent on specific HDAC isoforms; iii) which are the predictive markers for a successful therapy with HDAC inhibitors and iv) do HDAC inhibitors synergize with other chemotherapeutic drugs to induce the death of tumor cells?

The aim of this study was to identify the mechanism by which VPA, an HDAC inhibitor that preferentially inhibits class I HDACs, induces cell death in colon cancer cells. Several questions were addressed: i) which are the VPA-induced changes that mediate initiation of cell death; ii) to which extent do these responses depend on the HDAC2 isoform overexpressed in HT-29 colon cancer cells; iii) does VPA synergize with other chemotherapeutic drugs to inhibit the survival of colon cancer cells.

The primary approach was to use the microarray technique to find candidate genes which are involved in the induction of the cell death upon VPA treatment. Subsequent functional analyses were performed to: i) identify the key target(s) specifically required for the VPA-induced cell death and ii) determine if the expression of the VPA key target(s) is HDAC2 dependent.

5-FU is one of the most widely used drugs in chemotherapy of colon cancer, but development of drug resistance is the primary obstacle to an efficient 5-FU therapy. Combining HDAC inhibitors with chemotherapeutic agents to obtain better anti-tumor effects compared to those observed using single agents is a recently proposed therapeutic approach for colon cancer. In this study it was investigated if VPA synergizes with 5-FU to inhibit the survival of colon cancer cells which are either sensitive or resistant to 5-FU. First the effect of VPA on the expression of markers specifically associated with the resistance of colon cancer cells to the cytotoxic effect of 5-FU was evaluated. Further on, survival assays were performed to determine if combined treatment with VPA and 5-FU can inhibit the survival of colon cancer cells more efficiently than the 5-FU treatment alone.

2 MATERIALS AND METHODS

2.1 Cell lines

HT-29 human colon adenocarcinoma cell line was maintained in McCoy's 5A Medium Modified supplemented with 10 % heat inactivated fetal bovine serum (FCS), 2 mM Glutamine and 1 % Penicillin/Streptomycin.

Mouse Embryonic Fibroblasts (MEFs) derived from mouse embryos from either wildtype mice or HDAC2-deficient mice as published elsewhere [95] were cultured in Dulbecco's MEM medium with 4.5 g/L glucose supplemented with 10 % FCS, 2 mM glutamine and 1 % Penicillin/Streptomycin.

HT-29 parental human colon adenocarcinoma cell line (HT-29p) sensitive to 5-fluorouracil (5-FU) and the corresponding 5F12 cells resistant to 5-FU were kindly provided by Dr. Lesuffleur [172, 173]. The cells were grown in Dulbecco's MEM medium with 4.5 g/L glucose supplemented with 10 % FCS, 2 mM glutamine and 1 % Penicillin/Streptomycin.

DLD-1 human colon adenocarcinoma cell line and the corresponding DLD1-5-FU/R cells resistant to 5-FU were kindly provided by Dr. Fang from M.D. Anderson Cancer Center, Huston, USA [162]. The cells were grown in RPMI 1640 medium supplemented with 8 % heat-inactivated fetal bovine serum (FCS), 2 mM glutamine and 1 % Penicillin/Streptomycin.

All cells were cultured at 37˚C in a humified HEPA filtered IR Incubator containing 5 % CO_2 (LaborTect, Göttingen, Germany).

Reagents and materials used for cell culture:

Product	**Company**
HT-29 human colon adenocarcinoma cell line	American Type Culture Collection (ATTC), Rockville, USA
McCoy's 5A Medium Modified	Sigma-Aldrich Chemie, Steinheim, Germany
Dulbecco's MEM Medium	Biochrom AG, Berlin, Germany
RPMI 1640 Medium	Sigma-Aldrich Chemie, Steinheim, Germany
Fetal bovine serum (FCS)	Biochrom AG, Berlin, Germany
L-Alanyl-L-Glutamine (200 mM)	Biochrom AG, Berlin, Germany
Penicillin/Streptomycin (10.000 ug/mL)	Biochrom AG, Berlin, Germany
Cell culture flasks 25 cm^2, 50 cm^2 , 175 cm^2	Nunc, Thermo Fisher Scientific Langenselbold, Germany

2.2 Microarray analysis

Gene expression profile of HT-29 cells treated or not with 2 mM VPA for 3, 6 and 24 h was evaluated using the GeneChip Human Genome U133 Plus 2.0 Array (Affymetrix Inc., Santa Clara, USA) according to the Affymetrix Inc. protocols. The GeneChip Human Genome U133 Plus 2.0 Array is designed for whole-genome expression profiling of human samples with 61.000 of probe sets targeting a total of 41.000 transcripts. Total RNA was isolated from 4 biologically independent replicates per treatment using High Pure RNA Isolation Kit according to the manufacturer's protocol. The integrity of total RNA samples was measured with the RNA 6000 Lab Chip using Agilent 2100 Bioanalyzer (Agilent, Santa Clara, USA) following manufacturer's instructions. All samples displayed ribosomal 18 S and 28 S RNA sharp peaks in a high quality ratio of about 2.

First-strand cDNA was generated from 8 µg of total RNA by reverse transcription reaction using the GeneAmp PCR System 9700 (Applied Biosystems, Darmstadt, Germany). Total RNA was mixed in a final volume of 12 µL with 2 µL of poly–A RNA controls (diluted 1:6250 in Poly-A control dilution buffer) and 2 µL of T7-oligo(dT) primer (50 µM), then heated at 70˚C for 10 min. A solution prepared from 4 µL of first-strand buffer (5X), 2 µl of DTT (0.1 M) and 1 µL of dNTP (10 mM) was added to the first mix and heated further on for 2 min at 42˚C. Subsequently, 1 µl SuperScript II reverse transcriptase (200 U/µL) was added to the samples, followed by incubation for 1 h at 42˚C.

Second-strand cDNA synthesis mediated by RNase H was performed by mixing the first-strand synthesis sample in a final volume of 150 µL with the second-strand master mix, containing 30 µL of second strand reaction mix (5X), 3 µL of dNTP (10 mM), 1 µL of E.coli DNA ligase, 4 µL of E. coli DNA polymerase I and 1µL of E. coli RNase H. The samples were incubated for 2 h at 16˚C and then 2 µL of T4 DNA polymerase was added to each sample and incubated for 5 min at 16˚C. After incubation 10 µL of EDTA 0.5 M was added to the samples.

The cleanup of double-stranded cDNA was performed using the Sample Cleanup Module. The double-stranded cDNA sample was mixed with 600 µL of cDNA binding buffer, applied to the cDNA cleanup spin column, centrifuged at 8000 x g for 1 min. The column was washed with 750 µL of 1X cDNA wash buffer by centrifugation at 8000 x g for 1 min and then the double-stranded cDNA was eluted from the column with 14 µL of cDNA elution buffer.

The synthesis of biotin-labelled cRNA was performed by the IVT (*in vitro* transcription) reaction in a final volume of 40 µL with 6 µL of cDNA, 4 µL of IVT labelling buffer (10X), 12 µL of IVT labelling NTP mix and 4 µL of IVT labelling enzyme mix.

Samples were incubated at 37˚C for 16 h and then were cleaned up from the unincorporated NTPs and further on fragmented with the Sample Cleanup Module. RNase-free water (60 µL), 350 µL of IVT cRNA binding buffer and 250 µL of ethanol were added to each sample, then the samples were applied to the IVT cRNA cleanup spin column and centrifuged at 8000 x g for 15 sec. The column was washed first with IVT cRNA wash buffer, then with 500 µL of 80 % ethanol by centrifugation at 8000 x g for 15 sec. The cRNA was eluted from the column with 20 µL of RNase-free water. The biotinylated cRNA was quantified by UV spectroscopy at 260 nm (RNA concentration (µg/mL) = OD_{260} x 40 x dilution factor) and the purity of cRNA samples was determined by the ratio of absorbance at 260–280 nm using an Eppendorf Bio Photometer (Eppendorf, Hamburg, Germany). Further on 15 µg of biotinylated cRNA were fragmented at 94˚C for 35 min by metal-induced hydrolysis in a final volume of 30 µL with 6 µL fragmentation buffer (5X).

Subsequently, the fragmented biotin-labelled cRNA (15 µg) was mixed with the hybridization cocktail containing 50 pM of control oligonucleotide B2, 1.5 pM of Eukaryotic Hybridization Controls, 0.1 mg/mL of herring sperm DNA, 0.5 mg/mL of BSA, 1X hybridisation buffer, 10 % of DMSO. The samples were heated at 99˚C for 5 min, cooled at 45˚C for 5 min and then hybridized for 16 h in the hybridization oven at 45˚C to the GeneChip Human Genome U133 Plus 2.0 Array.

The probe arrays were further on washed and stained automatically using the Fluidic Station 450 (Affymetrix, Santa Clara, USA). Briefly, after hybridization the arrays were washed with non-stringent wash buffer A, stringent wash buffer B, stained with SAPE solution containing 1X stain buffer, 2 mg/mL BSA, 10 µg/mL streptavidine phycoerythrin, washed with wash buffer A, stained with antibody solution containing 1X stain buffer, 2 mg/mL BSA, 0.1 mg/mL goat IgG, 3 µg/mL biotinylated antibody, stained once again with SAPE solution and then washed with wash buffer A.

Data acquisition was performed using the GeneChip Scanner 3000 (Affymetrix, Santa Clara, USA). Subsequently, the data was imported as .CEL files, processed using the MAS 5.0 algorithm and normalized by nonlinear transformation employing the LOESS function (localy weighted scatterplot smoothing) by Dr. Mader (Institute for Bio-Informatics, GSF, Munich). For each incubation time point an arithmetic mean of the fluorescence signals of the 4 biologically independent replicates was calculated. The expression levels of the VPA-treated samples were normalized against the expression level of the untreated samples. Relative differences of $\geq$ 1.5 fold upregulation or downregulation were considered biologically significant.

The generation of the self organizing map (SOM) is explained in the paragraph 3.1.1. The generation of the heat map using the ChipInspector software (Genomatix Software, Munich, Germany) is explained in paragraph 3.1.1. The number and percent of genes changed by VPA treatment associated with different signaling pathways were calculated using GenMAPP and GenFinder software (Gladstone Institutes UCSF, San Francisco, USA).

Reagents used:

Product	**Company**
Valproic acid sodium salt (VPA)	Sigma-Aldrich Chemie, Steinheim, Germany
GeneChip Human Genome U133 Plus 2.0 Array	Affymetrix Inc., Santa Clara, USA
High Pure RNA Isolation Kit	Roche Diagnostics, Mannheim, Germany
RNA 6000 Lab Chip	Agilent, Santa Clara, USA
Poly-A RNA control kit	Affymetrix Inc., Santa Clara, USA
T7-oligo(dT) promoter primer kit (50 µM)	Affymetrix Inc., Santa Clara, USA
dNTP (10 mM)	Invitrogen, Karlsruhe, Germany
SuperScript II Reverse Transcriptase kit	Invitrogen, Karlsruhe, Germany
Second strand reaction mix (5X)	Invitrogen, Karlsruhe, Germany
E.coli DNA ligase (10 U/µL)	Invitrogen, Karlsruhe, Germany
E.coli DNA polymerase I (10 U/µL)	Invitrogen, Karlsruhe, Germany
E.coli RNaseH (2 U/µL)	Invitrogen, Karlsruhe, Germany
T4 DNA polymerase (5 U/µL)	Invitrogen, Karlsruhe, Germany
NaCl 5M	Applied Biosystems / Ambion, Darmstadt, Germany
EDTA 0.5 M	Sigma-Aldrich Chemie, Steinheim, Germany
Sample Cleanup Module	Affymetrix Inc., Santa Clara, USA
IVT Labelling kit	Affymetrix Inc., Santa Clara, USA
GeneChip Expression 3 Amplification reagents – Hybridization control kit	Affymetrix Inc., Santa Clara, USA
DMSO	Sigma-Aldrich Chemie, Steinheim, Germany

Product	Company
Bovine serum albumin (BSA) solution (50 mg/mL)	Invitrogen, Karlsruhe, Germany
R-phycoerythrin Streptavidine (SAPE) (1 mg/mL)	Molecular probes, Invitrogen, Karlsruhe, Germany
Goat IgG (10 mg/mL)	Vector Laboratory, Burlingame, USA
Anti-streptavidine antibody (goat) biotinylated (0.5 mg/mL)	Vector Laboratories, Burlingame, USA
20X SSPE (3M NaCl, 0.2M NaH_2PO_4, 0.02M EDTA)	BioWhittaker Molecular Aplications / Cambrex Corporation, New Jersey, USA

Buffers	Receipt
1X hybridization buffer	100 mM MES, 1M Na^+, 20 mM EDTA, 0.01% Tween-20
12X MES	1.22M MES, 0.89 M Na^+
Non-stringent wash buffer A	6X SSPE, 0.01 % Tween-20
Stringent wash buffer B	100 mM MES, 0.1 M Na^+, 0.01 % Tween-20
1X Stain buffer	100 mM MES, 1 M Na^+, 0.05 % Tween-20

2.3 Total RNA Isolation

HT-29 cells were seeded in 24-well plates (2 x 10^5 cells / well) (Falcon) and the next day the cells were treated with 2 mM VPA for the indicated time periods. Total RNA was isolated using High Pure RNA Isolation Kit, according to the manufacturer's protocol. Briefly, cells were lysed with a guanidine-based lysis/binding buffer and then the cell lysate was transferred to a filter tube and centrifuged for 15 seconds (sec) at 8000 x g. The flowthrough liquid was removed and DNase I solution was added to the filter tube for 15 min at RT. Subsequently, the filter was washed with ethanol-based buffers I and II. Finally, the total RNA was eluted from the filter with 60 uL elution buffer (nuclease-free double distilled water). The concentration of the total RNA was measured by UV spectroscopy at 260 nm (RNA concentration (µg/mL) = OD_{260} x 40 x dilution factor) and the purity of total RNA samples was determined by the ratio of absorbance at 260–280 nm using an Eppendorf Bio Photometer (Eppendorf, Hamburg, Germany).

Reagents used:

Product	**Company**
High Pure RNA Isolation Kit	Roche Diagnostics, Mannheim, Germany

2.4 First-strand cDNA synthesis

First-strand cDNA was generated from 2 µg total RNA by reverse transcription reaction using the GeneAmp PCR System 9700 (Applied Biosystems, Darmstadt, Germany) and the SuperScript II Reverse Transcriptase manufacturer's protocol. Total RNA was mixed in a final volume of 12 µL with 1 µL Oligo(dT) $_{12\text{-}18}$ (500 µg/mL) and 1 µL dNTP Mix (10 mM of each dATP, dCTP, dGTP, dTTP), then heated at 65˚C for 5 min. A solution prepared from 4 µL First-strand buffer (5X), 2 µl DTT (0.1 M), 1 µL RNaseOUT (40 µL/ml) and 1 µl SuperScript II reverse transcriptase (200 U/µL) was added to the first mix and heated further on for 52 min at 42˚C. The reaction was inactivated by heating at 70˚C for 15 min. The samples were diluted with RNase-fee H_2O to the concentration of 20 ng/µl.

Reagents used:

Product	**Company**
SuperScript II Reverse Transcriptase kit	Invitrogen, Karlsruhe, Germany
Oligo(dT) $_{12\text{-}18}$ (0.5 µg/µL)	Invitrogen, Karlsruhe, Germany
dNTP Mix (10 mM)	Invitrogen, Karlsruhe, Germany
RNaseOUT (40 U/µL)	Invitrogen, Karlsruhe, Germany

2.5 PCR reaction

The first-strand cDNA was amplified by the PCR reaction with primers specifics for Bcl-XL (FW: 5'-gta aac tgg ggt cgc att gt-3'; 5'-RW: cag gta agt ggc cat cca ag-3') and β-actin (FW: 5´-cat tgc cga cag gat cca ga-3´; RW: 5´-gac tcg tcg tact cc tgc ttg -3´) using the GeneAmp PCR System 9700 (Applied Biosystems, Darmstadt, Germany). The PCR reaction was carried out in a final volume of 20 µL with 5 µL cDNA (20 ng/µL), 10 µL PCR Master Mix (2X), 1 µL forward primer (100 pmol/µL), 1 µL reverse primer (100 pmol/µL). The samples were heated at 94°C for 5 min, followed by a number of amplification cycles specific for each set of primers and then the reaction was inactivated by heating at 72°C for 10 min. The amplification procedure for Bcl-XL gene consisted of 29 cycles (denaturation at 94°C for 30 sec, annealing at 52°C for 30 sec, elongation at 72°C for 1 min) and for actin consisted of

25 cycles (denaturation at 94°C for 30 sec, annealing at 55°C for 30 sec, elongation at 72°C for 1 min).

The amplified PCR products were subjected to agarose gel electrophoresis and visualised by ethidium bromide staining. 10 µl of the PCR products diluted in 1X Coral Load PCR buffer, were resolved in 2 % agarose gel in 1X Rotiphorese TBE Buffer (Roth) supplemented with 0.5 µg/mL ethidium bromide. A 1 kb DNA ladder (Invitrogen) was used as a molecular weight marker. The gels were run at 80 V in 1X Rotiphorese TBE Buffer using Agagel Standard electophoresis system (Biometra, Göttingen, GE). The absence of contaminants was routinely checked by PCR reaction of negative control samples, in which the DNA samples were replaced by sterile water. The visualization of PCR products in ethidium bromide-stained gels was done with EPI-Chemi Darkroom (UVP Laboratory Products, CA, USA) using the Lab Works Analysis software (UVP Laboratory Products, CA, USA).

Reagents used:

Product	**Company**
PCR Master Mix (2X)	Promega, Mannheim, Germany
Primers sequences	Eurofins MWG Operon, Ebersberg, Germany
10X Coral Load PCR buffer	Qiagen, Hilden, Germany
Agarose GTQ	Carl Roth, Karlsruhe, Germany
10X Rotiphorese TBE Buffer	Carl Roth, Karlsruhe, Germany
Ethidium bromide (10 mg/ml)	Invitrogen, Heidelberg, Germany

2.6 Real time-PCR Assay

The first-strand cDNA was amplified by a real-time PCR reaction with primers specifics for Bak (FW: 5´-gta gcc cag gac aca gag ga-3´; RW: 5´-ggt ggc aat ctt ggt gaa gt-3´), TYMS (Fw: 5'-cgc ttg gaa tcc aag aga tct t-3'; RW: 5'-aca gct cac tgt tca cca cat aga a-3') and β-actin (FW: 5´-cat tgc cga cag gat cca ga-3´; RW: 5´-gac tcg tcg tact cc tgc ttg -3´) using the LightCycler FastStart DNA Master Plus SYBR Green I kit according to the manufacturer's instructions. Reactions were performed in a 20 µL volume with 100 ng cDNA, 0.25 µM primers and 4 µL of Master mix (5X), which contains FastStart Taq DNA Polymerase, reaction buffer, dNTP mix, $MgCl_2$ and SYBR Green dye I. The thermal cycle program

consisted of an activation preheating step of 10 min at 90°C, followed by 45 cycles of 10 sec at 95°C, 10 sec at 55°C and 20 sec at 72°C. The generation of products was monitored after each extension step by measuring the fluorescence intensity of the double-stranded DNA-binding SYBR Green I dye using the LightCycler instrument (Roche Diagnostics, Mannheim, Germany) equipped with the LightCycler software (version 5.32, Roche Diagnostics). A melting curve analysis was performed to ensure the specificity of the reaction, by measuring the melting point of the double-stranded DNA product produced.

Relative quantification of gene expression was determined by the ratio of the amount of the specific transcript to the amount of the house-keeping gene actin using the relative expression ratio formula published by Pfaffl et al., 2002 [174]. The Nonlinear Least Squares Regression software was used to calculate the real-time PCR efficiency (E) of the individual transcripts. Relative differences of ≥ 1.5 fold upregulation or downregulation were considered biologically significant.

$$\text{Ratio}_{\text{target / reference gene}} = \frac{(E_{\text{target}})^{\Delta CP_{\text{target}}\,(\textit{mean untreated samples} - \textit{mean treated samples})}}{(E_{\text{reference}})^{\Delta CP_{\text{reference}}\,(\textit{mean untreated samples} - \textit{mean treated samples})}}$$

Reagents used:

Product	**Company**
Primers sequences	Eurofins MWG Operon, Ebersberg, Germany
LightCycler FastStart DNA Master Plus SYBR Green I kit	Roche Diagnostics, Mannheim, Germany

2.7 Measurement of oligonucleosomal DNA fragmentation in apoptotic cells

The Cell Death Detection ELISA ^{Plus} kit (Roche, Mannheim, Germany) was used to quantitatively determine cytoplasmic histone-associated-DNA-fragments (mono- and oligo-nucleosomes) generated during the apoptotic process according to the manufacturer's protocol. Briefly, HT-29 cells were treated with 1 mM or 2 mM VPA for 18 or 48 hours (h) in combination or not with 20 µM Pan-caspase inhibitor (Apoptame Q, MP Biomedicals, Eschwege, Germany). Cells were lysed, centrifuged at 200 x g and the supernatant (cytoplasmic fraction) was 10 fold diluted in incubation buffer. 20 µL of the diluted supernatant was incubated for 2 h at RT with 80 µL Immunoreagent (a mixture of

4 µL biotin-labeled antihistone antibody, 4 µL peroxidase-conjugated anti-DNA antibody and 72 µL of incubation buffer) in a streptavidin-coated microplate under gently shaking at 350 rpm. The excess solution was removed from the wells and then the microplate was rinsed three times with 250 µL of incubation buffer. The amount of nucleosomes was determined spectrophotometrically at a wavelength of 405 nm (reference wavelengh of 492 nm) with ABTS as a substrate of peroxidase using µQuant Universal Microplate Spectrophotometer (Bio-TEK Instruments, Vermont, USA).

Reagents used:

Product	**Company**
Cell Death Detection ELISA ^{Plus} kit	Roche, Mannheim, Germany
Pan-caspase inhibitor	Apoptame Q, MP Biomedicals, Eschwege, Germany

2.8 Detection of apoptosis by Annexin V-APC/PI staining

HT-29 cells were treated with 2 mM VPA, detached with Accutase and washed with PBS. Floating and adherent cells (3 x 10^5) were stained with 5 µL Annexin V-APC and 20 µL propidium iodide (PI) (50 µg/mL) in incubation buffer for 20 minutes (min) at room temperature (RT) in the dark. The cells were immediately subjected to fluorescence-activated cell sorter (FACS) using a LSR II flow cytometer equipped with FACSDiva-software (BD Biosciences Pharmingen, San Diego, USA). Excitation of Annexin V-APC was supplied by the 633 nm laser, while PI excitation was supplied by the 488 nm laser. Annexin-V-APC signal was detected with a combination of a 635-nm longpass-filter and a 660/20-nm bandpass-filter, while the PI signal was acquired with a 600-nm-longpass and a 610/20-nm bandpass filter.

A total of 10000 cells were analyzed per sample, the percentage of living (Annexin V^-/PI^-), early apoptotic (Annexin V^+/PI^-), late apoptotic/necrotic (Annexin V^+/PI^+) and necrotic cells (Annexin V^-/PI^+) was determined using WinMDI 2.8 software (BD Biosciences Pharmingen, San Diego, USA).

Reagents used:

Product	**Company**
Accutase	PAA Laboratories, Pasching, DE
Phosphate Buffered Saline buffer (PBS)	PAA Laboratories, Pasching, DE
Annexin V–APC (recombinant human Annexin V- allophycocyanin conjugated)	CALTAG, Burlingame, CA
Propidium iodide	Sigma-Aldrich Chemie, Steinheim, Germany

Solutions	
Incubation buffer	10 mM Hepes/NaOH, 140 mM NaCl, 5 mM $CaCl_2$, pH 7.4

2.9 Mitochondrial fractionation

HT-29 cells were treated with 2 mM VPA for the indicated time periods and then harvested with 1 mM EDTA in PBS. The whole cell lysates were prepared by resuspending a fraction of the cells in Laemmli lyses buffer. The mitochondrial lysates were prepared from the other fraction of the cells, using a modified protocol for nitrogen cavitation described by Gottlieb and Adachi, 2000 [175]. The cells were resuspended in an isotonic mitochondrial buffer supplemented with 100 µl/mL of 1X protease inhibitor cocktail, lysed in isotonic buffer for 20 min at 10 Bar in a cell nitrogen disruption bomb (Kimble Kontes, Vineland, New Jersey, USA) and then homogenized in a Dounce homogenizer. The suspension was centrifuged at 1000 x g/5 min/4ºC, the cytosolic fraction, containing the mitochondria was saved and further on centrifuged at 10000 x g/15 min/4ºC. The mitochondrial pellet was resuspended in the isotonic buffer and the protein concentration was determined using the Bredford protein assay with Roti-Nanoquant. Subsequently, 25 µg of the mitochondrial samples were subjected to Western Blot analysis.

Reagents used:

Product	**Company**
PBS	PAA Laboratories, Pasching, DE
Ethylenediaminetetraacetic acid (EDTA)	Sigma-Aldrich Chemie, Steinheim, Germany
Complete Protease Inhibitor Cocktail Tablets	Roche Diagnostics, Mannheim, Germany
Roti-Nanoquant	Carl Roth, Karlsruhe, Germany

Solutions	
4X Laemmli lyses buffer	250 mM Tris-HCl (pH 6.8), 8 % SDS, 40 % glycerol, 0.004 % bromophenol blue, 5 % 2-mercaptoethanol
Isotonic mitochondrial buffer	20 mM HEPES, (pH 7.4), 10 mM KCl, 1.5 mM $MgCl_2$, 1 mM EGTA, 1 mM EDTA, 250 mM Sucrose
Complete Protease inhibitor cocktail	10X stock solution: 1 Complete tablet dissolved in 5 mL distilated H_2O

2.10 Nuclei fractionation

HT-29 cells were treated with 2 mM VPA for the indicated time periods, detached with Accutase and washed with PBS. A fraction of the cells was lysed in cell extraction buffer for 30 min at 4˚C, centrifuged at 13000 rpm/10 min/4˚C and then the supernatant, representing the whole cell lysate was subjected to protein quantification using the Bredfort protein assay, followed by Western Blot analysis.

In order to prepare nuclei lysates, the other fraction of the cells was resuspended in 3.5 ml ice cold sucrose buffer I supplemented with 1 mM DTT and homogenized 10 times at 700 rpm. The homogenate was mixed with 3.5 ml sucrose buffer II supplemented with 1 mM DTT, added carefully to 4.4 ml sucrose buffer II and centrifuged at 30000 x g/45 min/4ºC. The nuclei pellet was washed 2 times with ice cold buffer I, resuspended in cell extraction buffer (BioSource, Nivelles, Belgium) for 30 min on ice, frozen/thawed for 3 times in nitrogen liquid, sonified 3 times using Bandelin Sonorex (Bandelin, Berlin, Germany), centrifuged at 13000 rpm/10 min/4ºC and then the supernatant, containing the nuclei fraction was subjected to protein quantification using the Bredford protein assay. Subsequently, 25 µg of the nuclei lysates were subjected to Western Blot analysis.

Reagents used:

Product	**Company**
Accutase	PAA Laboratories, Pasching, Germany
PBS	PAA Laboratories, Pasching, Germany
Cell extraction buffer	BioSource, Nivelles, Belgium
Roti-Nanoquant	Carl Roth, Karlsruhe, Germany

Solutions	
4X Laemmli lyses buffer	250 mM Tris-HCl (pH 6.8), 8 % SDS, 40 % glycerol, 0.004 % bromophenol blue, 5% 2-mercaptoethanol
Sucrose buffer I	0.32 M sucrose, 3 mM $CaCl_2$, 2 mM magnesium acetate, 0.1 mM EDTA, 10 mM TRIS-Cl, pH 8.0, 0.5 % (v/v) Nonidet P-40
Sucrose buffer II	2 mM sucrose, 5 mM magnesium acetate, 0.1 mM EDTA, 10 mM Tris-Cl, pH 8.0

2.11 Western Blot analysis

The protein concentration of whole cell lysates, nuclei and mitochondrial lysates were determined by the Bredford protein assay with Roti-Nanoquant using an Eppendorf Bio Photometer (Eppendorf AG, Hamburg, Germany). Usually 25 µg of the protein lysate in 1X Laemmli buffer or 25 µL of the whole cell lysates in 1X Laemmli buffer were heated at 95˚C/5 min and then resolved in the SDS-polyacrilamide gel with the corresponding percent of polyacrilamide (12 or 15 %) according to the molecular weight of the protein being investigated. Protein Marker Broad Range was used as protein molecular weight marker. 10 µl of the marker was diluted in 1X Laemmli buffer, heated at 95˚C/5 min and resolved in the SDS-polyacrilamide gel. The proteins were then subjected to gel electrophoresis separation at constant voltage of 160 V in Rotiphorese 1X SDS-PAGE buffer, using NOVEX Mini-Cell electrophoresis system (Invitrogen, Karlsruhe, Germany).

After the gel electrophoresis proteins were transferred by wet or semi-dry blotting to an Immun-Blot PVDF membrane. The wet transfer was performed either at constant voltage of 80 V, with the transfer buffer I using Trans-Blot Cell system (Bio-RAD Laboratories, CA**,** USA) or at constant voltage of 32 V, with the transfer buffer II using X Cell II Blot Module (Invitrogen, Karlsruhe, Germany). The semi-dry transfer was performed at constant current of 90 mA with the Rotiphorese 1X SDS-PAGE buffer supplemented with 15 % methanol using the Semi Dry Electroblotter system (Sartorius, Goettingen, Germany).

Subsequently, the membranes were blocked for 15 min at RT in 5 % non-fat dry milk in TBS-T buffer and then incubated over night at 4˚C with the primary antibody (see the list of antibodies) diluted in 5 % non-fat dry milk or 5 % BSA (PAA Laboratories) in TBS-T, accordingly to the manufacturer's instructions. The next day the membranes were washed 3 times with TBS-T and incubated for 1 h at RT with the species specific HRP-conjugated secondary antibody (see the list of antibodies), diluted in 5% non-fat dry milk in TBS-T. As loading control rabbit anti-beta-actin antibody was used in whole cell lysates. The mouse anti-Tim 23 antibody was used as loading control in protein lysates of mitochondrial fractions. The rabbit anti-GSK-3-beta antibody was used as loading control in protein lysates of nuclei fractions.

The proteins were visualised by enhanced chemiluminescence (ECL) detection using SuperSignal West Dura Extended Duration Substrate and Molecular Light Imager Night OWL (EG&G Berthold Technology, Bad Wildbad, Germany). Signal intensities were quantified by densitometry using Image Master Software (Amersham Biosciences, Piscataway, USA). The relative expression ratio of proteins was calculated as: relative expression ratio of protein = (protein signal density / loading control signal density) X 100.

List of the antibodies used for Western Blot analysis:

Antiboy	**Company**
Rabbit anti-Bak	Cell Signaling Technology, Danvers, USA
Rabbit anti-Bax	
Rabbit anti-Bad	
Rabbit anti-Bid	
Rabbit anti-Bim	
Rabbit anti-Bik	
Rabbit anti-Bcl2	
Rabbit anti-Bcl-XL	
Rabbit anti-Puma	
Rabbit anti-GSK-3-beta (clone 27C10)	
Rabbit anti-beta-actin	
Horseradish peroxidase-conjugated anti-rabbit IgG	
Horseradish peroxidase-conjugated anti-mouse IgG	

Antiboy	**Company**
Rabbit anti-HDAC2 (clone H-54)	Santa Cruz Biotechnology, Heidelberg, Germany
Rabbit anti-Noxa (clone N-15)	
Rabbit anti-Ets2 (clone C-20)	
Rabbit anti-Ets2 (pT72)	
Mouse anti-Tim 23	BD Biosciences, CA, USA

Reagents used:

Product	**Company**
Protein Marker Broad Range	New England Biolabs, Frankfurt am Main, Germany
PBS	PAA Laboratories, Pasching, Germany
Cell extraction buffer	BioSource, Nivelles, Belgium
Roti-Nanoquant	Carl Roth, Karlsruhe, Germany
Rotiphorese 10X SDS-PAGE buffer	Carl Roth, Karlsruhe, Germany
Mini cassettes 1.0 mm	Invitrogen, Karlsruhe, Germany
Immun-Blot PVDF membrane	Bio-RAD Laboratories, CA**,** USA
Milk Powder	Carl Roth, Karlsruhe, Germany
Bovine serum albumine (BSA)	PAA Laboratories, Pasching, Germany
Rotiphorese Gel 30	Carl Roth, Karlsruhe, Germany
SuperSignal West Dura Extended Duration Substrate	Pierce Biotechnology, Rockford,USA

Buffers	
4X Laemmli lyses buffer	250 mM Tris-HCl (pH 6.8), 8 % SDS, 40 % glycerol, 0.004 % bromophenol blue, 5 % 2-mercaptoethanol
Wet Blotting Transfer buffer I	TRIS 50 mM, Glycine 40 mM, 0.025 % SDS
Wet Blotting Transfer buffer II	TRIS 50 mM, Glycin 40 mM, 0.025 % SDS, 20 % methanol
TBS-T buffer	10 mM Tris-Cl, (pH 8), 150 mM NaCl, 0.05 % Tween-20

SDS-polyacrilamide gel	**Concentration**	
Separation gel (30 ml)	12.5 % (ml)	15 % (ml)
Rotiphorese Gel 30 (37, 5:1) 30 % Acrylamide/0.8 % bisacrylamide	12.5	15
Tris-Cl/SDS, pH 8.8	7.5	7.5
dH_2O	10	7.5
10 % ammonium persulfate	0.10	0.10
TEMED	0.02	0.02
Note 1: 30 ml of separation gel, adequate for casting four minigels (Invitrogen, CA, USA)		
Stacking gel	**ml**	
Rotiphorese Gel 30 (37, 5:1) 30 % Acrylamide/0.8 % bisacrylamide	1.3	
4X Tris-Cl/SDS, pH 6.8	2.5	
dH_2O	6.1	
10 % ammonium persulfate	0.50	
TEMED	0.01	
Note: 10 ml of stacking gel adequate for casting four minigels		

2.12 Small interfering RNA experiments

HT-29 cells were seeded in 24-well plates (8×10^4 cells /well), the next day the cells were transfected with 20 pmol of either anti-Bak siRNA sequence or Stealth™ RNAi Negative Control Med GC and further on the transfected cells were subjected to cell survival assay. For siRNA transfections against HDAC2 gene, HT-29 cells were seeded either in 12-well plates (2×10^5 cells /well) or in culture slides (8×10^4 cells /well). The next day the cells in 12-well plate were transfected with 120 pmol of each siRNA sequence specific against HDAC2 or with anti-luciferase siRNA and then the cells were subjected to Western Blot analysis. The cells in culture slides were transfected with 80 pmol of each siRNA HDAC2 sequence or with anti-luciferase siRNA and then the cells were subjected to immunofluorescence analysis by microscopy. The siRNA sense sequences directed against luciferase (si luciferase) and Stealth™ RNAi Negative Control Med GC were used as transfection controls.

The transfection experiments were performed with Lipofectamine 2000, according to the manufacturer's instructions. For example, for the Bak siRNA transfection, 3 μL of Lipofectamine 2000 was diluted in 50 μL of OptiMEM at RT and 5 min later the lipofectamine solution was combined with either 1uL of anti-Bak siRNA sequence (20 pmol/μL) or 1 μL of Stealth™ RNAi Negative Control Med GC (20 pmol/μL) in 50 μL OptiMEM. Incubation was continued for 20 min at RT and then the mixture was added to the cells in culture wells.

siRNA sense strand sequences used:

siRNA	**Sense strand sequence**	**Company**
stealth siHDAC2	5'-guc auc cca uga agg cuc aua gaa u -3'	Invitrogen, Heidelberg, Germany
stealth siHDAC2	5'-ggg cug gag gau uac auc aug cua a -3'	Invitrogen, Heidelberg, Germany
siHDAC2	5'-aag ccu cau aga auc cgc aug -3'	Eurofines MWG Operon, Ebersberg, Germany
stealth siBak	5´-gcc agu uug ugg uac gaa gau ucu u -3'	Invitrogen, Heidelberg, Germany
siLuciferase	5´-aac gua cgc gga aua cuu cga -3'	Invitrogen, Heidelberg, Germany
Stealth™ RNAi Negative Control Med GC		Invitrogen, Heidelberg, Germany

Reagents and materials used:

Product	**Company**
Culture slides	BD Biosciences, MA, USA
MULTIWELL 12 well and 24 well	Falcon, BD Labware, NJ, USA
Lipofectamine 2000	Invitrogen, Heidelberg, Germany
OptiMEM	Invitrogen, Heidelberg, Germany

2.13 Indirect immunofluorescence assay followed by microscopy

HT-29 cells were transfected with a siRNA sequence specifically directed against HDAC2 or with a siRNA sequence directed against luciferase as a transfection control, on culture slides, as specified in paragraph 2.12. After 72 h cells were fixed with 2 % paraformaldehyde for 10 min at 37˚ C, permeabilized with 90 % methanol for 30 min on ice and blocked for 10 min at RT in incubation buffer. Cells were co-incubated with rabbit anti-Bak antibody (dilution 1:200 in incubation buffer) and mouse anti-HDAC2 antibody (# 05-814, Upstate) (dilution 1:300 in incubation buffer) for 2 h at RT, washed two times with incubation buffer and stained with goat anti-rabbit Alexa Fluor 594 or goat anti-mouse Alexa Fluor 488-labeled secondary antibodies (dilution 1:400 in incubation buffer) for 1 h at RT. The cells were washed two times with PBS, the slides were mounted with Vectrashield

mounting medium (Linaris, Wertheim, Germany) and staining was visualised using the confocal laser scanning microscope Zeiss LSM 510 META (Zeiss, Germany).

List of the antibodies used:

Antibody	**Company**
rabbit anti-Bak	Cell Signaling Technology, Danvers, USA
mouse anti-HDAC2	Upstate Group, Inc., NY, USA
Alexa Fluor 594 goat anti-rabbit IgG (H+L)	Invitrogen, Karlsruhe, Germany
Alexa Fluor 488 goat anti-mouse IgG (H+L)	Invitrogen, Karlsruhe, Germany

Reagents and materials used:

Product	**Company**
Culture slides	BD Biosciences, MA, USA
Vectrashield mounting medium	Linaris, Wertheim, Germany

Buffer	**Receipt**
Blocking buffer	0.5 % BSA in PBS

2.14 Transient DNA transfection assay

Overexpression of Bak in HT-29 cells was performed by Dr. Huber (now Stüzt) (Institute of Toxicology, GSF, Munich) using different Bak constructs vectors: pcDNA-Bak (Bak wild type), pcDNA-BakΔGD (lacking the BH3-domain), pcDNA-BakΔC (lacking the C-terminal domain), kindly provided by Dr. Chittenden and published elsewhere [176]. HT-29 cells (1×10^5) were cotransfected with 1 µg pEGFP and 1 µg pcDNA-Bak, pcDNA-BakΔGD, pcDNA-BakΔC, or the empty expression vector pcDNA, respectively, using lipofectamine 2000 (Invitrogen, Karlsruhe, Germany). Briefly, 5 µl Lipofectamine 2000 were incubated for 5 min in 150 µl OptiMEM, then lipofectamine was combined for 20 min with a second solution containing pEGFP and either of the Bak-expression vectors. The transfection reagent was applied for 48 h to the cells, then cells were harvested using Accutase (PAA Laboratories, Pasching, Germany) and subjected to FACS apoptosis analysis by Annexin V/PI-staining using a LSR II flow cytometer equipped with FACSDiva-software (BD Biosciences Pharmingen, San Diego, USA). Excitation of Annexin V-APC was supplied by the 633 nm laser, while PI and EGFP excitation was supplied by the 488 nm laser.

Annexin-V-APC signal was detected with a combination of a 635-nm longpass-filter and a 660/20-nm bandpass-filter. PI signal was acquired with a 600-nm-longpass and a 610/20-nm bandpass filter; EGFP (enhanced green fluorescent protein) signal was detected with a combination of 505-nm-lonpass and a 530/30-nm-bandpass filter. A total of 10000 cells per sample were acquired making a gate on the EGFP positive cells. Further on the early apoptotic cells (Annexin-V^+/PI^-) and the late apoptotic/necrotic (Annexin- V^+/ PI^+) cells were quantified using WinMDI software (BD Biosciences Pharmingen, San Diego, USA).

Reagents used:

Product	**Company**
Lipofectamine 2000	Invitrogen, Heidelberg, Germany
OptiMEM	Invitrogen, Heidelberg, Germany
pEGFP vector	Clontech Laboratories, Terra Bella, CA, USA

2.15 Indirect immunofluorescence assay followed by flow cytometry

HT-29 cells were transfected with the appropriate stealth RNAi (anti-Bak siRNA or Stealth™ RNAi Negative Control Med GC as negative control, respectively) as specified in paragraph 2.12. 24 h after transfection 8 x 10^4 cells were seeded per well of a 24-well plate. The next day cells were treated or not with 2 mM VPA, respectively. After 72 h of incubation with VPA, treated and untreated cells were processed for Bak-staining followed by flow cytometry analysis.

Cells (3 x 10^5 / sample) were fixed and permeabilised for 30 min with 100 µL of BD Fixation/Permeabilisation solution and then washed two times with 1X BD Perm/Wash buffer from BD Cytofix/Cytoperm^{TM} Plus Fixation/Permeabilization kit (BD Biosciences Pharmingen, San Diego, USA). The cells were blocked for 30 min with 5 % goat serum in 1X Cytowash/Cytoperm, incubated for 2 h at RT with rabbit anti-Bak antibody (dilution 1:200 in blocking buffer), washed 2 times with 1X Cytowash/Cytoperm solution and then incubated with AlexaFlour-647 conjugated goat anti-rabbit secondary antibody (dilution 1:500 in blocking buffer). The staining was visualised by flow cytometry using the LSR II flow cytometer equipped with FACS Diva-software (BD). Excitation of AlexaFluor-647 was supplied by the 633 nm laser and the signal was detected with a combination of a 635-nm longpass-filter and a 660/20-nm bandpass-filter. A total of 10000 cells were analyzed per sample with WinMDI 2.8 software.

List of the antibodies used:

Antibody	**Company**
rabbit anti-Bak	Cell Signaling Technology, Danvers, USA
Alexa Fluor 647 goat anti-rabbit IgG (H+L)	Invitrogen, Karlsruhe, Germany

Reagents and materials used:

Product	**Company**
MULTIWELL 12 well or 24 well	Falcon, BD Labware, NJ, USA
BD Cytofix/Cytoperm™ Plus Fixation/Permeabilization kit	BD Biosciences, San Diego, USA
Goat serum (10 mg/mL)	Gibco, Invitrogen, Karlsruhe, Germany

2.16 Cell survival assay

HT-29 cells were transfected with the appropriate stealth siRNA (anti-Bak siRNA or Stealth™ RNAi Negative Control Med GC as negative control) as specified in paragraph 2.12. 24 h after transfection 8 x 10^4 cells were seeded per well of a 24-well plate. The next day (day 1) cells were counted and untreated or treated with 2 mM VPA. For counting, cells were detached with Accutase, stained with trypan blue and then viable cells were counted microscopically using a Burker hemocytometer. After 72 h of incubation with VPA (day 4), treated and untreated cells were counted or processed for Bak-staining by indirect immunofluorescence followed by flow cytometry analysis.

To obtain growth curves total amounts of Bak-positive (wt) and Bak-depleted cells were assessed at day 1 and day 4 by determining the percentages of Bak-positive (wt) and Bak-depleted cells per sample using flow cytometry data and set in relation to total cell amounts per sample, also determined at day 1 and day 4.

Reagents and materials used:

Product	**Company**
MULTIWELL 24 well	Falcon, BD Labware, NJ, USA
Burker hemocytometer	Brand, Wertheim, Germany
Accutase	PAA Laboratories, Pasching, DE

2.17 Cell viability assay

DLD1 and DLD1-5-FU/R cells (3×10^4) were seeded into 24-well plates. Twenty-four hours later cells were treated with VPA 2 mM for 48 h, followed by the treatment with 50 µM 5-fluorouracil (5-FU) for 72 h. As control, after theVPA treatment for 48 h, the cells were grown in fresh medium for 72 h or the cells were grown in fresh medium for 48 h followed by 5-FU treatment for 72 h. The cells were detached with Accutase and counted using the Z1 Coulter Particle Counter (Beckman Coulter, USA).

HT-29p and 5F12 cells (5×10^3) were seeded in 96-well plates, twenty-four hours later cells were treated with VPA 2 mM for 48 h, followed by treatment with 1 µM, 5 µM, 10 µM or 20 µM 5-FU for 24 h. After 5-FU incubation cells were grown in fresh medium for 48 h. As control, the cells were treated with VPA for 48 h and then cells were grown in fresh medium for 72 h or the cells were grown in medium for 48 h, incubated with 1 µM, 5 µM, 10 µM or 20 µM 5-FU for 24 h and then grown in fresh medium for 48 h. The media was removed and cells were incubated with the tetrazolium salt MTT (0.5 mg/ml in medium) at 37˚C for 3 h, then DMSO was added to solubilize the MTT-formazan product. The amount of violet crystals reflecting cellular growth and viability was determined spectophotometrically by measuring the samples OD at a wavelength of 550 nm using a TECAN Sunrise spectrophotometer (TECAN Group Ltd., Germany).

Materials used:

Product	**Company**
MULTIWELL 24 well and 96-well plates	Falcon, BD Labware, NJ, USA
5-Fluorouracil (5-FU)	Sigma-Aldrich Chemie, Steinheim, Germany
Accutase	PAA Laboratories, Pasching, DE
MTT (3-(4,5-Dimethyl-2-thiazolyl)-2,5-diphenyl-2H-tetrazolium bromide)	Sigma-Aldrich Chemie, Steinheim, Germany
DMSO (dimethyl sulfoxide)	Sigma-Aldrich Chemie, Steinheim, Germany

2.18 Statistical analysis

Statistical significance was investigated using a paired two-tailed Student t-test. Differences were considered statistically significant at $p \leq 0.05$. Relative differences are represented in bar charts and error bars represent the standard deviation (SD).

3 RESULTS

3.1 Which is the mechanism used by VPA to induce cell death in colon cancer cells?

To identify the mechanism by which VPA induces cell death in colon cancer cells it was investigated:

i) which are the VPA-induced changes that mediate initiation of cell death? (The effect of VPA on the gene expression profile of HT-29 cells is presented in sections 3.1.1 and 3.1.2; the results showing that VPA induces characteristic features of apoptosis are presented in section 3.1.3; the results showing that VPA induces multiple alterations in the protein expression level of the Bcl-2 family members in HT-29 cells are presented in section 3.1.4.)

ii) which are the key target(s) specifically required for the VPA-induced cell death? (The results showing that Bak is the major player in the VPA-induced cell death are presented in sections 3.1.6 and 3.1.7.)

iii) if the expression of the VPA target(s) is HDAC2 dependent? (The results showing that VPA upregulates expression of Bak and Bim by an HDAC2-dependent mechanism, while the VPA-reduced Bcl-XL expression is not HDAC2-dependent are presented in section 3.1.5; the results showing that Bcl-XL expression depends on the Ets2 transcription factor activity are presented in sections 3.1.8, 3.1.9, 3.1.10 and 3.1.11.)

3.1.1 The effect of VPA on the gene expression profile of the HT-29 cells

In order to identify target genes, which were regulated by VPA treatment, an Affymetrix microarray analysis was performed using untreated HT-29 cells or ones treated with 2 mM VPA for 3, 6 and 24 h. To standardize data and to remove the non-biological variation between the samples, the microarray data was processed using the MAS 5.0 algorithm and normalized by nonlinear transformation employing the LOESS function (locally weighted scatterplot smoothing) before analysis. For each incubation time point an arithmetic mean of the fluorescence signals of 4 biologically independent replicates was calculated. A gene was considered as being expressed if the mean of the fluorescence signals of the untreated sample was at least 20 counts (the basal threshold was set to 20 counts).

To visualise the microarray data a heat map was created using ChipInspector software (Genomatix Software, Munich, Germany). To generate the heat map, the expression levels of the 4 replicates of the VPA-treated samples were normalized against the respective expression levels of the 4 replicates of the untreated samples. Two fields of the heat map are shown in **Figure 5**. The changes in the expression levels induced by VPA treatment were displayed

graphically by color saturation. A ratio of 1.0 between treated and untreated samples showing that the expression remained unchanged upon VPA treatment is depicted in black. A positive ratio (>1.0) showing an upregulation of the expression after VPA treatment is depicted in red. A negative ratio (< 1.0) showing a downregulation of expression after VPA treatment is depicted in green. The heat map showed that the VPA treatment resulted in both transcription activation and repression.

For a refined analysis of the microarray data a self organizing map (SOM) was generated. The expression levels were normalized against the smallest mean of the VPA-treated and untreated samples. If the smallest mean was lower than the basal threshold, the expression levels of the VPA-treated and untreated samples were normalized against the basal threshold. Then, the data was transformed by a log2 function and a SOM was generated. The probe sets were grouped within the SOM into 100 clusters according to their expression changes upon VPA treatment (**Figure 6**). Clusters of upregulated (red, upper left corner) and downregulated (green, lower right corner) genes were identified by the SOM. Additionally, early and late VPA responsive genes could be identified within the upregulated and downregulated clusters of genes. Furthermore, clusters of genes were identified which show neither a clear upregulation nor downregulation after the VPA treatment (center of the SOM).

To calculate the relative difference in gene expression between the VPA-treated and untreated samples, the ratio between the mean expression level of the VPA-treated samples and the mean expression level of the untreated samples was calculated. The data analysis showed that 1090 genes were at least 2 fold upregulated and 754 genes were at least 2 fold downregulated after VPA treatment for 24 h. The lowest ratio after treatment of cells with VPA for 24 h was 0.08 and the highest ratio was 80.6. Most of the changes in gene expression were in a range between 0.1 and 20.0. Only one probe set had a ratio of 0.08 after VPA treatment of HT-29 cells for 24 h. 15 probe sets showed a change in expression in a range between 20.3 and 37.0 after VPA treatment for 24 h. Only one probe set was 80.6 fold upregulated after VPA treatment of HT-29 cells for 24 h **(Supplementary Table 1)**. Due to the size of the data, the comprehensive list of genes changed by the VPA treatment (relative differences of ≥ 1.5 fold upregulation or downregulation between the expression levels of the VPA-treated and untreated samples) is given in Appendix 1 (excel table).

To determine which cell signaling pathways are regulated by the VPA treatment in HT-29 cells GenMAPP and GenFinder softwares (Gladstone Institutes, UCSF, San Francisco, USA) were used. In **Table 3** the number and the percentage of genes whose expression was changed upon treatment with VPA for 6 h and associated with a specific cell signaling pathway (according to the KEGG and Gene Ontology pathways) are given. The tables

showing the effect of 3 h and 24 h of VPA treatment on different signaling pathways are presented in the **Supplementary Tables 2** and **3**. The results from **Table 3** showed that the expression of genes involved in the control of apoptosis were changed by the VPA treatment (Z-score = 2.0, Z-score of 1.96 or -1.96 correlate with a p-value of 0.05). The map from **Figure 7** showed the effect of VPA treatment for 6 h on genes involved in the apoptosis control according to the KEGG pathways (the maps showing the effect of VPA treatment for 3 h and 24 h on genes associated with apoptosis are presented in the **Supplementary Figure 1** and **2**). VPA changed the expression of genes directly involved in the control of the intrinsic and extrinsic pathways of apoptosis. The genes found to be more than 1.5 fold upregulated (red squares) by VPA treatment were: BAK1[1] (Bak, BCL2L7), BNIP3L (NIX), BIRC2 (cIAP1, Hiap-2, API1), BIRC3 (CIAP2, MALT2) and APAF1 (CED4). The genes found to be more than 1.5 fold downregulated (green squares) were: BCL2L1 (Bcl-XL), CFLAR (c-FLIP) and BIRC4 (XIAP). Subsequent analysis of the microarray data showed that VPA changed the expression of several genes from the Bcl-2 family which are involved in the mitochondrial pathway of apoptosis (**Table 4**), while the expression of genes involved in the death receptor pathway of apoptosis was either downregulated or not changed (**Table 5**). The results presented in **Table 4** showed that VPA treatment upregulated expression of Bak, Bim, Bik and Bmf and downregulated the expression of Bcl-XL, Bid and Noxa. The expression of Bcl-2, Bax, Bad and Puma was not changed by VPA treatment at the mRNA level. These results indicated that VPA might induce a proapoptotic signal in HT-29 cells by changing the balance of the pro- and antiapoptotic members of the Bcl-2 family.

It has been reported that VPA induced cell cycle arrest in different types of tumor cells [138, 140, 141]. Therefore, the effect of VPA on the expression of genes involved in cell cycle control was also analysed. The results displayed in **Table 3** showed that the expression of genes encoding proteins involved in cell cycle regulation at the G1/S checkpoint were changed after treatment with VPA for 6 h (Z-score = 2.4). The map in **Figure 8** shows the effect of VPA treatment for 24 h on the expression of genes associated with G1/S cell cycle control according to the KEGG pathways (the maps showing the effect of VPA treatment for 3 h and 6 h on the expression of genes associated with G1/S cell cycle control are presented in the **Supplementary Figures 3** and **4**). Genes encoding for the cyclin-dependent kinase (CDK) inhibitors: CDKN1A (p21CIP1, WAF1), CDKN2B (p15, INK4B), CDKN2D (p19, INK4D) and CDKN1C (p57, KIP2) were found to be more than 1.5 fold upregulated by VPA

[1] The gene names are given as Official name (Alternative name).

in HT-29 cells. Other genes involved in the regulation of the cell cycle progression were found to be more than 1.5 fold downregulated (green squares) upon the VPA treatment e.g. genes involved in G1/S cell cycle progression: CCND1 (cyclin D), CCNE2 (cyclin E2), CDC25A (CDC25A2), CDK4 (CMM3; PSK-J3), CDKN2A (ARF, p16INK4); genes involved in DNA replication: CDC45L (CDC45; CDC45L2), ORC1L (PARC1, HSORC1), ORC3L (LAT, LATHEO), ORC6L, POLE, POLA2, RPA2 (REPA2), MCM2 (CCNL1, CDCL1, cdc19), MCM3 (HCC5, RLFB), MCM4 (CDC21, CDC54), MCM5 (CDC46), MCM6 (Mis5), MCM7 (CDC47), PRIM1 (p49), PRIM2A (p58); transcription factors: MYC (c-Myc), E2F1 (RBP3, RBAP1), E2F2, E2F3, E2F4, TP53 (p53; TRP53), TFDP1 (DP1, DRTF1), CREBL1 (G13, CREB-RP) and CREB3L1 (OASIS) (**Figure 8**).

Among the genes found to be upregulated by the VPA treatment was the cyclin-dependent kinase inhibitor CDKN1A (p21CIP1, WAF1). This is in accordance with the previously reported data [136, 138, 177] and proves the accuracy of the presented microarray data. The VPA-induced alterations in the balance between the expression of cyclins, CDKs and CDK inhibitors provides a good explanation for the cell cycle block associated with VPA treatment that has been reported in previous publications [136, 138, 140, 141]. In addition, these results showed that VPA not only induced changes in the expression of genes involved in the control of the cell cycle checkpoints (cyclins, CDKs, CDK inhibitors), but also downregulated the expression of transcription factors like E2F and c-Myc, which are involved in the transcriptional regulation of genes directly involved in the cell cycle progression [178, 179].

Taking into consideration the changes induced by VPA in the mRNA expression of genes encoding for Bcl-2 family members, subsequent functional analyses were performed in this study in order to: i) investigate if VPA treatment induces characteristic features of apoptosis in HT-29 cells and ii) determine if the alterations induced by VPA in the gene expression of the Bcl-2 family members are reflected on the protein level. This would allow the identification of specific Bcl-2 family members that are directly involved in the initiation of cell death.

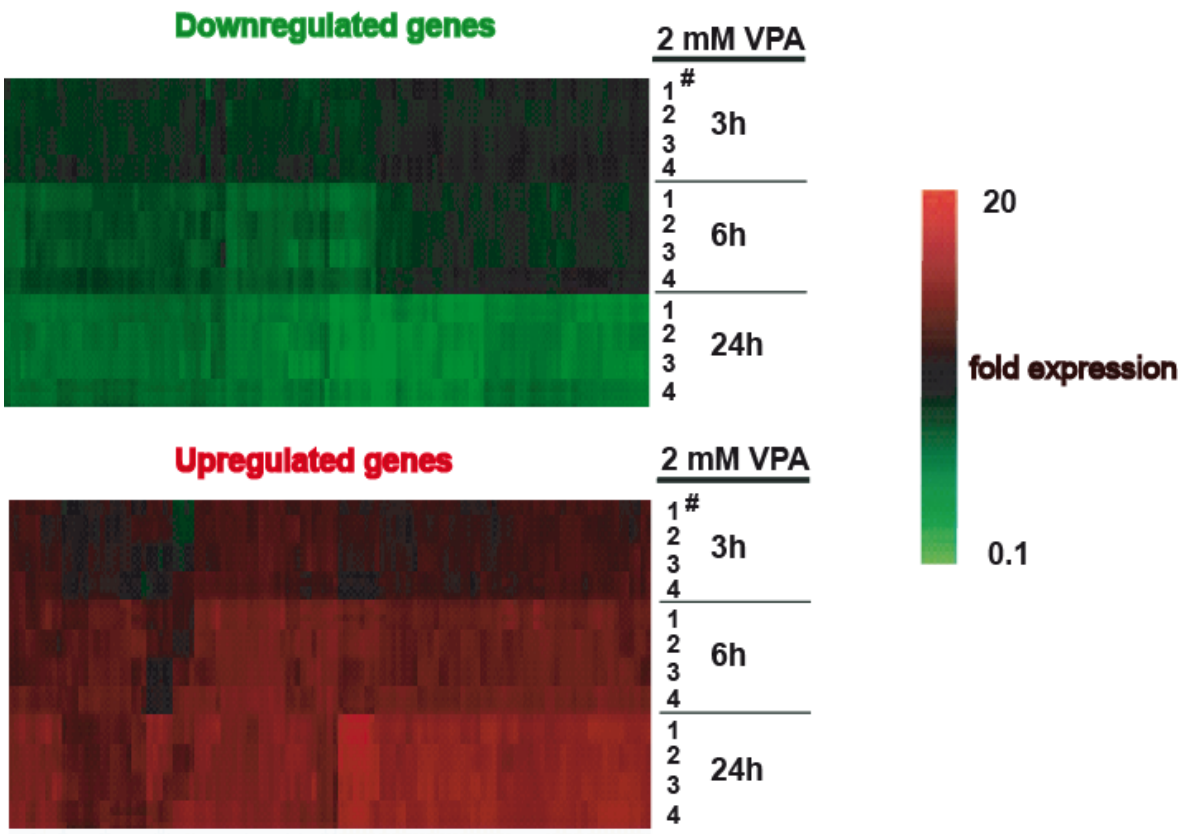

Figure 5. Heat map of the VPA-induced changes in the gene expression profile of HT-29 cells. HT-29 cells were untreated or treated with 2 mM VPA for 3, 6 and 24 h. Total RNA was isolated from 4 biologically independent replicates per treatment and then Biotin-labeled cRNA samples were hybridized to the GeneChip Human Genome U133 Plus 2.0 Array (Affymetrix Inc., Santa Clara, USA). The expression ratios between each VPA-treated and untreated sample replicate are presented graphically by a heat map using ChipInspector software (Genomatix Software, Munich, Germany). Genes not changed by the VPA treatment are depicted in black (ratio of 1.0 between treated and untreated samples). Genes upregulated by the VPA treatment are depicted in red (positive ratio between treated and untreated samples). Genes downregulated by the VPA treatment are depicted in green (negative ratio between treated and untreated samples) The figure shows two fields of the heat map. Each column represents a single probe set. The rows show the change in expression for each replicate of the VPA-treated samples. The color saturation gives the degree of expression change. #, 4 biologically replicates per treatment.

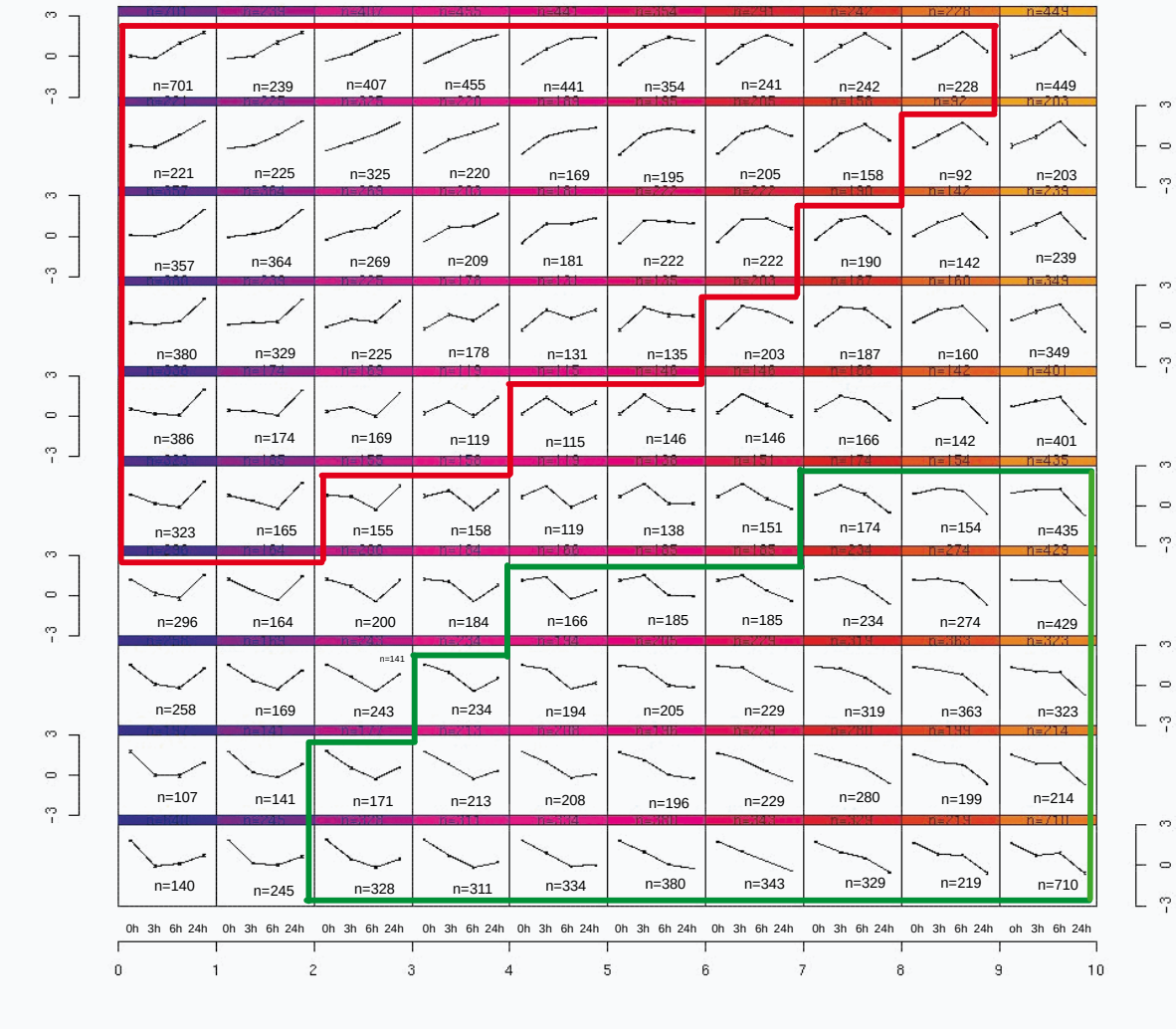

Figure 6. VPA-induced changes in the gene expression profile of HT-29 cells.

HT-29 cells were untreated or treated with 2 mM VPA for 3, 6 and 24 h. Total RNA was isolated from 4 biologically independent replicates per treatment and then Biotin-labeled cRNA samples were hybridized to the GeneChip Human Genome U133 Plus 2.0 Array (Affymetrix Inc., Santa Clara, USA). A self organizing map (SOM) is shown. The expression levels were normalized against the smallest mean of the VPA-treated and untreated samples. If the smallest mean was lower than the basal threshold, the expression levels of the VPA-treated and untreated samples were normalized against the basal threshold. For example, the expression level of the untreated sample was normalized against the basal threshold, if the smallest mean of the VPA-treated and untreated samples was lower than the basal threshold. Then, the data was transformed by a log2 function and a SOM was generated. Clusters of upregulated (red, upper left corner) and downregulated (green, lower right corner) genes could be identified within the SOM. Clusters of genes which show neither a clear upregulation nor downregulation after the VPA treatment were located at the center of the SOM.

Table 3. Cell signaling pathways regulated by VPA in HT-29 cells. The table shows the number and the percentage of genes whose expression was changed upon treatment with VPA for 6 h and which were associated with a specific cell signaling pathway, according to KEGG and Gene Ontology (GO) pathways. The number and percentage of genes were calculated using GenFinder software.

	Map name according to pathway	Number			Percentage		Z-score [4]
		Genes in pathway	Genes detected [1]	Genes changed	Genes detected [2]	Genes changed [3]	
KEGG pathways	**Androgen-Receptor**	112	98	18	87.5	18.4	3.4
	Apoptosis	82	71	11	86.6	15.5	2.0
	Cell Cycle-G1 to S control	67	64	11	95.5	17.2	2.4
	GPCRDB-Class A Rhodopsin-like	262	35	10	13.4	28.6	4.2
	Hedgehog	22	16	4	72.7	25.0	2.3
	Id-signaling	51	31	6	60.8	19.4	2.1
	IL-4	62	51	9	82.3	17.6	2.3
	Inositol phosphate metabolism	152	119	17	78.3	14.3	2.3
	Nicotinate and nicotinamide metabolism	156	111	21	71.2	18.9	4.0
	Nuclear Receptors	38	23	7	60.5	30.4	3.7
	Pantothenate and CoA biosynthesis	37	10	3	27.0	30.0	2.5
	Pyrimidine metabolism	98	63	11	64.3	17.5	2.6
	Smooth muscle contraction	156	88	13	56.4	14.8	2.0
	Sphingoglycolipid metabolism	144	118	18	81.9	15.3	2.7
	Starch and sucrose metabolism	208	119	16	57.2	13.4	2.0
	TGF-beta Receptor	151	133	22	88.1	16.5	3.2
	TGF-Beta Signaling	52	37	7	71.2	18.9	2.2
	TNF-alpha/NF-kB	187	175	23	93.6	13.1	2.1

(1) genes detected = the number of genes on array found to link to GO or Kegg pathway

(2) percentage of genes detected = genes detected on array / genes in pathway X 100

(3) percentage of genes changed = genes changed / genes detected on array X 100

(4) Z score = standard statistical test under the hypergeometric distribution; Z-score of 1.96 or -1.96 correlates with a p-value of 0.05

Table 3 (continued). Cell signaling pathways regulated by VPA in HT-29 cells. The table shows the number and the percentage of genes whose expression was changed upon treatment with VPA for 6 h and which were associated with a specific cell signaling pathway, according to KEGG and Gene Ontology (GO) pathways. The number and percentage of genes were calculated using GenFinder software.

	Map name according to pathway	Number			Percentage		Z-score [4]
		Genes in pathway	Genes detected [1]	Genes changed	Genes detected [2]	Genes changed [3]	
GO pathways	**Actin cytoskeleton**	217	126	4	58.1	3.2	-2.1
	Apoptosis	255	170	23	66.7	13.5	2.4
	Catalytic activity	167	117	3	70.1	2.6	-2.3
	Cell-cell signaling	274	76	13	27.7	17.1	2.7
	Chromatin modification	100	85	13	85.0	15.3	2.3
	Electron transporter activity	246	174	6	70.7	3.4	-2.4
	Golgi apparatus	296	223	10	75.3	4.5	-2.1
	Growth factor activity	157	53	12	33.8	22.6	3.7
	M phase	164	137	18	83.5	13.1	2.0
	Positive regulation of cell proliferation	113	58	10	51.3	17.2	2.4
	Primary active transporter activity	181	138	5	76.2	3.6	-2.0
	Rhodopsin-like receptor activity	265	34	9	12.8	26.5	3.8
	RNA polymerase II transcription factor activity	199	131	20	65.8	15.3	2.9
	Transcription coactivator activity	130	95	17	73.1	17.9	3.4
	Transcription cofactor activity	219	163	27	74.4	16.6	3.8
	Transcription factor binding	253	187	31	73.9	16.6	4.1

(1) genes detected = the number of genes on array found to link to GO or Kegg pathway

(2) percentage of genes detected = genes detected on array / genes in pathway X 100

(3) percentage of genes changed = genes changed / genes detected on array X 100

(4) Z score = standard statistical test under the hypergeometric distribution; Z-score of 1.96 or -1.96 correlates with a p-value of 0.05

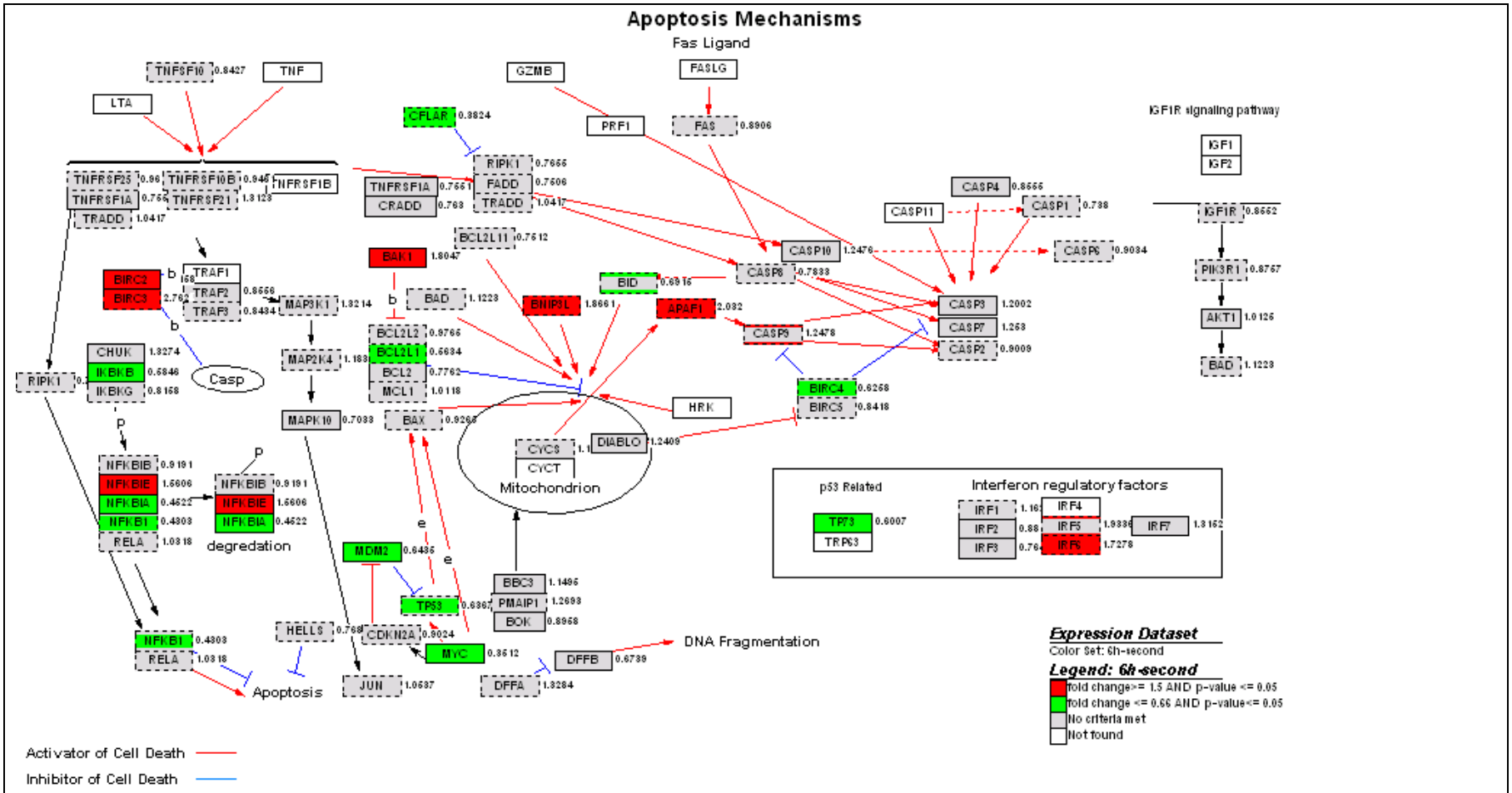

Figure 7. The effect of the VPA treatment for 6 h on the expression of genes associated with apoptosis in HT-29 cells.

The effect of VPA on expression of genes involved in apoptosis, according to the KEGG pathways is shown. In red: more than 1.5 fold upregulated genes; in green: more than 1.5 fold downregulated genes; in gray: unchanged genes; in white: gene expression level lower than basal threshhold. The map was generated using GenMAPP software.

Table 4. **The effect of the VPA treatment on the mRNA expression of the Bcl-2 family members in HT-29 cells**. VPA-induced changes in the gene expression of Bcl-2 family members were evaluated in HT-29 cells untreated or treated with 2 mM VPA for 3, 6 and 24 h using Affymetrix microarray analysis. The arithmetic mean of the fluorescence signals of 4 replicates per treatment was calculated for treated and untreated samples. The mean expression level of the VPA-treated samples was normalized against the mean expression level of the untreated samples.

Bcl-2 family	**Gene name**	**Affymetrix probe set number**	**GenBank accession no. of the transcript recognized by the probe set**	**2 mM VPA vs. 0 mM VPA**		
				3 h VPA	**6 h VPA**	**24 h VPA**
BH3-domain only proteins (proapoptotic function)	Bim	225606_at	NM_006538 NM_138621	1.3 ± 0.1 (p = 0.04)	1.4 ± 0.1 (p = 0.02)	1.6 ± 0.2 (p = 0.04)
	Bik	205780_at	NM_001197	3.1 ± 0.5 (p = 0.01)	2.7 ± 0.3 (p = 0.002)	2.8 ± 1.0 (p = 0.07)
	Bmf	226530_at	NM_001003940 NM_001003942 NM_001003943 NM_033503	3.0 ± 0.4 (p = 0.003)	2.9 ± 0.3 (p = 0.0007)	3.9 ± 0.4 (p = 0.0003)
	Bid	204493_at	NM_001196 NM_197966 NM_197967	0.9 ± 0.05 (p = 0.07)	0.7 ± 0.1 (p = 0.02)	0.6 ± 0.05 (p = 0.003)
	Noxa	204286_s_at	NM_021127	1.4 ± 0.2 (p = 0.06)	1.2 ± 0.2 (p = 0.08)	0.6 ± 0.1 (p = 0.002)
	Bad	209364_at	NM_004322 NM_032989	0.9 ± 0.07 (p = 0.1)	1.0 ± 0.1 (p = 0.7)	1.2 ± 0.1 (p = 0.1)
	Puma	211692_s_at	NM_014417	0.9 ± 0.2 (p = 0.6)	1.2 ± 0.1 (p = 0.08)	1.0 ± 0.1 (p = 0.8)
BH1-BH3 multidomain proteins (proapoptotic function)	Bak	203728_at	NM_001188	1.5 ± 0.7 (p = 0.00007)	1.8 ± 0.3 (p = 0.008)	1.6 ± 0.1 (p = 0.0004)
	Bax	208478_s_at	NM_004324 NM_138761 NM_138763 NM_138764 NM_138765	0.95 ± 0.08 (p = 0.002)	0.9 ± 0.1 (p = 0.3)	0.7 ± 0.07 (p = 0.01)
BH1-BH4 multidomain proteins (antiapoptotic function)	Bcl-XL	215037_s_at	NM_138578	0.6 ± 0.03 (p = 0.0006)	0.5 ± 0.02 (p = 0.0004)	0.7 ± 0.06 (p = 0.01)
	Bcl-2	207004_at	M13995	0.9 ± 0.4 (p = 0.1)	0.8 ± 0.1 (p = 0.2)	0.8 ± 0.2 (p = 0.3)
Actin	β-actin	200801_x_at	NM_001101	1.0 ± 0.08 (p = 0.2)	1.0 ± 0.04 (p = 0.6)	1.0 ± 0.03 (p = 0.1)

Table 5. The effect of VPA on the mRNA expression of the death receptors or their ligands in HT-29 cells. VPA-induced changes in the gene expression of death receptors or their ligands were evaluated in HT-29 cells untreated or treated with 2 mM VPA for 3, 6 and 24 h using Affymetrix microarray analysis. The arithmetic mean of the fluorescence signals of the 4 replicates per treatment was calculated for treated and untreated samples. The mean expression level of the VPA-treated samples was normalized against the mean expression level of the untreated samples. The results showed that VPA did not induce mRNA expression of the death receptors or their ligands in HT-29 cells.

Gene Name	**Affymetrix probe set number**	**GenBank accession number of the transcript recognized by probe set**	**2 mM VPA vs. 0 mM VPA**		
			3 h VPA	**6 h VPA**	**24 h VPA**
Fas (TNF receptor superfamily member 6)	204781_s_at	Fas transcript variant 1-8 (NM_000043, 152871, 152872, 152873, 152874, 152875, 152876, 152877)	1.0 ± 0.05 (p = 0.5)	0.9 ± 0.1 (p = 0.08)	0.6 ± 0.1 (p = 0.006)
TNFRSF1A (tumor necrosis factor receptor superfamily member 1A)	207643_s_at	NM_001065	0.8 ± 0.08 (p = 0.03)	0.8 ± 0.1 (p = 0.06)	0.9 ± 0.2 (p = 0.2)
TNFRSF6B (tumor necrosis factor receptor superfamily member 6b. decoy)	206092_x_at	TNFRSF6B transcript variant 1, 2 NM_016434, 032957	0.7 ± 0.04 (p = 0.05)	0.7 ± 0.2 (p = 0.04)	0.5 ±0.1 (p = 0.07)
TNFRSF10A (tumor necrosis factor receptor superfamily member 10a)	1552648_a_at	NM_003844	0.7 ± 0.06 (p = 0.003)	0.5 ± 0.1 (p = 0.002)	0.4 ± 0.07 (p = 0.001)
TNFRSF10D (tumor necrosis factor receptor superfamily member 10d. decoy)	227345_at	NM_003840	0.8 ± 0.3 (p = 0.1)	0.8 ± 0.001 (p = 0.1)	1.0 ± 0.3 (p = 0.8)

Table 5 (continued). The effect of VPA on the mRNA expression of the death receptors or their ligands in HT-29 cells. VPA-induced changes in the gene expression of death receptors or their ligands were evaluated in HT-29 cells untreated or treated with 2 mM VPA for 3, 6 and 24 h using Affymetrix microarray analysis. The arithmetic mean of the fluorescence signals of the 4 replicates per treatment was calculated for treated and untreated samples. The mean expression level of the VPA-treated samples was normalized against the mean expression level of the untreated samples. The results showed that VPA did not induce mRNA expression of the death receptors or their ligands in HT-29 cells.

Gene Name	**Affymetrix probe set number**	**GenBank accession number of the transcript recognized by probe set**	**2 mM VPA vs. 0 mM VPA**		
			3 h VPA	**6 h VPA**	**24 h VPA**
TNFRSF11A (tumor necrosis factor receptor superfamily member 11a)	207037_at	NM_003839	0.9 ± 0.1 (p = 0.2)	0.8 ± 0.1 (p = 0.1)	0.5 ± 0.1 (p = 0.004)
TNFRSF12A (tumor necrosis factor receptor superfamily member 12A)	218368_s_at	NM_016639	0.5 ± 0.04 (p = 0.0003)	0.5 ± 0.04 (p = 0.00001)	0.5 ± 0.03 (p = 00007)
TNFRSF13B (tumor necrosis factor receptor superfamily member 13B)	207641_at	NM_012452	1.2 ± 0.1 (p = 0.2)	0.9 ± 0.2 (p = 0.6)	0.8 ± 0.3 (p = 0.3)
TNFRSF14 (tumor necrosis factor receptor superfamily member 14)	209354_at	NM_003820	1.0 ± 0.2 (p = 0.8)	0.65 ± 0.2 (p = 0.004)	0.8 ± 0.1 (p = 0.08)
TRAIL (tumor necrosis factor (ligand) superfamily member 10)	202688_at	NM_003810	1.0 ± 0.1 (p = 1.0)	0.9 ± 0.04 (p = 0.2)	0.9 ± 0.1 (p = 0.3)

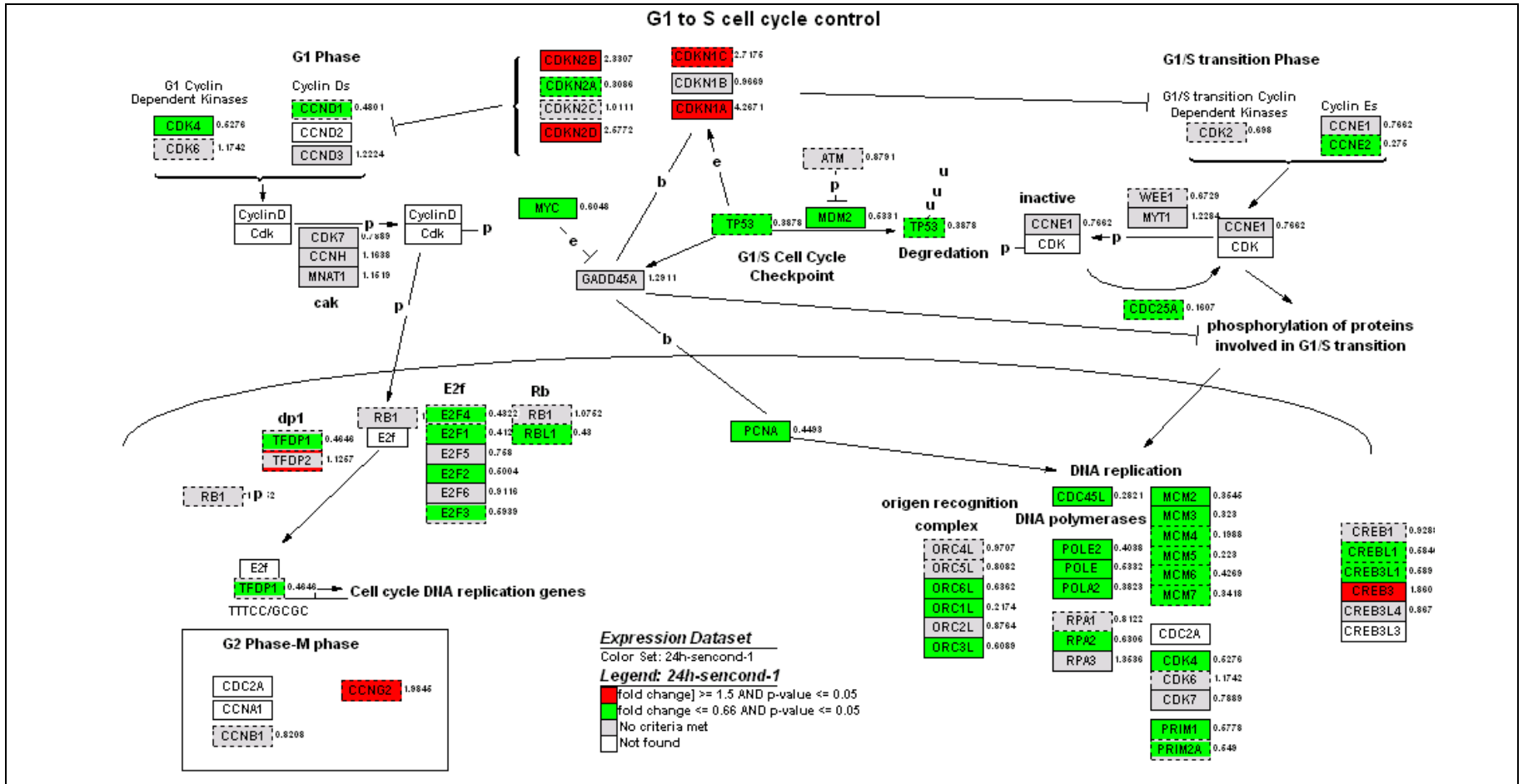

Figure 8. The effect of the VPA treatment for 24 h on the expression of genes associated with cell cycle control at the G1/S checkpoint in HT-29 cells. The effect of VPA on genes involved in the G1/S cell cycle control, according to the KEGG pathways is shown. In red: more than 1.5 fold pregulated genes; in green: more than 1.5 fold dowregulated genes; in gray: unchanged genes; in white: gene expression level lower than basal threshhold. The map was generated using GenMAPP software.

3.1.2 VPA upregulated the proapoptotic Bak mRNA expression and downregulated the antiapoptotic Bcl-XL mRNA expression

To validate the results obtained by the analysis of the microarray data, the effect of VPA treatment on the expression of genes encoding for proapoptotic Bak and antiapoptotic Bcl-XL proteins from the Bcl-2 family was investigated by two-step quantitative real time PCR or RT-PCR, respectively in HT-29 cells.

As shown in **Figure 9** the treatment of cells with 2 mM VPA for 6, 24 and 48 h induced a statistically significant increase in proapoptotic Bak gene expression, compared to untreated cells. The quantitative two-step real-time RT-PCR experiments showed that Bak mRNA expression normalized to the house keeping gene β-actin was already significantly upregulated after VPA treatment for 6 h compared to untreated cells (145.5 ± 16.0 % vs. 100 %, VPA-treated vs. untreated cells, $p = 0.02$). The Bak mRNA expression was increased to 213.7 ± 50.0 % after VPA treatment for 24 h ($p = 0.04$, VPA-treated vs. untreated cells) and to 196.0 ± 12.0 % after VPA treatment for 48 h ($p = 0.005$, VPA-treated vs. untreated cells). Similar results were obtained using Affymetrix microarray analysis, e.g. Bak expression was upregulated to 148.4 ± 7.3 % after 3 h ($p = 0.00007$, VPA-treated vs. untreated cells), 180.5 ± 27.5 % after 6 h ($p = 0.008$, VPA-treated vs. untreated cells) and 161.0 ± 12.2 % after 24 h ($p = 0.0004$, VPA-treated vs. untreated cells) of VPA treatment.

The mRNA expression of the gene encoding for the antiapoptotic protein Bcl-XL was downregulated by VPA treatment, as shown by the RT-PCR experiments performed with primers specific for the Bcl-XL isoform in HT-29 cells treated with 2 mM VPA for 3, 6 and 24 h (**Figure 10**).

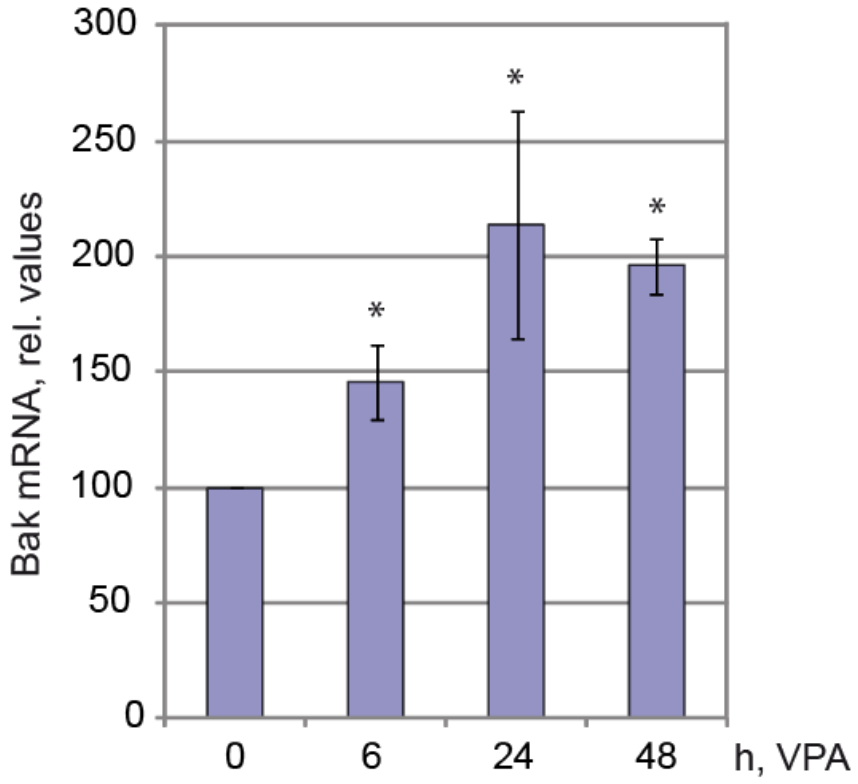

Figure 9. **VPA upregulated Bak expression at the mRNA level in HT-29 cells.**
HT-29 cells were treated with 2 mM VPA for the indicated time periods prior to extracting total RNA. Expression of Bak was determined by quantitative two-step real-time RT-PCR. Relative differences in Bak gene expression between VPA-treated and untreated samples were normalized to the expression of the house keeping gene β-actin. Data from three independent experiments was used to calculate the mean values and the S.E.M. (standard error of the mean); *****, $p \leq 0.04$ VPA-treated vs. untreated cells.

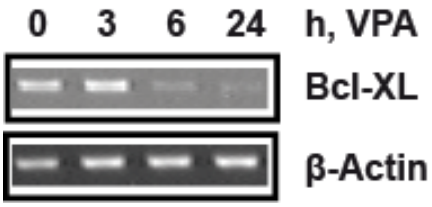

Figure 10. VPA downregulated Bcl-XL expression at the mRNA level in HT-29 cells.
HT-29 cells were treated with 2 mM VPA for the indicated time periods prior to extracting total RNA. Expression of Bcl-XL was determined by RT-PCR using primers specific for the Bcl-XL isoform. Data is representative of two independent experiments.

3.1.3 VPA induced characteristic features of apoptosis

The analysis of the microarray data (described in section 3.1.1) showed that VPA changed the expression of several proapoptotic and antiapoptotic genes in HT-29 cells. To investigate whether VPA induces apoptosis in HT-29 cells, the generation of mono- and oligonucleosomes upon treatment with different concentrations of VPA and various incubation times was tested in HT-29 cells. As shown in **Figure 11,** cytoplasmic histone-associated-DNA-fragments were induced by VPA in a dose and time dependent manner at VPA concentrations required for induction of apoptosis in other types of cells. The DNA fragmentation induced by treatment of cells with 2 mM VPA for 48 h was inhibited in the presence of a pan-caspase inhibitor. This is a characteristic feature of apoptotic cell death (**Figure 11**).

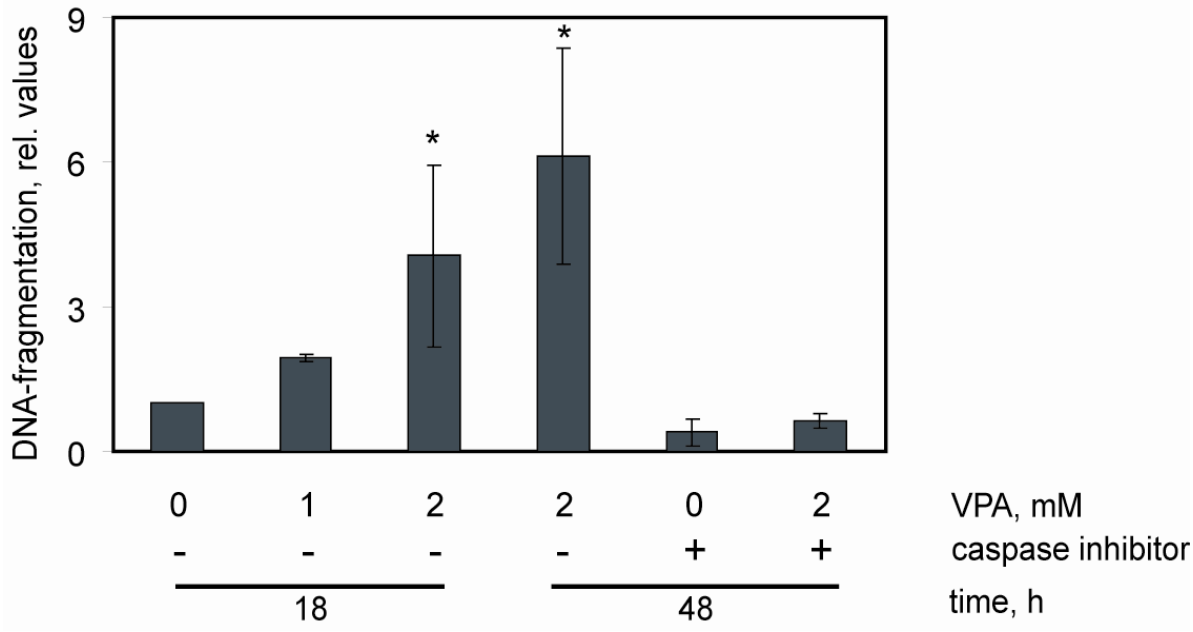

Figure 11. VPA induced caspase-dependent apoptosis in HT-29 cells.
Apoptosis was determined in adherent HT-29 cells after treatment with VPA alone or in combination with a pan-caspase inhibitor or the empty vehicle, respectively, at the indicated time points by scoring cytoplasmic histone-associated-DNA-fragments. Values of control cells were set to 1, values of the treated cells were set in relation to values of control cells. Data represents mean values ± SD from two independent experiments performed in triplicates. *****, $p < 0.05$ VPA-treated vs. untreated cells.

Further evidence that VPA induced apoptosis in HT-29 cells was obtained by double staining with Annexin-V and propidium iodide (PI). Annexin-V binds to cell surface-exposed phosphatidylserine. Staining with PI and Annexin-V allows discrimination of living, early apoptotic and late apoptotic/necrotic cells. As shown in **Figure 12**, VPA treatment increased the fraction of early apoptotic cells (Annexin V^+/PI^-) from 7.77 % in untreated cells to 18.04 % in VPA-treated cells. The fraction of cells in late apoptosis / necrosis stages (Annexin V^+/PI^+) was elevated from 13.41 % to 19.64 %. Altogether these results showed that VPA induced caspase-dependent apoptosis in HT-29 cells.

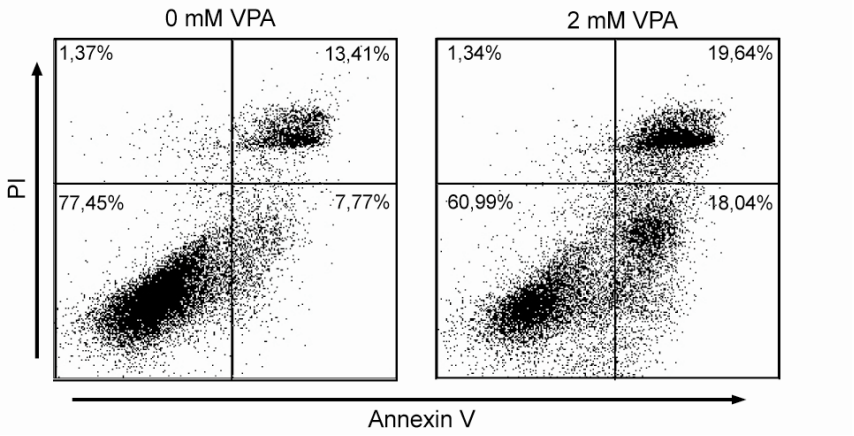

Figure 12. VPA induced apoptosis in HT-29 cells.
Apoptosis was determined in HT-29 cells after treatment with 2 mM VPA by double staining cells with APC-conjugated Annexin V and PI. The percentage of living, early apoptotic and late apoptotic/necrotic cells is shown in each quadrant. The scatter plots are representative of two independent experiments.

3.1.4 VPA regulated the expression of pro- and antiapoptotic Bcl-2 family members at the protein level

It was considered unlikely that the VPA induction of apoptosis was mediated by the death receptor signaling pathway, since the analysis of the microarray data (described in section 3.1.1) showed that the expression of death receptors or their ligands was not upregulated by VPA **(Table 5)**. Therefore, the effect of VPA on the expression of proapoptotic and antiapoptotic members of the Bcl-2 family at the protein level was investigated. The expression of: i) Bak and Bax as BH1-BH3 proapoptotic proteins; ii) Bad, Bid, Bim and Bik as BH3 domain-only proapoptotic proteins and iii) Bcl-XL and

Bcl-2 as antiapoptotic BH1-BH4 proteins was evaluated in total cell and mitochondrial extracts.

HT-29 cells were treated with 2 mM VPA for 6, 24 and 48 h, then whole cell lysates (left panel) and protein lysates from mitochondrial fractions (right panel) were subjected to Western Blot analysis. Actin or Tim23 were used as loading controls in whole cell or mitochondrial lysates, respectively (**Figure 13A**). Signal intensities were quantified and normalized expression levels in extracts from treated cells compared to untreated cells are shown in **Figure 13B**. It was considered that the changes in protein expression observed after 6 h and 24 h of VPA exposure are the most informative concerning potential mechanisms of apoptosis induction. The treatment with VPA induced prominent apoptosis promoting changes in the protein levels of Bak, Bid, Bim and Bcl-XL at the relevant sub-cellular localization, e.g. the mitochondria.

The expression of the proapoptotic protein Bak was upregulated more than 4-fold, particularly in mitochondrial extracts. A moderate and relatively late occurring downregulation of Bax was also observed in mitochondrial extracts. Among the regulatory BH3 domain-only proteins, VPA treatment for 24 h predominantly induced the expression of the active mitochondrial forms tBid and Bim-S. An upregulation of Bim-EL isoform was also observed in the mitochondrial lysates from VPA-treated cells after 24 h of drug exposure. The effects on Bid and Bim were specific responses since other BH3 domain-only proteins, e.g. Bad and Bik were not changed substantially in mitochondrial extracts (**Figure 13**).

VPA treatment clearly downregulated the expression of the antiapoptotic protein Bcl-XL in a time-dependent manner in whole cell lysates and mitochondrial extracts. Expression of Bcl-2, the other multidomain antiapoptotic protein was not changed after 24 h of VPA treatment and was found induced only after 48 h of treatment and only in whole cell lysates (**Figure 13**).

The expression of p53 targets, the proapoptotic proteins Puma and Noxa was also investigated in HT-29 cells treated for 6, 24 and 48 h with 2 mM VPA. The Western Blot analysis showed that expression of Puma and Noxa was downregulated after VPA treatment (**Figure 14**). This data suggested that VPA-induced cell death was not mediated by the p53 pathway in HT-29 cells.

The Western Blot analysis of the effect of VPA on the expression of the Bcl-2 family showed that VPA treatment had severe impact on the balance between pro- and antiapoptotic Bcl-2 protein family members. The proapoptotic response induced by VPA through upregulation of Bak protein levels was sustained by the VPA-induced changes in the protein levels of Bid, Bim and Bcl-XL.

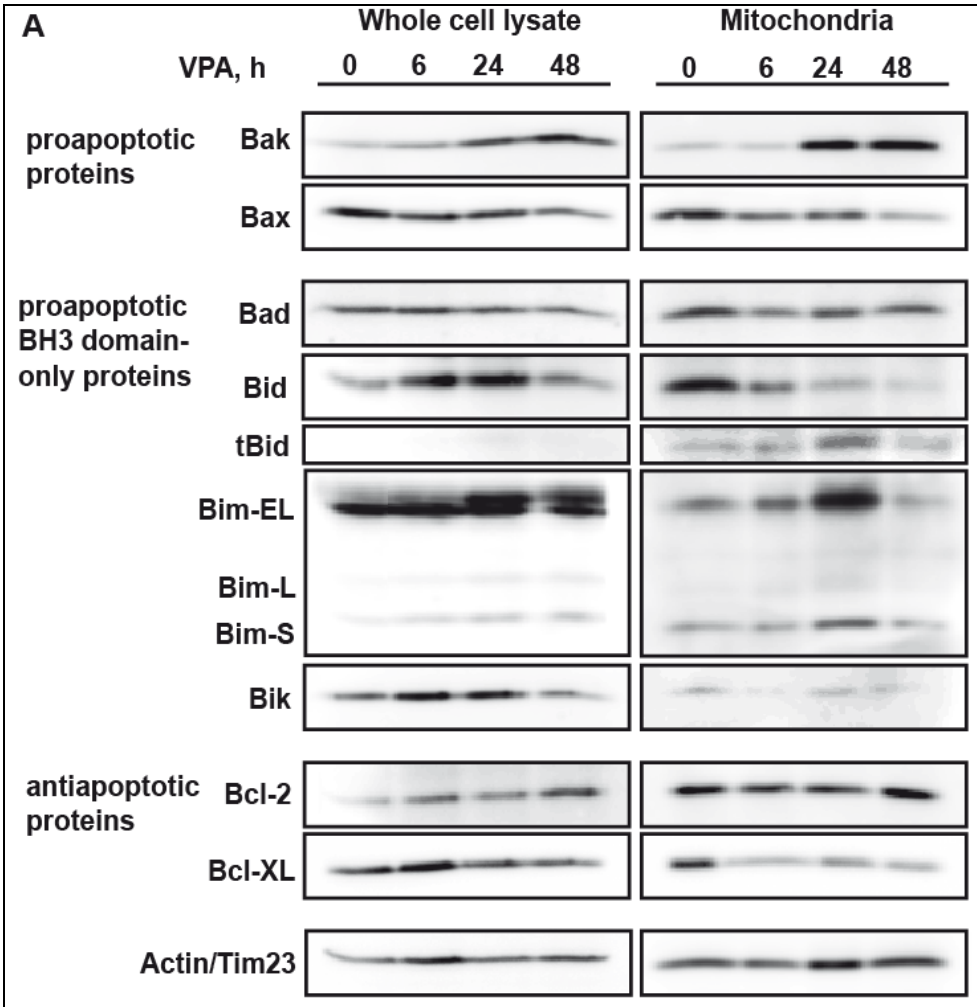

B

	Whole Cell Lysate				Mitochondria			
VPA, h	0	6	24	48	0	6	24	48
Bak	100	81	220	319	100	101	443	482
Bax	100	47	62	37	100	82	60	30
Bad	100	57	61	47	100	76	66	63
Bid	100	141	214	93	100	53	23	12
tBid					100	114	215	84
Bim-EL	100	64	93	62	100	134	207	68
Bim-S	100	94	153	136	100	104	185	58
Bik	100	94	115	47	100	50	84	72
Bcl-2	100	113	126	191	100	117	81	89
Bcl-XL	100	77	64	49	100	79	54	40

Figure 13. Expression of proapoptotic and antiapoptotic Bcl-2 family members in HT-29 cells. **A**) HT-29 cells were treated with 2 mM VPA for the indicated time periods before harvesting. Whole cell lysates (left panel) and protein lysates from mitochondrial fractions (right panel) were subjected to Western Blot analysis. Data is representative for three individual experiments. **B)** Densitometric analysis of Western Blot images from **Figure 13A**. Signal intensities were quantified using Image Master Software. The relative expression ratio of proteins was calculated as: relative expression ratio of protein = (protein signal density / loading control signal density) X 100.

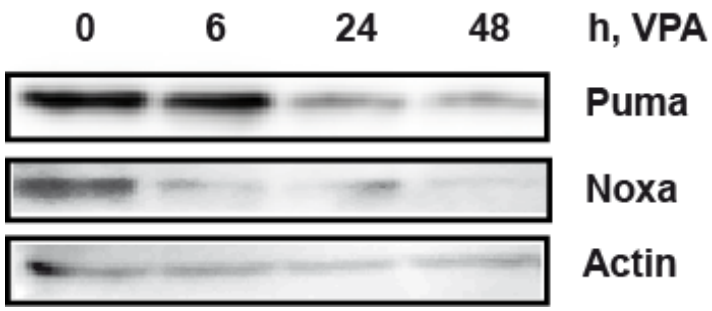

Figure 14. Expression of p53 target genes Puma and Noxa was not upregulated at the protein level after VPA treatment. HT-29 cells were treated with 2 mM VPA for the indicated time periods before harvesting. The expression of p53 target genes Puma and Noxa was evaluated in whole cell lysates by Western Blot analysis. Actin was used as loading control.

3.1.5 HDAC2-deficiency led to an increase in Bak and Bim expression, while Bcl-XL expression was not HDAC2 dependent

It has been previously shown that VPA, in addition to preferentially inhibiting the catalytic activity of class I HDACs, induces proteasomal degradation of HDAC2 isoform [131]. In the present study it was investigated whether the expression of VPA target genes Bak, Bim and Bcl-XL specifically depends on the expression of the HDAC2 isoform.

3.1.5.1 Expression of proapoptotic protein Bak is HDAC2-dependent

HDAC2 expression was knocked down by transfection of HT-29 cells with a siRNA sequence specifically directed against HDAC2. A siRNA sequence directed against luciferase was used as a transfection control. Western Blot analysis (**Figure 15**) and immunofluorescence microscopy (**Figure 16**) showed that HDAC2 downregulation resulted in an increase in Bak expression. HDAC2 protein levels were markedly reduced after 72 h of treatment with anti-HDAC2 siRNA, but not after treatment with control siRNA (**Figure 15**). The expression of Bak protein was upregulated after anti-HDAC2 siRNA transfection, compared to non-transfected cells or cells transfected with the control siRNA (**Figure 15**).

Figure 15. Expression of Bak was HDAC2-dependent. HT-29 cells were transfected with siRNA specific against HDAC2 (siRNA HDAC2) or with control siRNA (siRNA specific against luciferase). Subsequently, expression of Bak protein was determined in whole cell lysates by Western Blot analysis. Actin was used as loading control. Data is representative of three individual experiments.

Multicolor immunofluorescence images of identical microscopic fields stained for Bak and HDAC2 (**Figure 16**) showed upregulation of Bak expression in those cells that had lost HDAC2 protein as a result of siRNA transfection (e.g. cells in upper right corner of siRNA HDAC2 fields). Cells that still expressed HDAC2 after siRNA transfection (arrows in **Figure 16**) showed low expression levels of Bak protein compared to cells with efficient knockdown of HDAC2.

The specific role of HDAC2 for the expression of Bak was also confirmed in murine embryonic fibroblasts (MEFs) derived from either wildtype mice (HDAC2 +/+) or HDAC2-deficient mice (HDAC2 -/-). Western Blot analysis (**Figure 17**) indicated that HDAC2 deficient MEFs expressed increased levels of Bak protein compared to wildtype MEFs.

These results showed that HDAC2-deficiency led to an increase in Bak expression and further indicated that VPA-induced cell death was mediated by Bak upregulation.

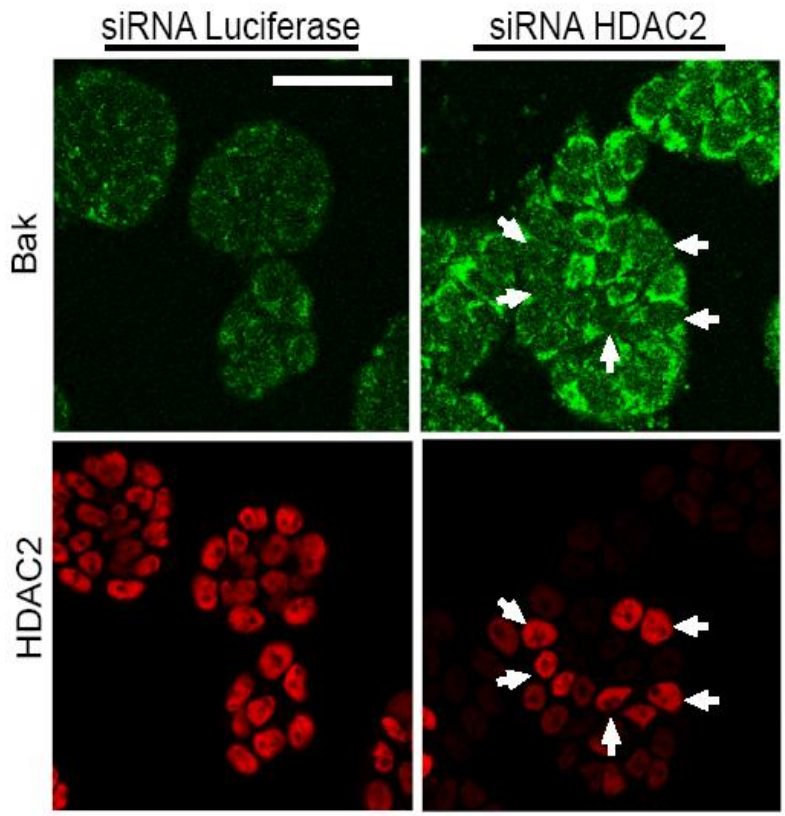

Figure 16. **HDAC2-deficiency led to an increase in Bak expression in HT-29 cells.**
HT-29 cells were transfected with siRNA specific against HDAC2 (siRNA HDAC2) or with control siRNA (siRNA specific against Luciferase) on chamber slides. After 72 h cells were probed with anti-Bak and anti-HDAC2 antibodies. Staining was visualised using AlexaFluor 594 or AlexaFluor 488-labeled secondary antibodies using a confocal laser scanning microscope. Representative single stains of the same fields for Bak (green) and HDAC2 (red) from three individual experiments are shown. Scale bar indicates 50 µm.

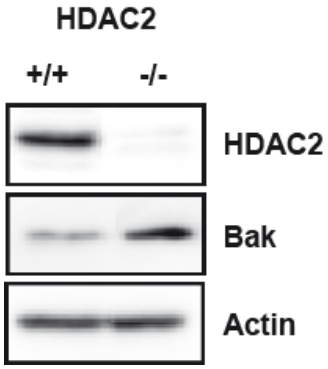

Figure 17. Expression of Bak was HDAC2-dependent in MEFs

Mouse Embryonic Fibroblasts (MEFs) lacking HDAC2 showed increased Bak expression. Bak and HDAC2 expression were determined in whole cell lysates of MEFs derived from either wildtype mice or HDAC2-deficient mice by Western Blot analysis. Actin was used as loading control. Data is representative of two individual experiments.

3.1.5.2 Expression of proapoptotic protein Bim, but not of antiapoptotic protein Bcl-XL was HDAC2-dependent

Several isoforms of proapoptotic protein Bim are generated by alternative splicing. The three major isoforms Bim-EL, Bim-L and Bim-S are reported to be involved in apoptosis induction [45, 46]. The analysis of the microarray data (described in section 3.1.1) from HT-29 cells treated with 2 mM VPA for 3, 6 and 24 h showed that VPA treatment significantly increased the Bim mRNA level of expression. The mRNA expression of Bim was upregulated by VPA already after 3 h of treatment (128.0 ± 9.5 % vs. 100 %, $p = 0.04$, VPA-treated vs. untreated cells). The Bim mRNA expression was increased to 140.0 ± 7.2 % after VPA treatment for 6 h ($p = 0.02$, VPA-treated vs. untreated cells) and to 160.7 ± 20.8 % after VPA treatment for 24 h ($p = 0.04$, VPA-treated vs. untreated cells) (**Figure 18**).

To investigate if the expression of Bim isoforms is regulated by HDAC2, the HT-29 cells were transfected with a siRNA sequence specifically directed against HDAC2 or with a siRNA sequence directed against luciferase as a transfection control. Western Blot analysis (**Figure 19**) showed that HDAC2-downregulation led to a marked increase of Bim-L expression and to a moderate increase of Bim-S expression compared to cells transfected with the control siRNA. HDAC2 protein levels were markedly reduced after 72 h of treatment with anti-HDAC2 siRNA, but not after treatment with the control siRNA. Expression levels of Bim-L and Bim-S isoforms were upregulated in cells transfected with anti-HDAC2 siRNA compared to cells transfected with the control siRNA.

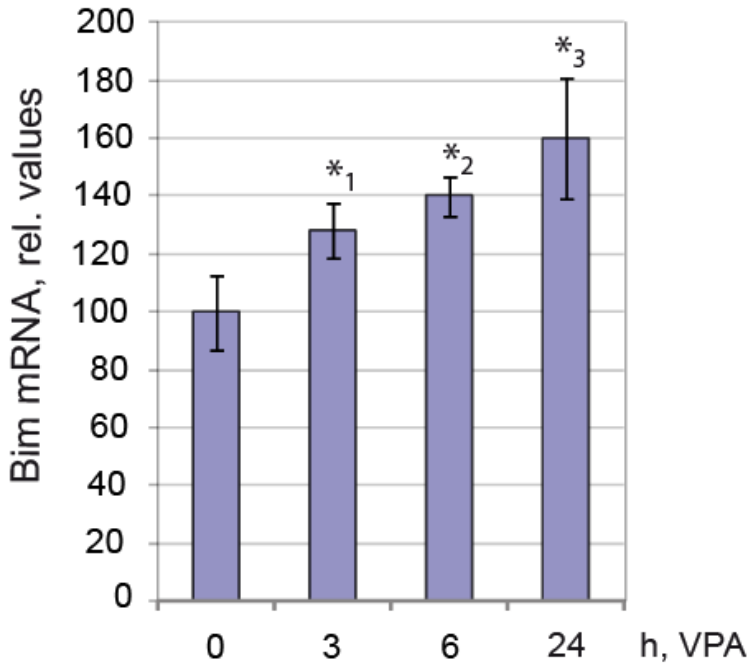

Figure 18. VPA upregulated Bim expression at the mRNA level in HT-29 cells.

VPA-induced changes in the Bim gene expression were evaluated in HT-29 cells untreated or treated with 2 mM VPA for 3, 6 and 24 h using Affymetrix microarray analysis (described earlier in paragraph 3.1.1). Relative differences in Bim mRNA expression between the VPA-treated and untreated samples are shown. Data from four independent replicates was used to calculate the mean values and SD. ***1**, p = 0.04 VPA-treated (3 h) vs. untreated cells; ***2**, p = 0.02 VPA-treated (6 h) vs. untreated cells; ***3**, p = 0.04 VPA-treated (24 h) vs. untreated cells.

Even if VPA downregulated the expression of Bcl-XL at the mRNA level (**Figure 10**) and at the protein level (**Figure 13**), the expression of the antiapoptotic protein Bcl-XL was not changed in HT-29 cells transfected with siRNA against the HDAC2 isoform, compared to cells transfected with the control siRNA (**Figure 19**).

These results showed that expression of Bim-L and Bim-S, but not of Bcl-XL was HDAC2-dependent.

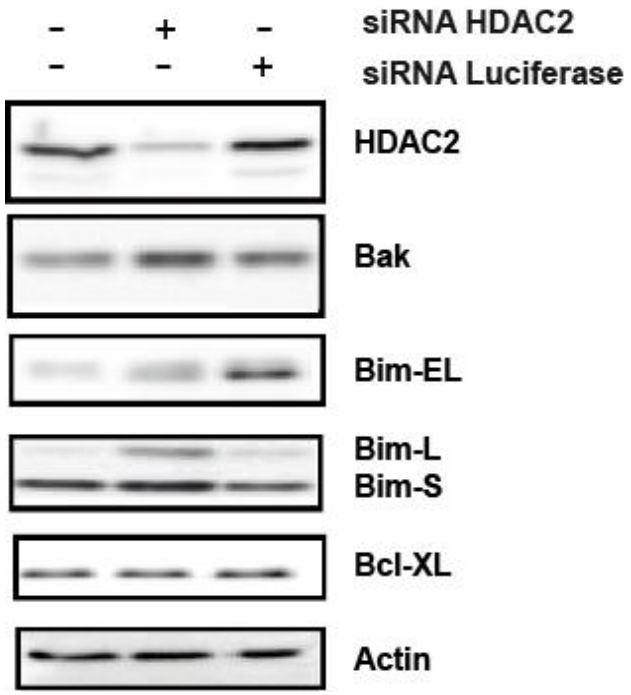

Figure 19. Expression of Bak and Bim, but not of Bcl-XL was HDAC2-dependent in HT-29 cells. HT-29 cells were transfected with siRNA specific against HDAC2 (siRNA HDAC2) or with control siRNA (siRNA specific against Luciferase). Subsequently, expression levels of Bak, Bim and Bcl-XL proteins were determined in whole cell lysates from the transfected cells by Western Blot analysis. Actin was used as loading control. Data is representative of two individual experiments.

In order to verify the results from the siRNA-mediated HDAC2 knockdown experiments, the expression of Bim and Bcl-XL proteins in MEFs that expressed either wildtype (HDAC2 +/+) or a catalytically inactive mutant form of HDAC2 (HDAC2 -/-) was investigated. The Western Blot analysis (**Figure 20)** showed that MEFs deficient in HDAC2 did not show any significant detectable changes in Bcl-XL expression compared to wildtype MEFs. Thus, the expression of antiapoptotic Bcl-XL protein is not dependent on the presence of the HDAC2 isoform. In the MEFs only the expression of Bim-EL could be detected, but not the expression of the other two isoforms Bim-L and Bim-S. The Western Blot analysis showed that Bim-EL was differentially expressed in wildtype MEFs and HDAC2-deficient MEFs.

In conclusion, these results showed that HDAC2 isoform regulated the expression of proapoptotic proteins Bak and Bim, while the expression of the antiapoptotic protein Bcl-XL was not HDAC2-dependent.

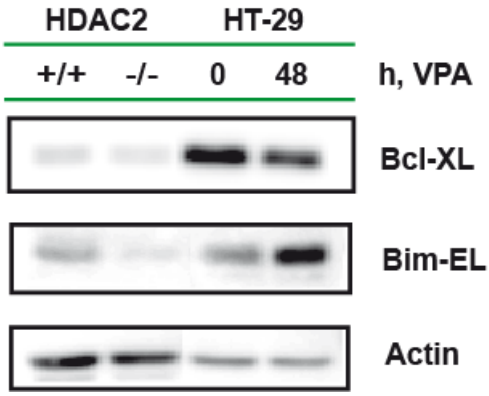

Figure 20. Expression of Bcl-XL and Bim in MEFs cells

Mouse Embryonic Fibroblasts (MEFs) lacking HDAC2 showed no change in Bcl-XL expression compared to wildtype MEFs. BimEL was differentially expressed in HDAC2-deficient MEFs compared to wildtype MEFs. Whole cell lysates of MEFs derived from either wildtype mice (+/+) or HDAC2-deficient mice (-/-) were subjected to Western Blot analysis. Whole cell lysates from HT-29 cells treated with 2 mM VPA for the indicated time periods were subjected to Western Blot analysis. Actin was used as loading control. Data is representative of two individual experiments.

3.1.6 Bak overexpression was sufficient to induce apoptosis

To test whether elevated Bak levels alone were sufficient to induce apoptosis in HT-29 cells, wildtype or mutant Bak were ectopically expressed by transient transfection of appropriate vectors provided by Chittenden [176]. Cells were cotransfected with pEGFP to allow identification of efficiently transfected cells. Ectopic expression of wildtype Bak or mutant Bak that lacks the C-terminal domain (BakΔC) induced apoptosis as indicated by Annexin-V staining of PI excluding cells (**Figure 21**). The induced rates of apoptosis were similar to those induced by VPA treatment (**Figure 12**). Transfection of mutant Bak that lacks the BH3-domain (BakΔGD) did not induce apoptosis, as expected from previous data [176]. The empty expression vector did not induce apoptosis (**Figure 21**).

These findings showed that overexpression of Bak alone was sufficient to induce apoptosis in HT-29 cells. This indicated that VPA-induced Bak upregulation may be sufficient to explain the observed VPA effects on apoptosis.

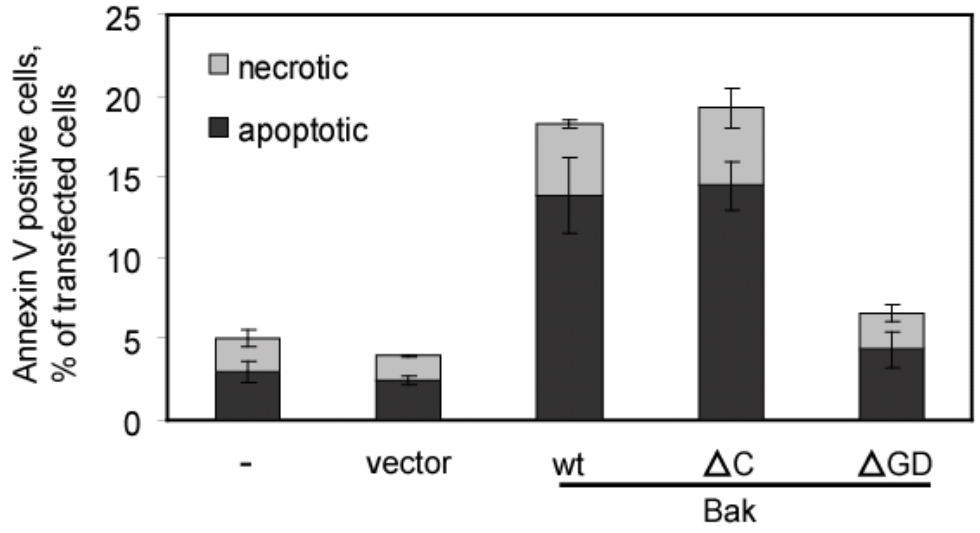

Figure 21. Bak overexpression alone was sufficient to induce apoptosis in HT-29 cells
HT-29 cells were cotransfected with pEGFP and the empty expression vector or expression vectors containing either wildtype Bak or mutant Bak (BakΔGD, BakΔC), respectively. After 72 h cells were double stained with APC-conjugated Annexin V and PI. The apoptosis was analyzed by flow cytometry. In black: Anexin V^+/PI^- cells; in gray: Anexin V^+/PI^+. Results are representative for two independent experiments performed in triplicates. Error bars indicate mean values ± SD.

3.1.7 Bak knockdown substantially protected HT-29 cells from VPA-induced cell death

3.1.7.1 Bak knockdown led to an accumulation of Bak-depleted cells after treatment with VPA

After having established that elevated Bak expression was sufficient to induce apoptosis of HT-29 cells, it was tested whether Bak is also essential for VPA-induced apoptosis. It was determined to which extent the knockdown of Bak by siRNA transfection could protect cells from VPA-induced apoptosis. Efficiently transfected cells were identified by reduced immunostaining of Bak using flow cytometry (FACS) and the relative abundance of these cells was compared to that of not efficiently transfected cells. FACS analyses (**Figure 22**, upper panel) performed 96 h after siRNA transfection indicated that transfection with siRNA specific against Bak, but not with control siRNA, resulted in the appearance of a second cell population, in which Bak expression was reduced compared to not efficiently transfected cells or cells transfected with a control siRNA. VPA treatment for 72 h starting 24 h after transfection (**Figure 22**, lower panel) increased the levels of Bak in not efficiently

transfected cells and in control transfected cells. VPA increased Bak expression only marginally in cells efficiently transfected with Bak siRNA. After 72 h of treatment with VPA the percentage of Bak-depleted cells (area of first peak in **Figure 22**, lower panel) was higher compared to untreated cells (area of first peak in **Figure 22,** upper panel) indicating that Bak depleted cells had an advantage to survive VPA exposure.

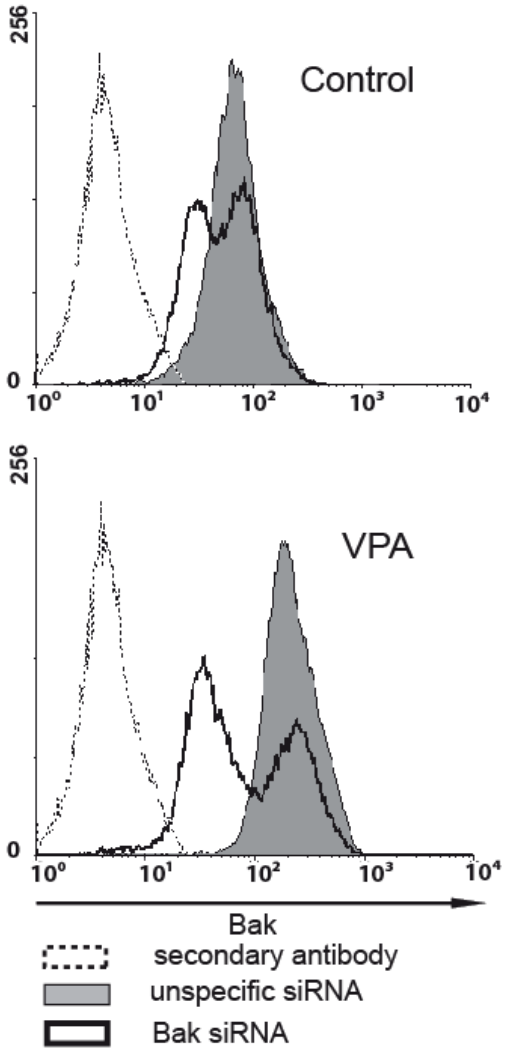

Figure 22. Bak knockdown led to an accumulation of Bak-depleted cells after treatment with VPA in HT-29 cells. HT-29 cells were transfected with anti-Bak siRNA or control siRNA. Transfected cells were untreated or treated with 2 mM VPA for 72 h and Bak expression was assessed by flow cytometry. In black: Bak-staining in cells transfected with siRNA specific against Bak; in gray, solid filled: Bak-staining in control transfected cells. Histograms are representative of 3 independent experiments.

3.1.7.2 Bak-depleted cells showed almost the same growth rate when treated with VPA compared to untreated cells.

The increase in number of Bak-positive and Bak-negative cells in the presence or absence of VPA could be calculated by determining the percentage of efficiently Bak-depleted cells at the onset of VPA treatment 24 h after transfection and counting absolute cell numbers at 24 h and 96 h in the absence or presence of VPA (**Figure 23A** and **B**). Accumulation of Bak-positive (wildtype) cells was reduced to 40.0 ± 16.0 % ($p = 0.02$) in the presence of VPA compared to Bak-positive cells not treated with VPA (**Figure 23B**). In contrast, accumulation of Bak-depleted cells was only marginally decreased to 75.6 ± 12.0 % ($p = 0.07$) in the presence of VPA compared to Bak-depleted cells not treated with VPA. The accumulation of cells as a result of cell division and apoptosis was calculated into net doubling times of individual cultures depending on Bak expression status and presence of VPA (**Figure 23B**). The most prominent finding was the increase of the doubling time from 25.6 ± 3.6 h to 50.7 ± 6.5 h ($p = 0.05$) in Bak wildtype cells upon treatment with VPA. The effect of VPA on Bak-depleted cells was moderate and not significant with an increase in net doubling time from 25.9 ± 5.4 h to only 31.7 ± 10.7 h ($p = 0.2$). The difference of the doubling time in the presence of VPA between Bak-depleted (31.7 ± 10.7 h) and Bak-positive (50.7 ± 6.5 h) cells was significant ($p = 0.02$). This suggested that Bak levels had an impact on survival of untreated HT-29 cells.

In summary, these results showed that knocking down Bak expression substantially protected HT-29 cells from VPA-induced cell death and indicated that VPA-induced apoptosis depended at least to a major part on induced expression of Bak.

A

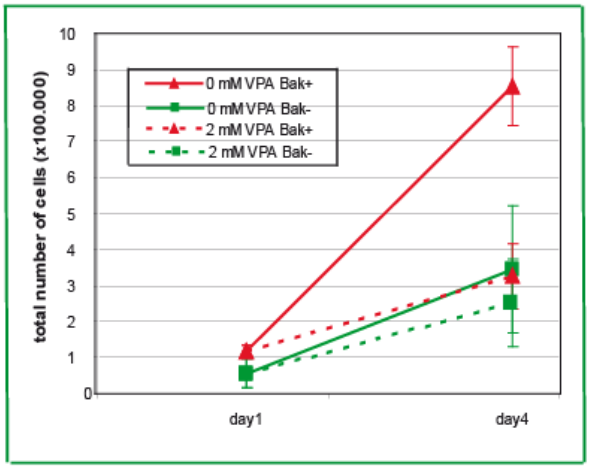

B

	Bak status	VPA treatment		p-value [2]
		0 mM	2 mM	
Cell numbers at day 1 ($x10^4$) [1]	wt	11.8 ± 1.8	11.8 ± 1.8	
	depleted	5.6 ± 3.9	5.6 ± 3.9	
Cell numbers at day 4 ($x10^4$) [1]	wt	85.0 ± 11.0	32.6 ± 9.0	0.04
	depleted	34.3 ± 17.6	25.0 ± 12.2	0.16
Cell numbers at day 4 relative to 0 mM VPA	wt	100 %	40.0 ± 16.0 % [3]	0.02
	depleted	100 %	75.6 ± 12.0 % [3]	0.07
Doubling time of cell numbers (h) [4]	wt	25.6 ± 3.6	50.7 ± 6.5 [3]	0.05
	depleted	25.9 ± 5.4	31.7 ± 10.7 [3]	0.22

Figure 23. Bak-depleted HT-29 cells showed almost the same growth rate when treated with VPA compared to untreated cells. **A**) Bak-depleted cells showed almost the same growth rate when treated with VPA compared to untreated cells. To obtain growth curves total amounts of Bak-positive (wt) and Bak-depleted cells were assessed at day 1 and day 4 by determining percentages of Bak-positive (wt) and Bak-depleted cells per sample using FACS and set in relation to total cell amounts per sample also determined at day 1 and day 4. The graph shows the mean of absolute cell numbers ± SD from three independent experiments. **B**) Total numbers of Bak-positive (wt) or Bak-depleted cells and doubling times were calculated from total cell counts and percentages of Bak-positive vs. Bak-depleted cells at day 1 and day 4. [1] mean of absolute cell numbers ± SD from three independent experiments; [2] p-value of VPA-treated vs. untreated cells; [3] difference between values of VPA-treated Bak-positive (wt) and VPA-treated Bak-depleted cells is significant ($p = 0.02$); [4] values are calculated from the increase of the cell numbers between day 1 and day 4.

3.1.8 VPA treatment downregulated the expression of Ets2 transcription factor

3.1.8.1 VPA downregulated Ets2 expression at the mRNA level in HT-29 cells

It has been found so far that the treatment of HT-29 cells with VPA induced multiple alterations in the expression of the Bcl-2 family members, with apoptosis promoting changes in the expression of the proapoptotic protein Bak and the antiapoptotic protein Bcl-XL. The expression of the proapoptotic protein Bak specifically depended on the HDAC2 isoform (**Figure 15 and 16**). VPA treatment downregulated expression of Bcl-XL at the mRNA (**Figure 10**) and at the protein level (**Figure 13**), but the expression of Bcl-XL was not HDAC2-dependent (**Figure 19**). Previous studies have shown that the transcription factor Ets2 regulated Bcl-XL expression in macrophages, osteoclasts, mesothelioma cells and malignant B-cells [180-183]. To further evaluate the underlying mechanism by which VPA downregulates expression of Bcl-XL at the mRNA level in HT-29 cells, the effect of VPA on expression of the Ets2 transcription factor was investigated.

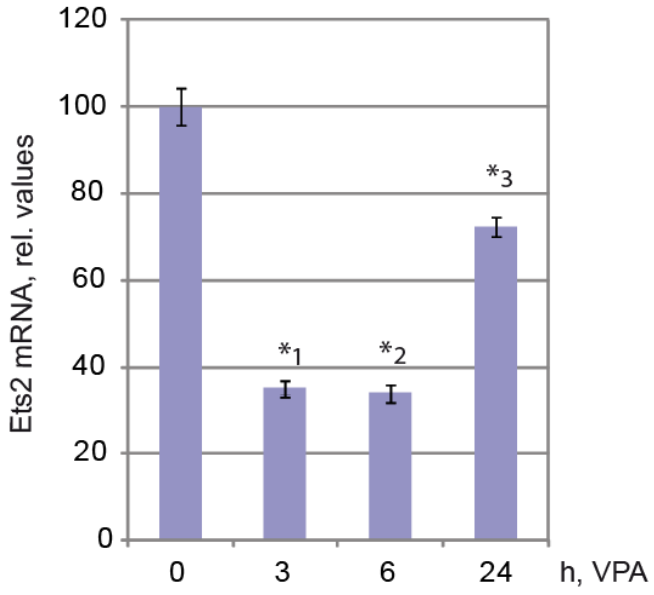

Figure 24. **VPA downregulated Ets2 expression at the mRNA level in HT-29 cells.** VPA-induced changes in the Ets2 gene expression were evaluated in HT-29 cells untreated or treated with 2 mM VPA for 3, 6 and 24 h by Affymetrix microarray analysis (described earlier in paragraph 3.1.1). Relative differences in Ets2 gene expression between the VPA-treated and untreated samples are shown. Data from four independent replicates was used to calculate the mean values and SD. ***1**, p = 0.00006 VPA-treated (3 h) vs. untreated cells; ***2**, p = 0.0001 VPA-treated (6 h) vs. untreated cells; ***3**, p = 0.0004 VPA-treated (24 h) vs. untreated cells.

The analysis of the microarray data (described in paragraph 3.1.1) showed that the treatment of HT-29 cells with 2 mM VPA for 3, 6 and 24 h resulted in downregulation of the Ets2 expression at the mRNA level. The treatment with VPA significantly decreased the mRNA level of Ets2 to 35.4 ± 1.6 % already after 3 h of exposure compared to untreated cells ($p = 0.00006$, VPA-treated vs. untreated cells). The expression of Ets2 at the mRNA level was downregulated to 34.0 ± 2.1 % after 6 h ($p = 0.0001$, VPA-treated vs. untreated cells) and to 73.0 ± 2.2 % after 24 h of VPA treatment ($p = 0.0004$, VPA-treated vs. untreated cells) compared to untreated cells (**Figure 24**).

3.1.8.2 VPA downregulated the expression of Ets2 at the protein level in HT-29 cells

The expression of the transcription factor Ets2 at the protein level was investigated by Western Blot analysis in HT-29 cells treated for 16, 24 and 48 h with 2 mM VPA. The Western Blot analysis (**Figure 25)** showed that VPA markedly downregulated the expression of Ets2 at the protein level after 16 h (41.1 % VPA-treated vs. 100 % untreated cels), 24 h (27.8 % VPA-treated vs. 100 % untreated cells) and 48 h (37.8 % VPA-treated vs. 100 % untreated cells) of VPA treatment compared to untreated cells. These results showed that despite the moderate downregulation of Ets2 expression at the mRNA level upon the VPA treatment for 24 h (**Figure 24**), the expression level of the Ets2 protein was found to be significantly downregulated after VPA treatment for 24 h.

In the same set of samples the expression of Bcl-XL was evaluated. It has been found that the downregulation of the Bcl-XL expression correlated with the reduced expression of the Ets2 transcription factor. For example, upon VPA treatment for 24 h, the expression of Ets2 transcription factor was downregulated to 27.8 % and the expression of Bcl-XL was reduced to 30.4 % (**Figure 25**). The expression of Ets2 protein after 16 h of VPA treatment also correlated with Bcl-XL expression. The expression of Bcl-XL was downregulated to 38.5 % after 16 h treatment with VPA and the expression of Ets2 transcription factor was reduced to 41.1 % (**Figure 25**).

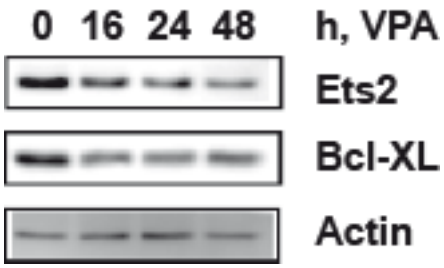

Figure 25. VPA downregulated the expression of Ets2 transcription factor at the protein level in HT-29 cells. HT-29 cells were treated with 2 mM VPA for the indicated time periods before harvesting. The expression of Ets2 and Bcl-XL was evaluated in whole cell lysates by Western Blot analysis. Actin was used as loading control.

3.1.8.3 Transcriptionally active form of Ets2 was downregulated by VPA in HT-29 cells

The observation that the VPA treatment downregulated the expression of both Bcl-XL and Ets2 led to the hypothesis that Bcl-XL expression might be regulated by Ets2 in HT-29 cells. This would explain the reduced Bcl-XL expression levels upon the VPA treatment. Previous studies have shown that the transcriptional activation function of Ets2 is enhanced by phosphorylation at threonine 72 [184-186]. The effect of the VPA treatment on the amounts of the total Ets2 and the phosphorylated active form of Ets2 (pT72-Ets2) was investigated by Western Blot analysis. Cytoplasmic and nuclear lysates were extracted from HT-29 cells treated for 16, 24 and 48 h with VPA. The lysates were probed with antibodies that recognized either total Ets2 indifferently of phosphorylation status or recognized only the pT72-Ets2 form. An anti-HDAC2 antibody was used to verify if the cytoplasmic extracts were contaminated with nuclei. An anti-GSK-3-beta antibody was used as a loading control in both cytoplasmic and nuclear lysates.

The Western Blot analysis (**Figure 26)** showed that the cytosolic extracts were not contaminated with nuclei, as HDAC2 could only be detected in the nuclear lysates, but not in the cytoplasmic lysates. The treatment with VPA decreased the expression of total Ets2 protein in cytoplasmic extracts (**Figure 26**). The amount of the pT72-Ets2 was also decreased in nuclear extracts after the VPA treatment. The apparent ratio between the total Ets2 and the pT72-Ets2 was not changed upon the VPA treatment. The Western Blot analysis (**Figure 26)** suggested that the lower amount of the transcriptionally active form of Ets2 led to downregulation of Bcl-XL expression upon the VPA treatment.

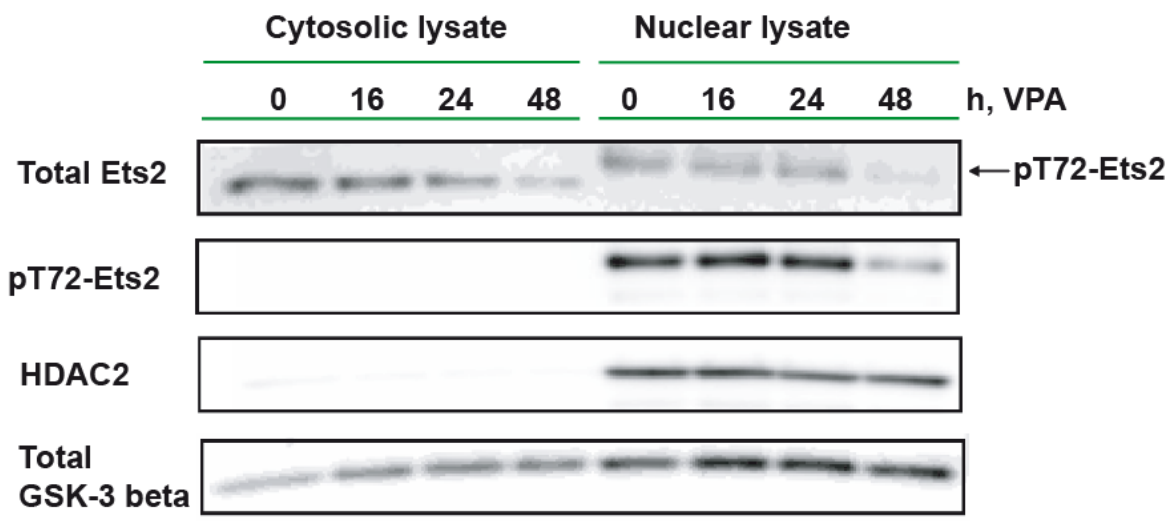

Figure 26. **Transcriptionally active form of Ets2 (pT72-Ets2) was downregulated by VPA in HT-29 cells.** HT-29 cells were treated with 2 mM VPA for the indicated time periods before harvesting. Cytoplasmic lysates and protein lysates from nuclei fractions were subjected to Western Blot analysis. Data is representative of two individual experiments.

3.1.9 Ets2 knockdown led to downregulation of Bcl-XL expression in HT-29 cells

To further investigate whether the Ets2 transcription factor is involved in the regulation of Bcl-XL expression in HT-29 cells, the effect of Ets2 knockdown by siRNA was tested. The cells were transfected with either a siRNA sequence specific against Ets2 (siRNA Ets2) or with a control siRNA sequence directed against luciferase (siRNA Luciferase). The siRNA experiments followed by Western Blot analysis showed that Ets2 protein level was reduced in cells transfected with siRNA Ets2, in comparison to cells transfected with the control siRNA (**Figure 27**). The expression of Bcl-XL was downregulated in cells transfected with siRNA Ets2, in comparison to cells transfected with control siRNA. This data showed that Ets2 deficiency led to downregulation of Bcl-XL expression in HT-29 cells.

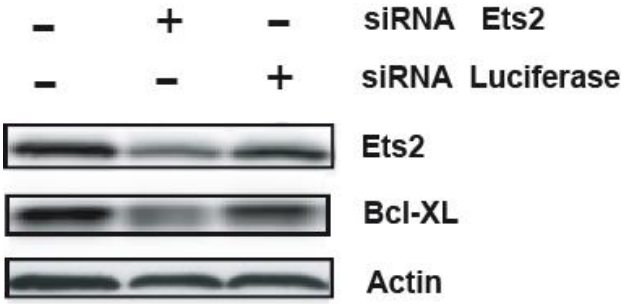

Figure 27. Ets2 knockdown led to downregulation of Bcl-XL expression in HT-29 cells. HT-29 cells were transfected with siRNA specific against Ets2 (siRNA Ets2) or with control siRNA (siRNA specific against Luciferase). Subsequently, expression of Ets2 and Bcl-XL proteins was evaluated in whole cell lysates by Western Blot analysis. Actin was used as loading control. Data is representative of three individual experiments.

3.1.10 VPA downregulated expression of Bcl-XL and Ets2 in DLD1 and DLD1-5-FU/R cells

After finding that Ets2 regulates the expression of Bcl-XL in HT-29 cells, it was investigated whether VPA also downregulates Bcl-XL and Ets2 expression in other colon tumor cell lines. DLD1 and DLD1-5-FU/R cells (DLD1 cells overexpressing Bcl-XL) were provided by Zhu [162]. DLD1 and DLD1-5-FU/R cells were treated with 2 mM VPA for 6, 24 and 48 h and the expression of Bcl-XL was analyzed by Western Blot analysis. The blots showed that the expression of Bcl-XL was higher in DLD1-5-FU/R cells compared to DLD1 cells (274 % DLD1-5-FU/R cells vs. 100 % DLD1 cells) (**Figure 28)**. VPA treatment for 48 h led to a reduced Bcl-XL expression in DLD1-5-FU/R in comparison to untreated cells (34 % VPA-treated vs. 100 % untreated DLD1-5-FU/R). VPA treatment for 48 h reduced more effectively the Bcl-XL expression in DLD1-5-FU/R (34 % VPA-treated vs. 100 % untreated DLD1-5-FU/R) than in DLD1 cells (75 % VPA-treated vs. 100 % untreated DLD1 cells). The Bcl-XL level in DLD1-5-FU/R after treatment with VPA for 48 h was similar to the Bcl-XL level in untreated DLD1 cells (94 % VPA-treated DLD1-5-FU/R cells vs. 100 % untreated DLD1 cells).

In the same set of samples the expression of Ets2 and pT72-Ets2 was also investigated by Western Blot analysis. The blots showed that Ets2 transcription factor was less expressed in DLD1-5-FU/R cells in comparison to DLD1 cells (56 % DLD1-5-FU/R cells vs. 100 % DLD1 cells) (**Figure 28)**. These results indicated that the elevated level of Bcl-XL in DLD1-5-FU/R cells was not a result of increased expression of Ets2. The VPA treatment for

48 h led to a reduced Ets2 expression in DLD-1 cells in comparison to untreated cells (41 % VPA-treated vs. 100 % untreated DLD-1 cells). The treatment with VPA for 48 h resulted in a decrease of Ets2 expression in DLD1-5-FU/R cells in comparison to untreated cells (34 % VPA-treated vs. 100 % untreated DLD1-5-FU/R cells). Similarly, the expression of pT72-Ets2 was reduced in DLD-1 cells treated with VPA for 48 h in comparison to untreated cells (44 % VPA-treated vs. 100 % untreated DLD-1 cells). The expression of pT72-Ets2 was reduced in DLD1-5-FU/R cells treated with VPA for 48 h in comparison with untreated cells (41 % VPA-treated vs. 100 % untreated DLD1-5-FU/R cells). A correlation between Bcl-XL and pT72-Ets2 expression levels was observed in DLD1-5-FU/R cells after 48 h of treatment with VPA, but not after 24 h of drug exposure **(Figure 28)**.

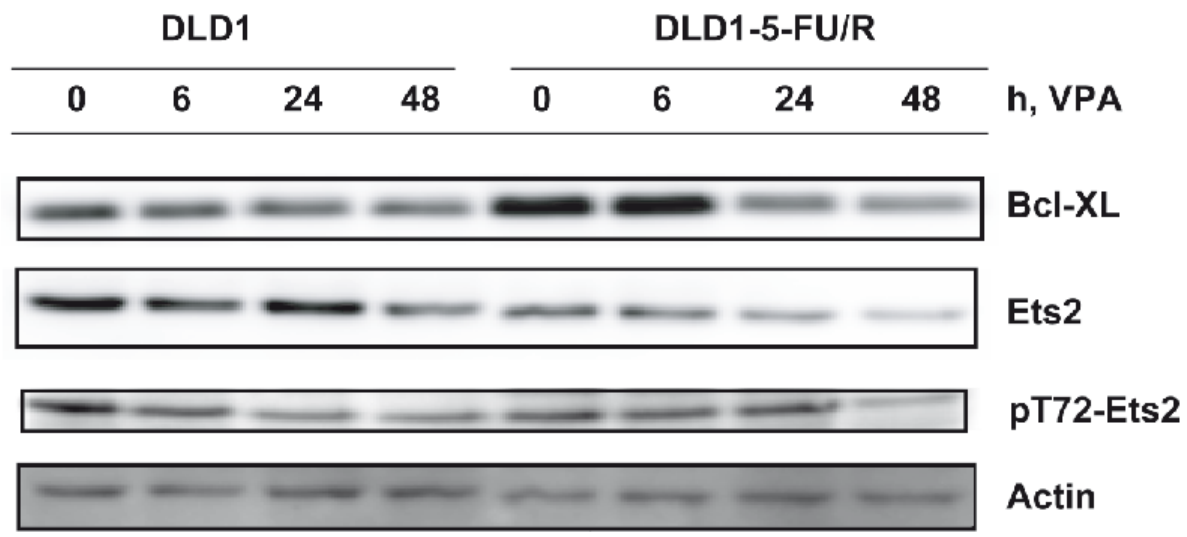

Figure 28. VPA downregulated the expression of Bcl-XL and Ets2 in DLD-1 and DLD1-5-FU/R cells. DLD1 and DLD1-5-FU/R cells were treated with 2 mM VPA for the indicated time periods before harvesting. Whole cell lysates were subjected to Western Blot analysis. Data is representative of two individual experiments.

These results showed that treatment with VPA markedly reduced the Bcl-XL expression in DLD1-5-FU/R cells, although overexpression of Bcl-XL in these cells appears to be due to a mechanism which is Ets2-independent. However, it was not clear if the reduction of Bcl-XL levels in DLD1-5-FU/R cells was related with Ets2 expression.

3.1.11 Ets2 knockdown by siRNA led to downregulation of Bcl-XL in DLD1-5-FU/R cells

To investigate whether the Ets2 transcription factor is involved in the regulation of Bcl-XL not only in HT-29 cells, but also in DLD1-5-FU/R cells, the effect of Ets2 knockdown by a siRNA approach was tested. DLD1-5-FU/R cells were transfected either with a siRNA sequence specific against Ets2 (siRNA Ets2) or with a control siRNA sequence directed against luciferase (siRNA Luciferase). The siRNA experiments followed by Western Blot analysis showed that Ets2 protein level was reduced in cells transfected with siRNA Ets2 in comparison to the cells transfected with the control siRNA (64 % vs. 100 %) (**Figure 29**). The expression of Bcl-XL was downregulated in cells transfected with siRNA Ets2, in comparison to cells transfected with control siRNA (50 % vs. 100 %).

This data showed that the Ets2 transcription factor was involved in the regulation of Bcl-XL expression in DLD1-5-FU/R cells, since Ets2 deficiency led to downregulation of Bcl-XL expression in these cells.

In summary, it has been found that VPA-increased expression of the proapoptotic protein Bak was a result of interference with the HDAC2 isoform. The reduced levels of the prosurvival protein Bcl-XL upon VPA treatment could be explained by the repression of Ets2 transcriptor factor. Next it was investigated whether combining VPA with other chemotherapeutic drugs could be a therapeutic option in colon cancer.

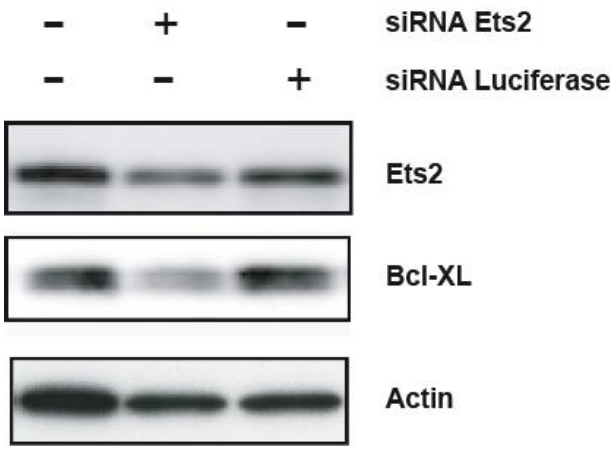

Figure 29. Ets2 knockdown led to downregulation of Bcl-XL expression in DLD1-5-FU/R cells. DLD1-5-FU/R cells were transfected with siRNA specific against Ets2 (siRNA Ets2) or with control siRNA specific against luciferase (siRNA Luciferase). Subsequently, the expression levels of Ets2 and Bcl-XL proteins were determined in whole cell lysates by Western Blot analysis. Actin was used as loading control. Data is representative of two individual experiments.

3.2 Does VPA synergize with 5-FU to inhibit the survival of colon cancer cells?

New therapeutic strategies are required to improve the response rate in advanced colon cancer [164]. Many HDAC inhibitors have been shown to enhance the antitumor activity of several conventional chemotherapeutic drugs. One proposed mechanism is that HDAC inhibitors lower the threshold for inducing tumor cell death in the presence of other chemotherapeutic drugs by decreasing the expression of antiapoptotic genes e.g. Bcl-XL [166, 171]. 5-FU based chemotherapy regimens are the standard treatment for colorectal cancer, but the response rates remain unsatisfactory, mainly due to drug resistance [164, 187, 188]. It has been shown that different HDAC inhibitors increase the 5-FU cytotoxicity by changing the expression of markers associated with resistance to 5-FU, e.g. TYMS [189]. To evaluate whether VPA synergizes with 5-FU to inhibit the survival of colon cancer cells which are either sensitive or resistant to 5-FU, it was investigated:

i) if VPA changes the expression of markers specifically associated with resistance of cancer cells to the cytotoxic effect of 5-FU, e.g. Bcl-XL and TYMS. (The results showing that VPA reduces the expression of Bcl-XL in both DLD1 (sensitive to 5-FU) and DLD1-5-FU/R cells (selected to be partially resistant to 5-FU) were presented in section 3.1.10. The results showing the effect of VPA on TYMS are presented in section 3.2.2).

ii) if the combined VPA and 5-FU treatment inhibits the survival of colon cancer cells more efficiently than the 5-FU treatment alone. (The results of the effect of combined treatment with VPA and 5-FU on survival of DLD-1 and DLD1-5-FU/R cells are presented in section 3.2.1. The results of the effect of combined treatment on survival of HT-29p (sensitive to 5-FU) and 5F12 (resistant to 5-FU) cells are presented in section 3.2.3).

3.2.1 The effect of combined treatment with VPA and 5-FU on survival of DLD-1 and DLD1-5-FU/R colon cancer cells

The effect of combined treatment with VPA and 5-FU on the survival of colon cancer cells was investigated by a cell viability assay using DLD1 cells (sensitive to 5-FU) and DLD1-5-FU/R cells (partially resistant to 5-FU, overexpressing Bcl-XL). The DLD1-5-FU/R cells were derived by Zhu et al, 2005 [162] from DLD-1 cells, that were treated with increasing concentrations of 5-FU (50 - 400 µM) and survived 8 days after the end of this treatment. In the present study, DLD1 and DLD1-5-FU/R cells were treated with 2 mM VPA for 48 h followed by the treatment with 50 µM 5-FU for 72 h. As controls, the cells were either incubated with 2 mM VPA for 48 h and then grown in fresh medium for 72 h or the cells were grown in fresh medium for 48 h and then incubated with 50 µM 5-FU for 72 h. The viable cells were counted after the treatment.

The treatment of the DLD-1 cells with 5-FU resulted in the survival of 39.0 ± 3.7 % of cells in comparison to untreated cells (p = 1.3E-06, 50 µM 5-FU vs. 0 µM 5-FU) (**Figure 30** and **Table 6**). The treatment of DLD-1 cells with VPA resulted in the survival of 73.0 ± 17.0 % of cells in comparison to untreated cells (p = 0.01, 2 mM VPA vs. 0 mM VPA). The treatment of DLD-1 cells with VPA and 5-FU resulted in the survival of only 14.1 ± 2.0 % of cells in comparison to untreated cells (p = 1.7E-07, combined treatment vs. untreated cells; p = 0.0006, combined treatment vs. 2 mM VPA; p = 1.9E-06, combined treatment vs. 50 µM 5-FU). The combined treatment with VPA and 5-FU resulted in a stronger reduction of the number of DLD-1 cells in comparison to individual treatment with VPA and 5-FU, respectively. In comparison to the cells surviving the VPA treatment (assumed as 100 %) the percentage of cells surviving the combined VPA and 5-FU treatment was reduced to 19.3 %. In comparison to the cells surviving the 5-FU treatment (assumed as 100 %) the percentage of cells surviving the combined VPA and 5-FU treatment was reduced to 36.1 %. Thus, 63.9 % of the DLD1 cells surviving the 5-FU treatment alone died upon combined treatment with VPA and 5-FU (**Table 6**).

The treatment of DLD1-5-FU/R cells with 5-FU resulted in the survival of 74.6 ± 2.6 % of cells in comparison to untreated cells (p = 0.0001, 50 µM 5-FU vs. 0 µM 5-FU) (**Figure 30** and **Table 7**). The treatment of the DLD1-5-FU/R cells with VPA resulted in the survival of 70.6 ± 3.0 % in comparison to untreated cells (p = 8.8E-07, 2 mM VPA vs. 0 mM VPA). The treatment of DLD1-5-FU/R cells with VPA and 5-FU resulted in the survival of 44.1 ± 3.1 % of cells (p = 4.4E-07, combined treatment vs. untreated cells; p = 3.3E-05, combined treatment vs. 2 mM VPA; p = 1.7E-05, combined treatment vs. 50 µM 5-FU). The combined treatment with VPA and 5-FU resulted in a stronger reduction of the number of DLD1-5-FU/R cells in comparison to the individual treatment with VPA and 5-FU, respectively. In comparison to the cells surviving the VPA treatment (assumed as 100 %) the percentage of cells surviving the combined VPA and 5-FU treatment was reduced to 62.5 %. In comparison to the cells surviving the 5-FU treatment (assumed as 100 %) the percentage of cells surviving the combined VPA and 5-FU treatment was reduced to 59.0 %. Therefore, 41.0 % of the DLD1-5-FU/R cells surviving the 5-FU treatment alone died upon combined treatment with VPA and 5-FU.

These results showed that VPA synergized with 5-FU to inhibit the survival of DLD-1 cells (sensitive to 5-FU) and DLD1-5-FU/R (partially resistant to 5-FU). The combined VPA and 5-FU treatment showed stronger inhibitory effects on cell survival than 5-FU or VPA treatment alone in both DLD1 and DLD1-5-FU/R cells. The combined treatment with VPA and 5-FU suppressed the survival more efficiently in DLD1 cells than in

DLD1-5-FU/R cells: 63.9 % of the DLD-1 cells surviving the 5-FU treatment alone died upon the combined treatment; 41.0 % of the DLD1-5-FU/R cells surviving the 5-FU treatment alone died upon the combined treatment.

In summary, the presented data indicated that combining VPA with 5-FU has the potential to enhance the efficacy of 5-FU-based chemotherapy in colon cancer.

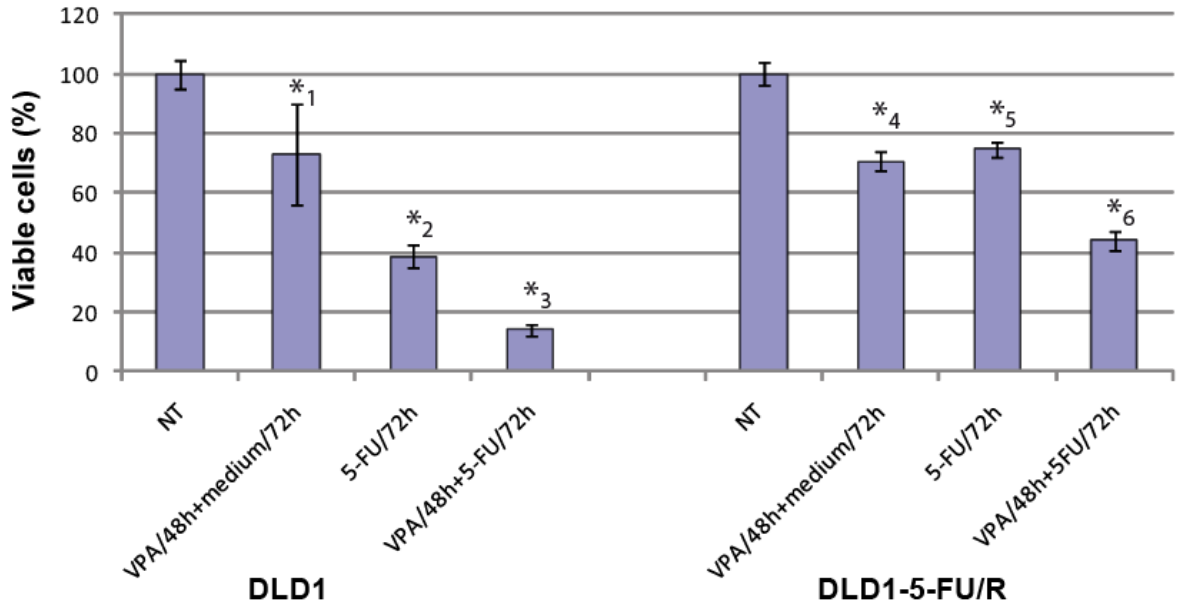

Figure 30. Combined VPA and 5-FU treatment provided stronger inhibition of survival than 5-FU or VPA treatment alone in both DLD-1 and DLD1-5-FU/R cells. DLD1 (5-FU sensitive) and DLD1-5-FU/R (partially resistant to 5-FU) cells were treated with 2 mM VPA for 48 h, followed by the treatment with 50 µM 5-FU for 72 h. As controls the cells were either incubated with VPA for 48 h and then grown in fresh medium for 72 h or the cells were grown in medium for 48 h and then incubated with 5-FU for 72 h. The results, expressed as mean values (%) ± SD, represent the percentage of treated viable cells relative to untreated (NT) viable cells from two independent experiments performed in triplicates.***1**,***2**, $p \leq 0.01$, VPA or 5-FU treated vs. untreated DLD1 cells; ***4**, ***5**, $p \leq 0.0001$, VPA or 5-FU treated vs. untreated DLD1-5-FU/R cells; ***3**, $p \leq 0.0006$, combined treatment vs. VPA or 5-FU or untreated DLD1 cells; ***6**, $p \leq 3.3E\text{-}05$, combined treatment vs. VPA or 5-FU or untreated DLD1-5-FU/R cells.

Table 6: The effect of combined treatment with VPA and 5-FU on survival of DLD-1 colon cancer cells.			
DLD1	**viable cells** [% ± SD]	**p-value**	**Significance**
untreated cells	100		The combined treatment with VPA and 5-FU provided stronger inhibition of survival than the VPA or 5-FU treatment alone.
cells surviving VPA treatment (a)	73.0 ± 17.0	0.01 (2 mM VPA vs. 0 mM VPA)	
cells surviving 5-FU treatment (b)	39.0 ± 3.7	1.3E-06 (50 µM 5-FU vs. 0 µM 5-FU)	
cells surviving combined treatment (c)	14.1 ± 2.0	1.7E-07 (combined treatment vs. untreated cells) 0.0006 (combined treatment vs. 2 mM VPA) 1.9E-06 (combined treatment vs. 50 µM 5-FU)	
cells surviving combined treatment (c) relative to cells surviving 5-FU treatment (b)	36.1 (14.1/39.0)	1.9E-06 (50 µM 5-FU vs. combined treatment)	36.1 % of the cells surviving the 5-FU treatment alone were viable after the combined treatment with VPA and 5-FU; therefore, 63.9 % of the cells surviving the 5-FU treatment alone died upon the combined treatment.
cells surviving combined treatment (c) relative to cells surviving VPA treatment (a)	19.3 (14.1/73.0)	0.0006 (2 mM VPA vs. combined treatment)	19.3 % of the cells surviving the VPA treatment alone were viable after the combined treatment with VPA and 5-FU; therefore, 80.7 % of the cells surviving the VPA treatment alone died upon the combined treatment.

Table 7: The effect of combined treatment with VPA and 5-FU on survival of DLD1-5-FU/R colon cancer cells.			
DLD1-5-FU/R	**viable cells** [% ± SD]	**p-value**	**Significance**
untreated cells	100		The combined treatment with VPA and 5-FU provided stronger inhibition of survival than the VPA or 5-FU treatment alone.
cells surviving VPA treatment (a)	70.6 ± 3.0	8.8E-07 (2 mM VPA vs. 0 mM VPA)	
cells surviving 5-FU treatment (b)	74.6 ± 2.6	0.0001 (50 µM 5-FU vs. 0 µM 5-FU)	
cells surviving combined treatment (c)	44.1 ± 3.1	4.4E-07 (combined treatment vs. untreated cells) 3.3E-05 (combined treatment vs. 2 mM VPA) 1.7E-05 (combined treatment vs. 50 µM 5-FU)	
cells surviving combined treatment (c) relative to cells surviving 5-FU treatment (b)	59.0 (44.1/74.6)	1.7E-05 (50 µM 5-FU vs. combined treatment)	59.0 % of the cells surviving the 5-FU treatment alone were viable after the combined treatment with VPA and 5-FU; therefore, 41% of the cells surviving the 5-FU treatment alone died upon the combined treatment.
cells surviving combined treatment (c) relative to cells surviving VPA treatment (a)	62.5 (44.1/70.6)	3.3E-05 (2 mM VPA vs. combined treatment)	62.5 % of the cells surviving the VPA treatment alone were viable after the combined treatment with VPA and 5-FU; therefore, 37.5 % of the cells surviving the VPA treatment alone died upon the combined treatment.

3.2.2 VPA downregulated TYMS gene expression in HT-29p and 5F12 colon cancer cells

3.2.2.1 VPA downregulated TYMS expression at the mRNA level in HT-29 cells

It has been found that VPA has the potential to increase the 5-FU cytotoxic effect in DLD1-5-FU/R cells which overexpress Bcl-XL. Besides the overexpression of Bcl-XL leading to resistance of tumor cells to 5-FU, high expression levels of TYMS have also been reported as being associated with a poor response and resistance to the 5-FU treatment in colon cancer [67, 158-160, 164, 190, 191]. Analysis of the microarray data (described in paragraph 3.1.1) showed that TYMS mRNA expression was significantly downregulated to 13.7 ± 2.0 % after treatment of HT-29 cells with VPA for 24 h in comparison to untreated cells ($p = 0.00002$, VPA-treated vs. untreated cells) (**Figure 31**). TYMS expression was downregulated to 80.0 ± 9.0 % after 3 h ($p = 0.007$, VPA-treated vs. untreated cells) and to 75.4 ± 6.0 % after 6 h ($p = 0.0007$, VPA-treated vs. untreated cells) of VPA treatment.

These results showed that VPA reduced the expression of TYMS, which is a key determinant for the resistance of cancer cells to the cytotoxic effect of 5-FU.

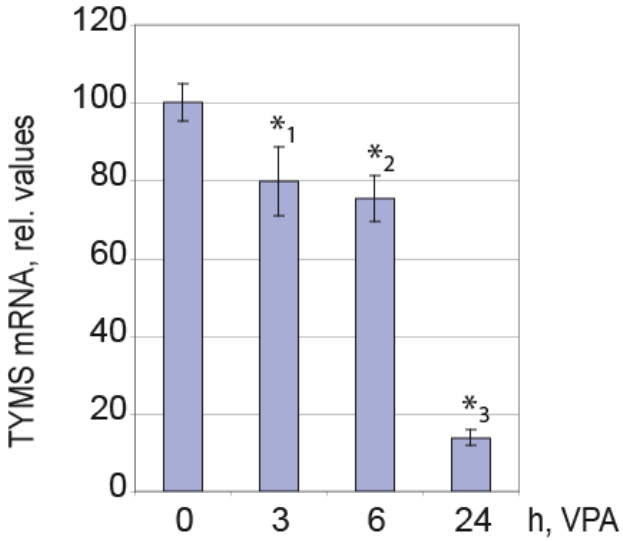

Figure 31. **VPA downregulated TYMS expression at the mRNA level in HT-29 cells**
VPA-induced changes in the TYMS gene expression were evaluated in HT-29 cells untreated or treated with 2 mM VPA for 3, 6 and 24 h using Affymetrix microarray analysis (described earlier in paragraph 3.1.1). Relative differences in TYMS gene expression between the VPA-treated and untreated samples are shown. Data from four independent replicates was used to calculate the mean values and SD. ***1, *2, *3** $p \leq 0.007$, VPA-treated vs. untreated samples.

3.2.2.2 VPA downregulated TYMS expression at the mRNA level in 5F12 cells

Given that low tumoral TYMS expression is predictive for sensitivity to 5-FU-based chemotherapy [160, 190], it was investigated whether VPA can downregulate the expression of TYMS in colon cancer cells which are resistant to 5-FU treatment. 5F12 colon cancer cells are resistant to 5-FU, presumably due to overexpression of TYMS by gene amplification. The 5F12 cells and their parental HT-29 cells (HT-29p, sensitive to 5-FU) were provided by Leteurtre. The 5F12 cells were obtained by growing HT-29p cells at passage 144 in the presence of increasing concentrations of 5-FU (1 µM, 5 µM, 10 µM and 20 µM) [172, 173].

First, it was determined by quantitative two-step real-time RT-PCR, whether VPA can downregulate the TYMS expression at a comparative level in HT-29 cells (passage 20) and HT-29p cells (HT-29 cells at passage 165) **(Figure 32)**. The TYMS basal gene expression was similar in HT-29p cells compared to HT-29 cells (130.4 ± 13.0 % HT-29p cells vs. 100 % HT-29 cells, $p = 0.02$). The treatment of HT-29 cells with VPA for 6 h resulted in downregulation of TYMS expression to 56.8 ± 14.35 % compared to untreated HT-29 cells ($p = 0.009$, VPA-treated vs. untreated HT-29 cells). The treatment of HT-29 cells with VPA for 24 h resulted in downregulation of TYMS expression to 20.2 ± 7.0 % compared to untreated HT-29 cells ($p = 0.0002$, VPA-treated vs. untreated HT-29 cells). The treatment of HT-29p cells with 2mM VPA for 6 h resulted in downregulation of TYMS gene expression to 87.2 ± 11.5 % compared to HT-29 untreated cells ($p = 0.1$, VPA-treated HT-29p cells vs. untreated HT-29 cells). The treatment of HT-29p cells with 2 mM VPA for 24 h resulted in downregulation of TYMS gene expression to 60.0 ± 7.0 % compared to untreated HT-29 cells ($p = 0.002$, VPA-treated HT-29p cells vs. untreated HT-29 cells)**.** These results showed that TYMS expression was less efficiently repressed by VPA in HT-29p cells compared to HT-29 cells.

The effect of VPA treatment on TYMS expression was investigated in 5F12 cells (resistant to 5-FU) compared to HT-29p **(Figure 33)**. The cells were treated with VPA for 6 or 24 h and subjected to quantitative two-step real-time RT-PCR analysis. The results showed that TYMS was 12.2 ± 2.8 fold higher expressed in 5F12 cells compared to HT-29p cells ($p = 0.004$ 5F12 cells vs. HT-29p cells). The treatment of HT-29p cells with 2 mM VPA for 6 h resulted in downregulation of TYMS gene expression to 65.0 ± 8.9 % compared to HT-29p untreated cells ($p = 0.004$, VPA-treated vs**.** untreated HT-29p cells). The treatment of HT-29p cells with 2 mM VPA for 24 h resulted in downregulation of TYMS gene expression to 44.1 ± 5.7 % compared to HT-29p untreated cells ($p = 0.0003$ VPA-treated vs. untreated HT-29p cells). The treatment of 5F12 cells with VPA for 6 h downregulated the expression of

TYMS to 59.7 ± 10.3 % compared to untreated 5F12 cells (p = 0.02, VPA-treated vs. untreated 5F12 cells). The treatment of 5F12 cells with VPA for 24 h downregulated the expression of TYMS to 47.7 ± 8.4 % compared to untreated 5F12 cells (p = 0.03,VPA-treated vs. untreated 5F12 cells). However, the level of TYMS expression after 6 h treatment with VPA was 730.4 ± 126.1 % higher in 5F12 cells compared to untreated HT-29p cells (p = 0.002 VPA-treated 5F12 cells vs. untreated HT-29 cells). The level of TYMS expression after 24 h treatment with VPA was 583.9 ± 104.0 % higher in 5F12 cells compared to untreated HT-29p cells (p = 0.003 VPA-treated 5F12 cells vs. untreated HT-29 cells).

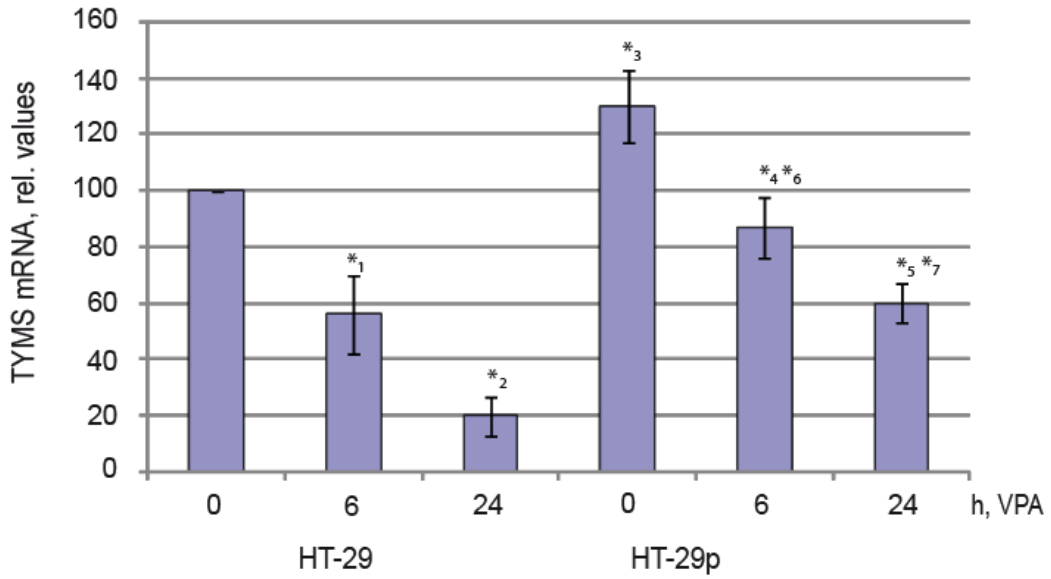

Figure 32. **TYMS expression was less efficiently repressed by VPA in HT-29p cells compared to HT-29 cells.** HT-29 cells (passage 20) and HT-29p cells (HT-29 cells at passage 165) were treated with 2 mM VPA for the indicated time periods prior to extracting total RNA. Expression of TYMS was determined by quantitative two-step real-time RT-PCR. Relative differences in TYMS gene expression compared to the untreated HT-29 cells were normalized to the expression of the β-actin. Data from two independent experiments performed in duplicates was used to calculate the mean values and SD. ***1**, p = 0.009, VPA-treated HT-29 cells (6 h) vs. untreated HT-29 cells;***2**, p = 0.0002,VPA-treated HT-29 cells (24 h) vs. untreated HT-29 cells; ***3**, p = 0.02, untreated HT-29p cells vs. untreated HT-29 cells;***4**, p = 0.1, VPA-treated HT-29p cells (6 h) vs. untreated HT-29 cells;***5**, p = 0.002, VPA-treated HT-29p cells (24 h) vs. untreated HT-29 cells; ***6**, p = 0.01, VPA-treated HT-29p cells (6 h) vs. untreated HT-29p cells; ***7**, p = 0.0008, VPA-treated HT-29p cells (24 h) vs. untreated HT-29p cells.

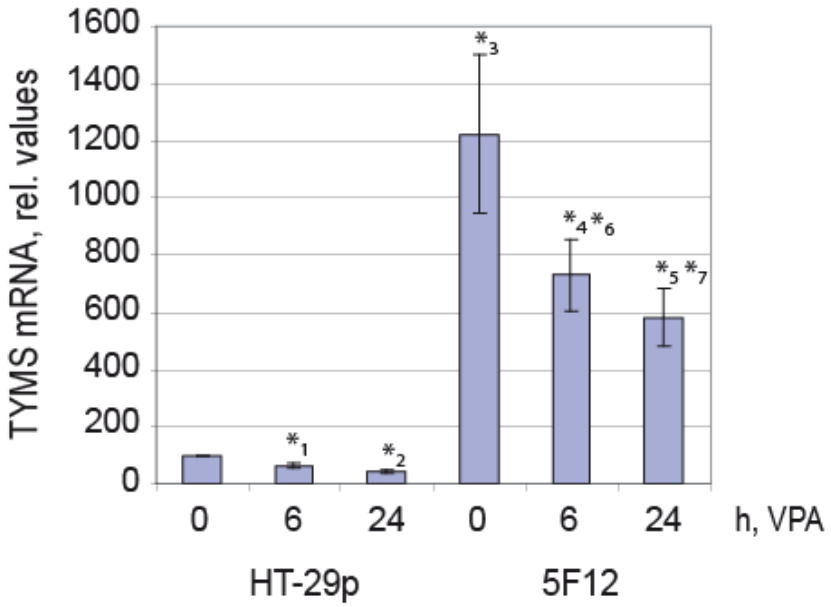

Figure 33. **VPA downregulated TYMS expression at the mRNA level in HT29p and 5F12 cells. Higher levels of TYMS were present in the VPA-treated 5F12 cells compared to untreated HT-29p cells.** HT-29p (5-FU sensitive) and 5F12 (5-FU resistant) cells were treated with 2 mM VPA for the indicated time periods prior to extracting total RNA. Expression of TYMS was determined by quantitative two-step real-time RT-PCR. Relative differences in gene expression compared to the untreated HT-29p cells were normalized to the expression of the β-actin. Data from two independent experiments performed in duplicates was used to calculate the mean values and SD. $*_1$, p = 0.004, VPA-treated HT-29p cells (6h) vs. untreated HT-29p cells; $*_2$, p = 0.0003, VPA-treated HT-29p cells (24 h) vs. untreated HT-29p cells; $*_3$, p = 0.004, untreated 5F12 cells vs. untreated HT-29p cells; $*_4$, p = 0.002, VPA-treated 5F12 cells (6 h) vs. untreated HT-29p cells; $*_5$, p = 0.003, VPA-treated 5F12 cells (24 h) vs. untreated HT-29p cells; $*_6$, p = 0.02, VPA-treated 5F12 cells (6 h) vs. untreated 5F12 cells; $*_7$, p = 0.03, VPA-treated 5F12 cells (24 h) vs. untreated 5F12 cells.

These results showed that VPA markedly downregulated the expression of TYMS in both HT-29p cells (sensitive to 5-FU) and 5F12 cells (resistant to 5-FU). As TYMS expression levels are a determinant of 5-FU resistance, these results led to the hypothesis that combining VPA with 5-FU might sensitize HT-29p and 5F12 colon cancer cells to the 5-FU cytotoxic effect by VPA-mediated downregulation of TYMS.

3.2.3 The effect of combined treatment with VPA and 5-FU on survival of HT-29p and 5F12 colon cancer cells

To investigate whether combining VPA with 5-FU enhances the sensitivity of colon cancer cells to the 5-FU cytotoxic effect and increases the efficacy of the 5-FU-based therapy, the effect of combined treatment with VPA and 5-FU on the viability of HT-29p (sensitive to 5-FU) and 5F12 (resistant to 5-FU) cells was investigated by a MTT cell viability assay. The cells were treated with 2 mM VPA for 48 h and then treated for 24h with 1µM, 5 µM, 10 µM or 20 µM 5-FU, since 5F12 cells were reported to be resistant to 5-FU at these concentrations [172, 173]. After the 5-FU treatement the cells were grown in fresh medium for 48 h. As controls, cells were either: i) incubated with 2 mM VPA for 48 h and then grown in fresh medium for 72 h or ii) grown in fresh medium for 48 h, incubated with 1 µM, 5 µM, 10 µM or 20 µM 5-FU for 24 h and then grown in fresh medium for 48 h.

The treatment of HT-29p cells with 2 mM VPA resulted in the survival of 81.6 ± 3.4 % of cells in comparison to untreated cells ($p = 0.01$, 2 mM VPA vs. 0 mM VPA) (**Figure 34** and **Table 8)**. The treatment of HT-29p cells with 10 µM 5-FU resulted in the survival of 63.7 ± 10.1 % of cells compared to untreated cells ($p = 0.02$, 10 µM 5-FU vs. 0 µM 5-FU). The treatment of the HT-29p cells with combination VPA and 10 µM 5-FU resulted in the survival of 53.6 ± 14.7 % of cells ($p = 0.2$, 10 µM 5-FU vs. combined treatment; $p = 0.03$, combined treatment vs. untreated cells, $p = 0.1$, 2 mM VPA vs. combined treatment). These results showed that the combined treatment with VPA and 10 µM 5-FU did not significantly reduce the percentage of the viable HT-29p cells compared to the 5-FU treatment alone. The same results were obtained when the cells were incubated with 1 µM, 5 µM or 20 µM 5-FU.

The treatment of 5F12 cells with VPA resulted in the survival of 85.0 ± 4.0 % of cells in comparison to untreated cells ($p = 0.02$, 2 mM VPA vs. 0 mM VPA) **(Figure 34** and **Table 8)**. The treatment of 5F12 cells with 10 µM 5-FU resulted in the survival of 97.0 ± 4.0 % of cells ($p = 0.3$, 10 µM 5-FU vs. 0 µM 5-FU). The treatment of the 5F12 cells with VPA and 10 µM 5-FU resulted in the survival of 77.1 ± 7.6 % of cells ($p = 0.05$, 5-FU vs. combined treatment; $p = 0.1$, VPA vs. combined treatment; $p = 0.03$, combined treatment vs. untreated cells). These results showed that the combined treatment with VPA and 10 µM 5-FU did not significantly reduce the percentage of the viable cells compared to the VPA treatment alone. Therefore, the reduced percentage of the viable cells observed after the combined treatment in comparison to 5-FU treated or untreated cells is an effect of the VPA treatment alone.

VPA did not synergize with 5-FU to inhibit the survival of HT-29p and 5F12 colon cancer cells. The pre-treatment with VPA could not overcome the resistance of the 5F12 cells to the cytotoxic effect of 5-FU. Therefore, combining VPA with 5-FU did not increase the efficacy of the 5-FU treatment in these cells. The amounts of TYMS still present in the cells upon VPA treatment might be responsible for the lack of response to the combined treatment with VPA and 5-FU of the HT-29p and 5F12 cells.

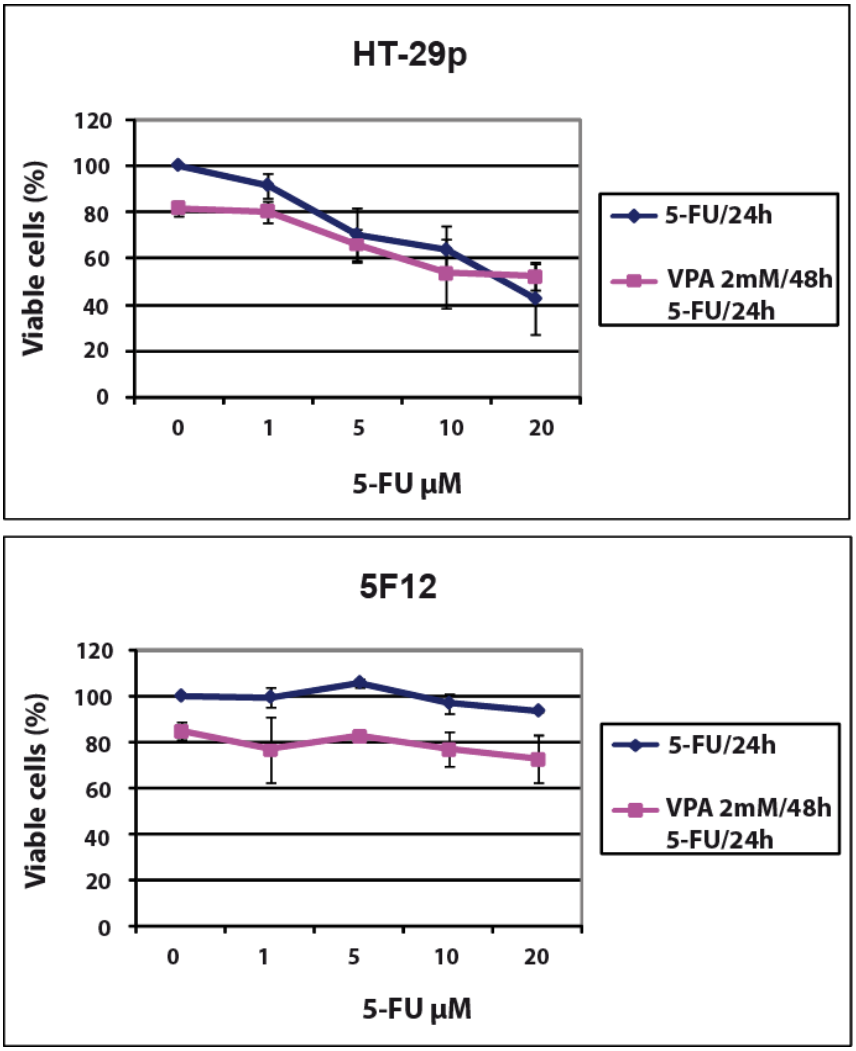

Figure 34. VPA did not synergize with 5-FU to inhibit the survival of HT-29p and 5F12 colon cancer cells. HT-29p (5-FU sensitive) and 5F12 (5-FU resistant) cells were treated with 2 mM VPA for 48 h, followed by treatment with 1 µM, 5 µM, 10 µM or 20 µM 5-FU for 24 h; after 5-FU incubation cells were grown in fresh medium for 48 h. As controls, the cells were treated with VPA for 48 h and then grown in fresh medium for 72 h or the cells were grown in fresh medium for 48 h, incubated with 1 µM, 5 µM, 10 µM or 20 µM 5-FU for 24 h and then grown in fresh medium for 48 h. The cellular viability was determined by the MTT assay. The results from three independent experiments expressed as mean values ± SD are given. The values of treated viable cells were normalized to the values of untreated cells (100 %).

Table 8: The effect of combined treatment with VPA and 5-FU on survival of HT-29p and 5F12 colon cancer cells			
HT-29p	**viable cells** [% ± SD]	**p-value**	**Significance**
untreated cells	100		The combined treatment with VPA and 10 µM 5-FU did not significantly reduce the percentage of the viable cells compared to the 5-FU treatment alone.
cells surviving VPA treatment	81.6 ± 3.4	0.01 (2 mM VPA vs. 0 mM VPA)	
cells surviving 5-FU treatment	63.7 ± 10.1	0.02 (10 µM 5-FU vs. 0 µM 5-FU)	
cells surviving combined treatment	53.6 ± 14.7	0.03 (combined treatment vs. untreated cells) 0.2 (combined treatment vs. 10 µM 5-FU) 0.1 (combined treatment vs. 2 mM VPA)	
5F12	**viable cells** [% ± SD]	**p-value**	**Significance**
untreated cells	100		The combined treatment with VPA and 10 µM 5-FU did not markedly reduce the percentage of the viable cells compared to the 5-FU and VPA treatment alone.
cells surviving VPA treatment	85.0 ± 4.0	0.02 (2 mM VPA vs. 0 mM VPA)	
cells surviving 5-FU treatment	97.0 ± 4.0	0.3 (10 µM 5-FU vs. 0 µM 5-FU)	
cells surviving combined treatment	77.1 ± 7.6	0.03 (combined treatment vs. untreated cells) 0.05 (combined treatment vs. 10 µM 5-FU) 0.1 (combined treatment vs. 2 mM VPA)	

4 DISCUSSION

Transcriptional repression by aberrant expression of HDACs or recruitment of HDACs to target genes is involved in cancer initiation and progression [72, 75, 81, 87]. Consequently, HDAC inhibitors are considered to be promising anti-cancer agents and are currently investigated in clinical trials as monotherapy or in combination with chemotherapy or radiotherapy in a variety of hematological and solid tumors. Vorinostat (SAHA) is the first HDAC inhibitor approved by FDA in 2006 for the treatment of cutaneous T-cell lymphoma [114] However, many questions still remain open: i) which HDAC isoforms have to be inhibited in a given tumor type; ii) is the expression of key mediators of cell death dependent on specific HDAC isoforms; iii) which are the predictive markers for a successful therapy with HDAC inhibitors and iv) do HDAC inhibitors synergize with other chemotherapeutic drugs to induce the death of tumor cells?

This study focuses on the following challenges in the field: i) to define the mechanism by which the HDAC inhibitor VPA induces cell death in colon cancer cells and ii) to investigate whether VPA synergizes with 5-FU to inhibit the survival of colon cancer cells sensitive and resistant to 5-FU.

4.1 Which is the mechanism used by VPA to induce cell death in colon cancer cells?

The HDAC inhibitor VPA preferentially inhibits the catalytic activity of class I HDACs. In addition, VPA induces proteasomal degradation of HDAC2 isoenzyme [131]. To identify the mechanism by which VPA induces cell death in colon cancer cells it was investigated: i) which are the VPA-induced changes that mediate initiation of cell death in colon cancer cells?; ii) which are the key target(s) specifically required for the VPA-induced cell death?; and iii) if the expression of the VPA key target(s) is HDAC2 dependent.

4.1.1 The effect of VPA on the gene expression profile of the HT-29 cells

Previous studies have shown that different HDAC inhibitors induced similar changes in the gene expression profile, but there were also differences, which were a result of their specificity against HDAC isoenzymes. In addition, the cell line dependency of the changes in gene expression induced by HDAC inhibitors was also shown [192, 193].

To identify target genes regulated by VPA treatment in colon cancer cells, the effect of VPA on the gene expression profile of the HT-29 cells was investigated using Affymetrix microarray analysis. The microarray data analysis showed that the expression of 4.7 % of the genes recognized by the chip array (1844 genes out of 39.000 genes) have been at least 2 fold changed upon the VPA treatment (either positively or negatively). Thus, only a small fraction of genes was regulated in response to VPA treatment. These findings are in line with previous

studies which showed that in various types of cells the HDAC inhibition has not induced global changes in gene expression, but resulted in transcriptional changes of a limited set of genes [192, 194-196]. For example, Reid et al., 2005 [194] showed that only 6 % of the genes analyzed responded specifically to the VPA treatment in breast and ovarian cell lines.

The results of the present study showed that 1090 genes were at least 2 fold upregulated and 754 genes were at least 2 fold downregulated after VPA treatment for 24 h in HT-29 colon cancer cells. This is in agreement with other studies reporting that: i) the ratio of upregulated to downregulated genes was close to 1:1 and ii) treatment with HDAC inhibitors resulted in transcription activation, but also in gene repression, explaining the complex response to the action of HDAC inhibitors [75, 81]. Reid et al., 2005 [194] also reported that identical proportions of genes were activated and repressed greater than 2 fold by VPA in breast and ovarian cell lines.

Previous studies reported complex cellular consequences of the treatment with HDAC inhibitors, which include cell cycle arrest, apoptosis, differentiation, suppression of angiogenesis and immunomodulation [72, 80]. Various HDAC inhibitors, including VPA blocked the cell cycle progression by transcriptional activation of CDK inhibitor p21 [74, 78, 177]. Upregulation of Bax/Bcl-2 ratio, activation of caspases or release of cytochome c were proposed to mediate HDAC-induced apoptosis [72, 81]. These findings were obtained using several HDAC inhibitors in various cell lines and it is unclear whether they are universally applicable. Therefore, the changes induced by VPA in the gene expression profile of the HT-29 colon cancer cells were analyzed in the present study.

In the present study it was found that VPA affected positively and negatively multiple signaling pathways involved in regulation of cell cycle G1/S checkpoints, apoptosis, DNA repair, RNA synthesis, maintenance of chromatin architecture and cytoskeleton organization (**Table 3, Supplimentary Tables 2** and **3**). These pathways are regarded as potential targets for cancer therapy. The gene activation induced by VPA was most probably mediated through hyperacetylation of gene promoters by HDAC inhibition. VPA-induced downregulation of gene expression might result from secondary effects, like transcriptional activation of negative regulatory factors.

The microarray data analysis showed that VPA changed the expression of a subset of genes specifically associated with apoptosis already after 3 h and 6 h of treatment (**Figure 7** and **Supplementary Figure 1**). Taking into consideration the early time points of the gene changes, the modulation of apoptotic genes was not a simple consequence of the VPA effects, but it was considered to play causative roles. The analysis of the microarray data revealed that VPA induced proapoptotic changes in expression of the Bcl-2 family members involved in the mitochondrial (intrinsic) pathway of apoptosis regulation, e.g. Bak and Bcl-XL, but not of the components involved in regulation of the death receptor (extrinsic) signaling pathway

(e.g. members of the TNFR superfamily) (**Table 4** and **Table 5**). Thus, VPA-mediated induction of apoptosis was most probably triggered by the mitochondrial pathway through the Bcl-2 family protein members, rather than being induced through the death receptor pathway. The VPA-induced changes in expression of genes encoding for Bcl-2 protein family members were complex: i) Bak, Bim, Bik and Bmf were upregulated; ii) Bcl-XL, Bid and Noxa were downregulated; iii) the expression of Bcl-2, Bax, Bad and Puma remained unchanged (**Table 4**). The microarray data indicated that VPA changed the expression of Bak and Bcl-XL. This finding was confirmed by two-step quantitative real time PCR or RT-PCR in HT-29 cells (**Figure 9** and **Figure 10)**. The gene expression of other proapoptotic components of mitochondrial pathway, like BNIP3L and APAF-1 were also upregulated by the VPA treatment (**Figure 7**). Although, the gene expression of inhibitory apoptosis proteins such as cIAP1 (BIRC2) and cIAP2 (BIRC3) was upregulated (**Figure 7**), the overall response of the mitochondrial pathway components was one that could provide a proapoptotic signal in VPA-treated HT-29 cells.

The upregulation of Bak mRNA expression by VPA in HT-29 colon cancer cells is in accordance with Fortunati et al., 2008 [138], who reported that VPA upregulated Bak mRNA expression in breast cancer cells. It was reported that SAHA and TSA increased Bim transcription in HCT116 colon tumor cells [124]. In the present study HDAC inhibition by VPA also upregulated Bim gene expression in HT-29 cells. The upregulation of Bmf mRNA expression is in accordance with Zhang et al., 2006 [125], who reported that Bmf was transcriptionaly activated by FK228 and CBHA. Bax gene expression was upregulated by SBHA in melanoma cells [118], while in the present study VPA did not change Bax gene expression in HT-29 cells. It has been reported that VPA decreased Bcl-2 mRNA expression levels in chronic lymphocytic leukaemia cells (CLL) [129] and breast cancer cells [138]. In the present study Bcl-2 gene expression was not changed. Facchetti et al., 2004 reported that expression of Noxa at the mRNA level was not changed by VPA in human melanoma cells [135]. In contrast to this finding, in the present study VPA treatment downregulated Noxa gene expression in HT-29 cells. It has been reported that SAHA did not change the Bcl-XL mRNA expression level in hepatoma cells [197], while SBHA downregulated Bcl-XL gene expression in melanoma cells [118]. In the present study VPA also downregulated Bcl-XL gene expression in HT-29 cells.

The analysis of the microarray data showed that VPA changed the expression of a large number of genes involved in cell cycle progression. Downregulation of genes required for progression from G1 to the S phase of the cell cycle and of several genes involved in inhibition of the DNA replication was observed upon treatment with VPA (**Figure 8**). This supports the previous reports showing that VPA inhibits proliferation of various cancer cells [136, 138, 140, 141]. Changes in the gene expression of cyclins, CDKs and MCM were

associated with cell cycle arrest induced by other HDAC inhibitors, like SAHA, FK288, TSA and MS-275 [193, 198-200].

In addition to cyclin-dependent kinase (CDK) inhibitor p21, which is a common responsive gene of HDAC inhibitors action [74, 78, 177], other key regulatory components of the cell cycle checkpoints were identified as being changed by VPA at the mRNA level. For example, the gene expression of several CDK inhibitors such as CDKN2B (p15, INK4B), CDKN2D (p19, INK4D), CDKN1C (p57, KIP2) was upregulated by VPA (**Figure 8**). These results showed that VPA targeted a specific set of CDK inhibitors, different of other HDAC inhibitors. For example, many HDAC inhibitors have been reported to induce G1 cell cycle block by p21 and p27 upregulation [73, 78, 80].

In summary, the major finding of the gene expression analysis performed in this study is the identification of multiple alterations induced by VPA in the mRNA expression of Bcl-2 family members involved in regulation of the mitochondrial pathway of apoptosis. The VPA-induced changes in gene expression of Bcl-2 family members, but not in the expression of death receptors have the potential to trigger apoptosis in HT-29 colon cancer cells. Further analysis were performed to estabilish if the changes induced by VPA in the gene expression of the Bcl-2 family members resulted in cell death of HT-29 cells and to identify the VPA key targets required for VPA-mediated cell death.

4.1.2 VPA mediated apoptosis by the mitochondrial pathway

Zhu et al., 2004 [94] showed that HDAC2 overexpression upon loss of the APC tumor suppressor protected HT-29 colon cancer cells against apoptosis. It was reported in the same study that HDAC2 knockdown induced cell death in HT-29 cells. Previous studies have shown that VPA preferentially inhibited class I HDACs and interfered with HDAC2 by inducing its proteasomal degradation [131].

The microarray data analysis performed in the present study showed that the treatment of HT-29 cells with VPA resulted in proapoptotic changes in the gene expression of the components of the mitochondrial pathway of apoptosis, but not in the gene expression of the components of the death receptor pathway of apoptosis (**Table 4** and **Table 5**). Therefore, it was investigated whether VPA treatment induced apoptosis in HT-29 cells. The VPA treatment increased the fraction of early apoptotic cells (Annexin V^+/PI^-) and induced DNA fragmentation. Moreover, the VPA-induced DNA fragmentation was significantly decreased in the presence of a pan-caspase inhibitor (**Figure 11** and **12**).

Cell death mediated by caspases is regulated at multiple steps. One of these steps is controlled by Aven, an antiapoptotic protein that inhibits caspase activation. It has been reported that Aven inhibits Apaf-1 oligomerization and thereby suppresses the activation of caspase-9 and apoptosis [201]. The microarray data showed that the mRNA expression of

AVEN was downregulated to 14 ± 3.4 % after treatment of HT-29 cells with VPA for 24 h compared to untreated cells (p = 0.000002, VPA-treated vs. untreated cells) (**Supplementary Table 4).** Therefore, inhibition of Aven upon VPA treatment might facilitate the activation of downstream effector caspases, leading to apoptosis.

Previous studies showed that HDAC inhibitors, including VPA induced apoptosis in a variety of tumor cells. Several potential mechanisms have been proposed including effects on both intrinsic and extrinsic apoptotic pathways in a caspase-dependent or independent manner [75, 80, 136, 202], [139], [129]. The specific mechanism used by each HDAC inhibitor to induce apoptosis depends on the specific HDAC isoenzymes inhibited. Moreover, the response to HDAC inhibitors strongly depends on the tumor cell type [72, 80].

In the present study it has been shown that VPA induced characteristic features of apoptosis in HT-29 colon cancer cells. VPA-mediated apoptosis in HT-29 cells was induced through the mitochondrial pathway, which finally resulted in the activation of effector caspases. Inhibition of the effector caspases led to the significant decrease in VPA-induced DNA fragmentation in the presence of the pan-caspase inhibitor.

4.1.3 VPA induced multiple alterations in the protein expression levels of the Bcl-2 family proteins in HT-29 cells

To further characterize the underlying mechanism of VPA-induced apoptotic cell death in HT-29 colon cancer cells, the effect of VPA treatment on the expression of proteins from Bcl-2 family was investigated. VPA induced apoptosis promoting changes in the protein levels of apoptotic activators t-Bid, Bim-S and Bim-EL isoforms, proapoptotic effector Bak and antiapoptotic Bcl-XL protein, at the relevant sub-cellular localization, e.g. the mitochondria. VPA upregulated the protein expression levels of Bak, Bim-S, Bim-EL and tBid, and downregulated the expression of Bcl-XL protein (**Figure 13**). Although, some proapoptotic proteins were downregulated, (e.g. Bax, Noxa, Puma) or not substantially changed (Bad and Bik) and expression of antiapoptotic protein Bcl-2 was not influenced by the VPA treatment (**Figure 13**), the overall changes in the ratio of pro- and antiapoptotic proteins would facilitate induction of apoptosis. The VPA-induced changes in Bim, tBid and Bcl-XL promoted the proapoptotic function of Bak.

The proapoptotic effector protein Bak is negatively regulated at the mitochondria by Mcl-1 and Bcl-XL, which sequester Bak by binding to its BH3 pocket and thereby preventing its oligomerization [11]. In the present study, VPA significantly upregulated the expression of Bak protein and reduced the expression of Bcl-XL protein in HT-29 cells. The microarray data showed that the expression of Mcl-1 was not changed following VPA treatment in HT-29 cells (**Supplementary Table 5**). Thus, adequate conditions for Bak activation and oligomerization were present in VPA-treated HT-29 cells.

Upon apoptosis induction Mcl1-Bak and Bcl-XL-Bak interactions are disrupted by the regulatory BH3 domain-only proteins (e.g. Bim, tBid), allowing the pore forming Bak to oligomerize and trigger apoptosis [4, 11, 16, 35, 55]. In the present study, the expression levels of the BH3-only proteins Bim and tBid were higher than those of the antiapoptotic proteins upon VPA treatment. Therefore, the effector function of Bak in triggering apoptosis was facilitated.

The expression of the proapoptotic effector protein Bax was downregulated by the VPA treatment in HT-29 cells (**Figure 13**). Reduced levels of Bax did not impair apoptosis induction, since significant levels of Bak were present in HT-29 cells upon VPA treatment. This is in accordance with Hemmati et al., 2006 [203] who showed that Bak functionally complements for loss of Bax in HCT116 colon cancer cells. Degenhardt et al., 2002 and Wei et al. 2001 [57, 68] showed that Bak and Bax function in a redundant capacity to facilitate apoptosis induction. Brooks et al., 2007 [62] reported that mitochondrial fragmentation was attenuated in Bak-deficient cells, while Bax-deficiency did not prevent mitochondrial fragmentation. The resistance to etoposide and cisplatin of Bak-deficient leukemia cells could not be reverted by ectopic expression of Bax or truncated Bid, while ectopic expression of Bak induced apoptosis in Bax -/- or Bid -/- mice [63]. All these reports show that Bak can function independently of Bax.

In healthy cells, the regulatory BH3 domain–only Bim isoforms, Bim-EL and Bim-L are maintained in an inactive conformation through binding to the microtubules**.** These proteins act like sensors of the cytoskeletal integrity and are involved in mediating apoptosis induced by microtubule stabilizing drugs [42-44]. Bim-S, the most potent Bim isoform in apoptosis induction is not sequestered by microtubules and it is not normally found in healthy cells [45, 46]. VPA treatment of HT-29 colon tumor cells resulted in upregulation of total Bim protein levels. The expression of Bim-EL and Bim-S isoformes was increased by VPA predominantly in the mitochondria (**Figure 13**). Tubulin is one of the non-histone targets that undergo acetylation following VPA treatment [204]. Therefore, VPA-induced changes in the acetylation level of the microtubules could mediate the release of Bim from microtubules and its translocation to mitochondria. This is in accordance with Puthalakath et al., 1999 [44] and Bratton et al, 2001 [43], who reported that microtubules damaging drugs induced Bim translocation to mitochondria.

The regulatory BH3 domain–only protein Bid is cleaved by caspase 8 upon activation of the death receptor extrinsic pathway. The active tBid fragment translocates to mitochondria where promotes Bak oligomerization [16]. Numerous studies reported that HDAC inhibitors induced apoptosis through the extrinsic pathway by induction of death receptor and their ligands. In the present study, the expression of the death receptors or their ligands was not upregulated upon VPA treatment (**Table 5**). However, cleavage of Bid was detected in the

mitochondrial fractions of VPA-treated HT-29 cells, even though the mRNA expression was moderately repressed (**Figure 13, Table 4**). It is most likely that tBid translocation to mitochondria was a secondary event, subsequent to activation of the intrinsic pathway. This is in line with Cowling and Downward, 2002 [17], who reported that the intrinsic apoptotic pathway may feed-back to extrinsic pathway by cleaving caspase-8, which in turn would generate tBid.

The expression of the antiapoptotic protein Bcl-XL plays an important role in the survival and protection against apoptosis of various tumor cells, including prostate, breast and colon cancer cells [67, 205, 206]. It has been reported that the anti-apoptotic protein Aven binds to Bcl-XL and enhances Bcl-XL anti-apoptotic activity [201]. VPA treatment significantly downregulated the expression level of Bcl-XL in HT-29 cells (**Figure 13**). The mRNA expression of Aven was also significantly downregulated by the VPA treatment in HT-29 cells (**Supplementary Table 4**). Thus, the proapoptotic response induced by VPA through upregulation of Bak, Bim and tBid was augmented by the decrease in Bcl-XL expression.

The expression of the p53 targets, the proapoptotic proteins Puma and Noxa was downregulated after VPA treatment in HT-29 cells (**Figure 14**). Thus, it was considered that the p53 pathway was not involved in the VPA-induced cell death in HT-29 cells. Degenhardt et al., 2002 reported that Bak could mediate suppression of tumorigenesis in a p53-independent manner [68]. Therefore, it is plausible that VPA induced Bak-mediated apoptosis in HT-29 cells, in the absence of p53-mediated signals.

Stress signals from the endoplasmic reticulum (ER) mediated through proapoptotic protein Bik were reported to initiate mitochondrial apoptosis [47]. The protein expression level of Bik was not increased upon VPA treatment (**Figure 13**). Therefore, it is unlikely that the stress from ER contributed to VPA-induced apoptosis in HT-29 cells.

Most of the changes found on protein expression levels of Bcl-2 family members after treatment with VPA were a result of the VPA-induced changes on mRNA expression level (e.g changes in Bak, Bax, Bim, Bcl-XL, Bcl-2, Noxa) (**Table 4**, **Figures 13** and **14)**. Differences in gene and protein expression levels of certain Bcl-2 members (e.g. PUMA, Bik, Bmf) have also been observed following the VPA treatment. A possible explanation is that these Bcl-2 proteins were degraded by a proteasome-dependent mechanism activated by VPA. VPA is linked to the ubiquitin-proteasomal pathway by increasing the expression of the E2 ubiquitin-conjugating enzyme Ubc8 [131]. It has been shown that protein degradation or processing by ubiquitin-proteasome system is involved in the regulation of the Bcl-2 proteins [207, 208].

The VPA treatment resulted in increased expression of Bik at the mRNA level (**Table 4**). However, the expression level of Bik protein was not upregulated upon the VPA

treatment (**Figure 13**). Several reports have shown that Bik protein was targeted to the proteasome-dependent degradation [47]. It has been reported that in ZR75-1 breast cancer cells which constitutively express Bik mRNA, the Bik protein was rapidly degraded by the proteasomal machinery [209]. Inhibition of proteasome resulted in accumulation of Bik at the mitochondria [210]. In colon cancer cell lines, Bik degradation was blocked by treatment with Bortesomib and MG132. Bortezomib induced rapid accumulation of Bik, but not of Bax, Bak, Bcl-2 or Bcl-XL [211].

Despite the increased expression of Bmf at the mRNA level upon the VPA treatment, the expression level of the Bmf protein was not upregulated after the VPA treatment. (**Supplementary Figure 6**). The reason of this discrepancy is not clear. Significant regulation of the BH3-only proteins is exerted at the post-transcriptional level. In contrast, little is known about the post-translational regulation of Bmf. It has been reported that infection with C. trachomatis resulted in reduction of the constitutively expressed Bmf protein [212]. Other BH3-only proteins e.g. Bax, Bak, Bcl-2 or Bcl-XL were not affected. Degradation of PUMA in cells infected with C. trachomatis was blocked by inhibition of proteasome with MG132. Thus, it was suggested that the same proteasome-dependent mechanism might be involved in degradation of Bmf.

The expression of PUMA was not changed by VPA at the mRNA level (**Table 4**), while PUMA protein expression was clearly downregulated in HT-29 cells upon VPA treatment (**Figure 14**). Previous reports have shown that the proteasome system is involved in the regulation of the protein expression levels of PUMA [213]. Inhibition of the proteasome by epoxomicin [214] and bortexomib [215] induced expression of PUMA in HCT116 colon cancer cells.

The published data show that in general HDAC inhibitor treatment induced proapoptotic signals in tumor cells by increase of the Bax/Bcl-XL or Bax/Bcl-2 ratios. For example, VPA increased Bax/Bcl-XL and Bax/Bcl-2 ratios together with Bid cleavage in hepatoma and chronic lymphocytic leukaemia cells, respectively [129, 133, 216]; MS-275 increased Bax/Bcl-2 ratio in colangiocarcinoma cells [121]; SAHA and CBHA increased the Bax/Bcl-2 and Bax/Bcl-XL ratios in tyroid carcinoma cells [122].

Few reports indicated that Bak expression was upregulated upon HDAC inhibitor treatment. For example, VPA upregulated Bak and downregulated Bcl-2 protein levels in breast cancer cells [138]. SAHA upregulated Bak, Bax, Bim and downregulated Bcl-2 and Bcl-XL protein levels [128]; SBHA upregulated Bak, Bax and Bim levels and downregulated Bcl-XL and Mcl1 expression levels [130]. In several publications, Bak was not reported as being involved in HDAC inhibitors-induced apoptosis [127, 217].

In summary, the major finding in this section is that VPA upregulated the expression of the proapoptotic effector Bak at the protein level in HT-29 colon cancer cells. The

proapoptotic function of Bak was promoted by the VPA-induced changes in the protein expression of Bid, Bim and Bcl-XL. This profile of VPA-induced changes in Bcl-2 family proteins is distinct from the frequently described HDAC inhibitors profile that involves an increase in Bax/Bcl-2 or Bax /Bcl-XL ratio.

4.1.4 VPA upregulated Bak and Bim expression at the mRNA level by an HDAC2-dependent mechanism, while the VPA-reduced Bcl-XL expression was not mediated by HDAC2 interference

Evidence that the HDAC2 isoform is involved in tumorigenesis came from the observation that HDAC2 is overexpressed in colon [94], prostate [98] and cervical carcinomas [100] in comparison to the normal tissues. Zimmermann et al., 2007 reported that HDAC2 played an important role for tumor development *in vivo*, since the number of intestinal tumors were significantly reduced in HDAC2-deficient APC^{min} mice compared with HDAC2 wild-type APC^{min} mice [95]. Weichert et al., 2008 showed that elevated HDAC2 levels are an independent marker of poor prognosis in gastric cancer [92]. Thus, HDAC2 appears to play a prominent role in the pathogenesis of gastrointestinal cancer. Zhu et al., 2004 showed that HDAC2 is overexpressed upon loss of the APC tumor suppressor in HT-29 colon cancer cells and that RNAi-mediated knockdown of HDAC2 resulted in cell death, indicating a role of HDAC2 in protecting cancer cells against apoptosis in HT-29 cells [94]. Recently, Fritsche et al., 2009 showed that HDAC2 mediates therapeutic resistance of pancreatic cells to etoposide via the BH3-only protein Noxa [218].

Taking into consideration these previous findings, it was investigated if the expression of VPA-responsive proteins from the Bcl-2 family (Bak, Bim and Bcl-XL) depends on the HDAC2 isoform. The mRNA levels of Bak and Bim were upregulated and those of Bcl-XL were repressed by VPA to an extent that could plausibly account for most of the changes found on protein levels (**Figure 9, Figure 10** and **Figure 18**).

To investigate whether the changes induced by VPA in expression of Bak, Bim and Bcl-XL proteins specifically depend on the HDAC2 isoform an RNAi (RNA interference) approach was used to knockdown the expression of HDAC2 in HT-29 cells. Increased expression of Bak, Bim-L and Bim-S proteins was found in cells that had lost HDAC2 as a result of siRNA transfection (**Figure 15, Figure 16** and **Figure 19**). The results of the RNAi experiments, were confirmed in mouse embryonic fibroblasts (MEFs) that expressed either wildtype (HDAC2 +/+) or a catalytically inactive mutant form of HDAC2 (HDAC2 -/-). HDAC2 deficient MEFs expressed markedly increased levels of Bak protein, compared to wildtype MEFs (**Figure 17**). The HDAC2 knockdown by siRNA in HT-29 cells and HDAC2 deficiency in MEFs had no influence on the expression of the antiapoptotic protein Bcl-XL

(**Figure 19** and **Figure 20**). These results showed that Bak and Bim expression depended on the HDAC2 isoform, while Bcl-XL expression was not associated with HDAC2 knockdown.

Several studies showed that HDAC inhibitors induced expression of Bak in tumor cells, but the mechanism of this effect is not understood [128, 130, 138]. For example, Fortunatti et al., 2007 [138] showed that VPA upregulated Bak expression at the mRNA and protein level in breast cancer cells, but the mechanism underlying the effect of VPA was not clarified. Zhao et al., 2005 [124] showed that SAHA and TSA increased the Bim transcription by the activation of the E2F1 transcription in HCT116 colon tumor cells. In the present study, VPA downregulated the expression of the E2F1 transcription factor (**Supplementary Table 7**). Therefore, the expression of Bim could not be E2F1 dependent in VPA-treated HT-29 cells.

This is the first report showing that the induction of the proapoptotic proteins Bak and Bim is associated with a specific HDAC isoform, namely HDAC2. The results showed that VPA-induced expression of Bak and Bim was specifically mediated by the interference with HDAC2. The mechanism by which VPA reduced the expression of Bcl-XL in HT-29 cells was not HDAC2 dependent, but might be mediated by VPA effects independent of interference with HDAC2. These results also showed that the HDAC2 isoform was involved in the protection of tumor cells against apoptosis by the repression of Bak and Bim gene expression.

4.1.5 Bak overexpression was sufficient to induce apoptosis of HT-29 cells and Bak knockdown protected HT-29 cells from VPA-induced apoptosis

Since the proapoptotic Bak protein was clearly found to be upregulated by VPA treatment in HT-29 cells, it was further evaluated whether elevated Bak levels alone are sufficient to induce apoptosis in HT-29 cells. Ectopic expression of wildtype Bak or mutant Bak that lacks the C-terminal domain (BakΔC) induced apoptosis at similar rates compared with those induced by VPA treatment (**Figure 12** and **Figure 21**). Chittenden et al., 1995 showed that the BakΔC mutant reduced only slightly the cytotoxic function of Bak in transfected Rat-1 cells and reported that the C-terminal hydrophobic tail is not required for the apoptotic function of Bak [176]. Transfection of mutant Bak that lacks the BH3-domain (BakΔGD) did not induce apoptosis in HT-29 cells (**Figure 21)**. Chittenden et al., 1995 [176] showed that the BH3-domain deleted in the BakΔGD mutant was required for the proapoptotic function of Bak.

This data showed that Bak overexpression alone was sufficient to promote apoptosis in HT-29 cells. In addition, this data showed that the VPA increased expression of one specific component of the intrinsic pathway of apoptosis e.g. proapoptotic effector Bak was sufficient for induction of apoptosis.

To test whether Bak is required for VPA-induced apoptosis, the effect of Bak knockdown on protection of HT-29 cells from the VPA-induced cell death was evaluated. The VPA treatment of the Bak siRNA transfected cells resulted in the increase of the percentage of Bak-depleted cells (**Figure 22,** lower pannel). This data indicated that Bak depleted cells had an advantage to survive VPA exposure. In contrast, accumulation of Bak-positive cells was reduced in the presence of VPA (**Figure 22,** lower pannel). These results are consistent with the cell doubling time results (**Figure 23**). Upon VPA treatment the doubling time of Bak-positive cells was increased, while the effect of VPA on Bak-depleted cells was moderate with insignificant increase in the net doubling time. This minor effect of VPA in Bak-deficient cells maybe explained by the VPA-induced cell cycle inhibition through upregulation of p21 expression in HT-29 cells [177]. *These results showed that Bak was required for VPA-induced cell death, since Bak knockdown protected HT-29 cells from the apoptotic effect of VPA.*

In summary, the results from the Bak overexpression and Bak knockdown experiments showed that Bak was the major player in the VPA-induced cell death.

4.1.6 Bcl-XL expression depended on Ets2 transcription factor in HT-29 and DLD1-5-FU/R colon cancer cells

It was proven that the increased Bak expression levels upon VPA treatment were a result of the interference of VPA with HDAC2 isoform. However, the reduced expression levels of the prosurvival protein Bcl-XL upon VPA treatment were not an effect of HDAC2 inhibition (**Figure 16 and 19**). The analysis of the microarray data showed that VPA reduced the expression of a transcription factor involved in the regulation of the Bcl-XL, namely Ets2 (**Figure 24**) [180-183]. Ets2 belongs to the Ets family of transcription factors, which consists of more than 20 members. They act as transcription activators or repressors of multiple genes involved in cellular proliferation, differentiation and apoptosis [219]. It has been shown that Ets2 overexpression contributes to neoplasic transformation in prostate [220], breast [221] and thyroid cancer [222]. Targeting this transcription factor is thought to be a valid anticancer therapeutic strategy [223, 224].

To understand the mechanism by which VPA reduced the levels of the prosurvival protein Bcl-XL, the expression of Ets2 protein upon VPA treatment was further investigated. It has been found that the downregulation of the Bcl-XL expression at the mRNA and protein level (**Figure 10 and 25**) correlated with the reduced expression of the Ets2 transcription factor upon VPA treatment (**Figure 25**). The amount of the phosphorylated transcriptionally active form of Ets2 also decreased upon VPA treatment in HT-29 cells (**Figure 26**). The VPA treatment had the same effect on Ets2 expression in another colon tumor cell line, DLD1

(**Figure 28**). These results led to the hypothesis that the repression of the transcription factor Ets2 by VPA resulted in the downregulation of Bcl-XL expression in HT-29 cells.

Bcl-XL is one of the alternative splicing variants of Bcl-x gene. Bcl-XL expression is controlled by several transcription factors such as Ets2, STAT, Rel/NFkB, PU.1, GATA-1, Brn-3a or PAX3 in response to specific stimuli [41]. [213]. In this study a RNAi approach was used to determine whether Ets2 is required for Bcl-XL expression in HT-29 cells. The treatment of HT-29 cells with a siRNA sequence designed to specifically knockdown Ets2 expression resulted in a marked decrease in the Bcl-XL expression level (**Figure 27**). Ets2 silencing inhibited Bcl-XL protein expression, not only in HT-29 cells, but also in DLD-1 colon tumor cells overexpressing Bcl-XL (DLD1-5-FU/R) (**Figure 29**).

These results are consistent with previous publications. Sevilla et al., 1999 [180] reported that transient expression of Ets2 resulted in upregulation of Bcl-XL transcription in macrophages. Zhang Q et al., 2005 [181] showed that overexpression of Ets2 increased Bcl-XL mRNA in osteoclasts. Cao et al, 2009 [183] showed that transient expression of Ets-2 cDNAs in mesothelioma cell lines resulted in an increase in the promoter activity of Bcl-XL and consequently in its mRNA and protein expression levels.

Since many transcription factors are involved in the regulation of Bcl-XL expression in different cells, the effect of VPA on the expression of these transcriptor factors was also analysed in HT-29 cells. Constitutive activation of STAT transcription factors was associated with increased expression of Bcl-XL [41]. It was considered unlikely that in HT-29 cells the downregulation of Bcl-XL observed upon VPA treatment was mediated by STAT transcription factors since: i) the mRNA STAT3 level was upregulated after VPA treatment for 6 h (151.5 ± 10.0 % VPA-treated vs. 100 % untreated cells, $p = 0.003$); ii) the level of STAT5A expression at the mRNA level was very low and close to the basal threshold in the microarray data analysis (43.4 ± 9 vs. basal threshold = 20); iii) the mRNA expression of STAT6 was minimally downregulated after VPA treatment for 6 h (73.9 ± 3.2 % VPA-treated vs. 100 % untreated cells, $p = 0.0001$), while the expression of Ets2 was significantly downregulated after VPA treatment for 6 h (34.0 ± 2.1 % VPA-treated vs. 100 % untreated cells, $p = 0.0001$) (**Supplementary Table 8**).

The transcription factors from Rel/NFkB family (RELA, RELB, NFkB1, NFkB2) increase expression of genes involved in apoptosis, including Bcl-XL [225, 226]. The microarray data showed that the mRNA expression of RELA and RELB was not significantly changed by VPA treatment (RELA: 100.5 ± 4.0 % VPA-treated (24 h) vs. 100 % untreated cells, $p = 0.9$; RELB: 72.32 ± 15.9 % VPA-treated (24h) vs. 100 % untreated cells, $p = 0.07$). The expression of NFkB1 was downregulated after 6 h of VPA treatment (43.0 ± 2.2 % VPA-treated vs. 100 % untreated cells, $p = 0.005$). The expression of NFkB2 was upregulated after 6 h of VPA treatment (180.0 ± 10.6 % VPA-treated vs. 100 % untreated cells, $p = 0.002$)

(**Supplementary Table 9)**. It could be concluded that Rel/NFkB transcription factors were not involved in the downregulation of Bcl-XL by VPA treatment, since other downstream targets of Rel/NFkB signaling pathway involved in apoptosis e.g. cIAP1 (inhibitory apoptosis protein 1), tumor suppression e.g. IRF1 (interferon regulatory factor 1) and angiogenesis e.g. VEGF were not downregulated after VPA treatment (**Supplementary Table 9)**.

The transcription factors PU.1, GATA-1, Brn-3a and PAX3 have been reported to activate expression of Bcl-XL [41]. The expression of these transcription factors was not detected by micrroarray analysis in HT-29 cells.

It was also reported that STAT1, TEL and p53 transcription factors are involved in repression of Bcl-XL expression [41]. The microarray analysis showed that their expression was not upregulated by VPA in HT-29 cells. The expression of STAT1 and TEL transcription factors was not changed by VPA treatment (STAT1: 107.4 ± 8.4 % VPA-treated (24 h) vs. 100 % untreated cells, p = 0.03; TEL: 92.55 ± 2.7 % VPA-treated (24 h) vs. 100 % untreated cells, p = 0.3). The expression of p53 was downregulated upon VPA treatment for 24 h (38.8 ± 1.2 % VPA-treated vs. 100 % untreated cells, p = 0.001) (**Supplementary Table 10**).

This data showed for the first time that Ets2 regulated Bcl-XL expression in two different colon tumor cell lines (HT-29 and DLD1-5-FU/R). Taken together with the data showing that VPA reduced the expression level of Ets-2, these results identified the transcriptor factor Ets-2 as a mediator of the VPA effect on the expression of the prosurvival protein Bcl-XL.

4.2 Does VPA synergize with 5-FU to inhibit the survival of colon cancer cells?

Colorectal cancer is the third most common form of cancer and the second leading cause of cancer-related death in the Western world [148]. Colon carcinoma often show multidrug resistance, which is one of the most serious problems of a successful therapy in advanced colon cancer [164]. One of the most widely used drugs in chemotherapy of advanced colon cancer is 5-fluorouracil (5-FU), but clinical efficacy of 5-FU is reduced due to drug resistance [149, 187, 188]. Combining 5-FU with newer chemotherapeutic agents like irinotecan and oxaliplatin improves the response rate only to ~50%. Therefore, novel strategies to improve the response rate to 5-FU are of great clinical relevance [164].

It has been shown that combinations of HDAC inhibitors with well established chemotherapeutic drugs, including 5-FU can provide synergistic anti-tumor effects. The mechanism underlying this synergy is thought to be related to: i) simultaneous activation of different apoptosis pathways leading to an overall increase in proapoptotic signaling [166, 171, 189] and ii) downregulation of markers associated with resistance of tumor cells to

chemotherapeutic drugs by HDAC inhibitors [168] Considering this, it was proposed that VPA might synergize with 5-FU and increase 5-FU cytotoxicity in colorectal cancer cells.

4.2.1 VPA synergized with 5-FU to inhibit the survival of DLD1 and DLD1-5-FU/R colon cancer cells

Overexpression of Bcl-XL has been reported in colon cancer and it has been shown to be associated with resistance to 5-FU treatment and poor prognosis in colon cancer [67, 191]. New therapeutic approaches that may help to increase the 5-FU cytotoxicity are needed to improve the clinical outcome in colon cancer. Wacheck et al, 2003 [227] reported that reduction of the Bcl-XL protein levels is a promising therapeutic strategy to increase the effect of chemotherapy in colon cancer. It has been shown here that VPA reduced the expression of Bcl-XL not only in DLD-1 (sensitive to 5-FU), but also in DLD1-5-FU/R colon cancer cells (partially resistant to 5-FU, overexpressing Bcl-XL) (**Figure 28**). On the basis of this observation, it has been proposed that VPA might enhance the 5-FU cytotoxic effect in these cells. To test it, the effect of combined treatment with VPA and 5-FU on the survival of colon cancer cells was investigated by a cell viability assay in DLD1 and DLD1-5-FU/R cells. The results showed that the combined VPA and 5-FU treatment inhibited the survival of DLD1 and DLD1-5-FU/R cells to a higher extend than the 5-FU treatment alone **(Figure 30, Table 6 and 7**). This data showed that VPA increased the 5-FU cytotoxicity in DLD-1 and DLD1-5-FU/R colon cancer cells.

The Bcl-XL expression level in DLD1-5-FU/R cells after treatment with VPA for 48 h was comparable to the Bcl-XL expression in untreated DLD1 cells (**Figure 28**). However, the effect of combined VPA and 5-FU treatment was more pronounced in DLD-1 than in DLD1-5-FU/R cells. It has been previously proposed that the cell death susceptibility is determined by a critical ratio of pro- and antiapoptotic Bcl-2 proteins, rather than the total amounts present in the cell [228]**.** VPA-mediated Bcl-XL downregulation changed the balance between pro- and antiapoptotic Bcl-2 proteins in both DLD-1 and DLD1-5-FU/R cells. DLD-1 parental cells might be more susceptible than DLD1-5-FU/R cells to the VPA-induced change in the balance between Bcl-2 family of proteins. This would lead to the observed increase in cytotoxicity upon combined treatment of DLD-1 cells with VPA and 5-FU compared to 5-FU treatment alone. DLD1-5-FU/R cells acquired the ability to evade the 5-FU cytotoxic effect, which might allow them to be also less susceptible to the changed balance between pro- and antiapoptotic Bcl-2 proteins induced by VPA. This would explain the reduced effect of the combined VPA and 5-FU treatment in DLD1-5-FU/R cells compared to DLD-1 cells.

It has been found that the combined VPA and 5-FU treatment inhibited the survival more efficiently in DLD-1 than in DLD1-5-FU/R cells **(Figure 30, Table 6 and 7**). These

results are partially contradictory to the ones of Zhu et al., 2005 [162] who used a siRNA aproach to knockdown the expression of Bcl-XL. Zhu et al., 2005 [162] reported that combined treatment with Bcl-XL siRNA and 5-FU suppressed the proliferation more efficiently in DLD1-5-FU/R cells than in DLD-1 cells. One possible explanation for the different results of the present study and those of Zhu et al [162] is that siRNA interference is known to be very specific and thus more effective in the inhibition of Bcl-XL gene expression than the VPA treatment. The amount of Bcl-XL still present in the DLD1-5-FU/R cells after VPA treatment can be sufficient to partially protect the cells against the 5-FU cytotoxic action. In spite of this minor discrepancy between the results of this study and the one of Zhu, it could be shown that 41 % of the DLD1-5-FU/R cells surviving the 5-FU treatment alone were killed by the combined treatment with VPA and 5-FU (**Table 7**). This proved that combining VPA with 5-FU enhanced the cytotoxic effect of 5-FU in these cells.

DLD-1 cells are sensitive to 5-FU exposure. Nevertheless, the combined treatment with VPA and 5-FU resulted in stronger inhibition of survival than the 5-FU treatment alone (**Figure 30** and **Table 6**). Combined VPA and 5-FU treatment has clinical significance due to the fact that any additional reduction of survival of tumor cells is important for the clinical outcome. Long term treatment with 5-FU results in the development of clones with a resistance phenotypes, which have a proliferative advantage and can drive the tumor progression [157].

The findings of the present study are in accordance with several studies showing that HDAC inhibitors enhanced the cytotoxicity of 5-FU. For example, MS275 synergized with 5-FU to inhibit the survival of colon cancer cells [229], phenylbutyrate potentiated growth inhibition by 5-FU in colon cancer [170] and TSA enhanced 5-FU cytotoxicity in colon cancer cells [168].

In summary, the data presented here indicated that VPA exerted synergistic interaction with 5-FU reducing the survival of DLD1 and DLD1-5-FU/R colon tumor cells. The combined treatment with VPA and 5-FU may be promising due to the VPA potential to increase the 5-FU cytotoxicity in colon cancer cells.

4.2.2 VPA did not synergize with 5-FU to reduce the survival of HT-29p and 5F12 colon cancer cells

It has been reported that an elevated TYMS level is another major contributing factor towards the mechanism of 5-FU resistance [158, 159, 164]. TYMS is a key enzyme in DNA synthesis and is the target enzyme of the 5-FU cytotoxic action. The inhibition of TYMS activity mediates the 5-FU antiproliferative effects [149]. An inverse correlation between TYMS expression in colon cancer cells and sensitivity to 5-FU has been reported [160, 190]. Increased TYMS expression was found to be a negative prognostic factor of survival in colon

cancer [160, 231]. As TYMS overexpression is a well-documented mechanism of resistance to the 5-FU therapy in colon cancer, there is a significant need to develop therapeutic strategies to overcome TYMS-mediated resistance to 5-FU.

The results showing that TYMS was significantly downregulated at the mRNA expression level after treatment of HT-29 cells with VPA (**Figure 31**) suggested that combining VPA with 5-FU might overcome the 5-FU resistance of colon cancer cells. As a model of 5-FU resistant and sensitive cells, the 5F12 (resistant to 5-FU, presumably due to TYMS overexpression) and their parental cells HT-29p (sensitive to 5-FU) cells were used. To test the mentioned assumption it was first investigated if VPA is effective in reducing the TYMS expression in 5F12 cells expressing ~12 fold more TYMS, than their parental cells (**Figure 33**). The results showed that VPA treatment significantly downregulated the expression of TYMS at the mRNA level in 5F12 cells, but the expression of TYMS after VPA treatment was still ~6 fold higher in 5F12 cells, compared with the parental cells sensitive to 5-FU (**Figure 33**). These findings suggested that the level of residual TYMS still expressed in cells after VPA treatment might influence the response to 5-FU therapy. To test this, a cell proliferation assay was used to determine if sensitization to 5-FU chemotherapy is possible by VPA-mediated downregulation of TYMS, even if VPA treatment was not efficient in reducing the TYMS expression to a level comparable with the one in parental cells.

The results showed that the combined treatment with VPA and 5-FU has not significantly reduced the percentage of the HT-29p viable cells in comparison to the 5-FU treatment alone ($p = 0.2$, 10 μM 5-FU vs. combined treatment) (**Figure 34** and **Table 8**). These results indicated that there is no therapeutic benefit for the combined treatment vs. single 5-FU treatment in HT-29p colon cancer cells. The combined treatment with VPA and 5-FU has not shown a strong additive effect on inhibition of survival of 5F12 cells in comparison to VPA or 5-FU treatment alone (**Figure 34** and **Table 8**). The combination VPA and 5-FU inhibited the growth of 5F12 cells (by 20 %) compared to 5-FU treatment alone. Thus, a combined VPA and 5-FU treatment might be beneficial in clinical application due to the fact that any additional reduction of proliferation of 5-FU resistant cells is important for the clinical outcome, as the resistant clones are the ones who drive the tumor progression. On the other hand the combined treatment has not shown an additive effect on inhibition of cell survival compared with VPA treatment alone, which suggested that the 20 % of reduction in cell growth observed in the case of the combined treatment was a result of the VPA treatment alone.

These results showed that the pre-treatment with VPA did not sensitize HT-29p and 5F12 colon cancer cells to the 5-FU cytotoxic effect, despite the VPA-mediated downregulation of the TYMS levels to ~50 % in both cell lines (**Figure 33**). A possible

explanation is that the amounts of TYMS still present after the VPA treatment protect the cells against the 5-FU cytotoxic effect.

Previous studies evaluating the ability of various HDAC inhibitors to synergize with 5-FU showed that combination of these agents potently inhibited the growth of tumor cells. Tumber et al., 2007 [169] showed that PXD101 in combination with 5-FU inhibited the growth of HCT116 colon cancer cells by downregulation of TYMS by PXD101. In the same cell line, Lee et al, 2006 [168] reported that sequential treatment with TSA followed by 5-FU enhanced 5-FU cytotoxicity by TSA-mediated downregulation of TYMS. Similarly, Fazzone et al., 2009, [189] reported that SAHA and LBH589 downregulated TYMS gene expression and that the combination of these HDAC inhibitors with 5-FU enhanced growth inhibition in a panel of colon cancer cell lines. Differences between these previously published studies and the data of the present study could be due to a number of factors including the different mode of action of different HDAC inhibitors and the level of TYMS overexpression in the cell lines investigated.

In summary, the results presented here showed that VPA has not synergized with 5-FU to reduce the survival of 5F12 cells (resistant to 5-FU, overexpressing TYMS) and of their parental cells (sensitive to 5-FU). Nevertheless, the 5-FU cytotoxicity has been enhanced in the presence of VPA in the other colon cancer cell lines analysed: DLD-1 (sensitive to 5-FU) and DLD1-5-FU/R (partially resistant, overexpressing BCl-XL). It appears that a major limiting factor in the success of the combined VPA and 5-FU therapy in HT-29p and 5F12 cells is the expression level of TYMS still present in these cells after the VPA treatment. In the DLD-1 and DLD1-5-FU/R cells, the VPA-induced change in the balance between the pro- and antiapoptotic Bcl-2 family might explain the increase in cytotoxicity observed upon the combined treatment.

5 CONCLUSION

The results presented in this study showed that HDAC inhibition by VPA induced a set of changes which collectively promoted apoptosis. The profile of VPA-mediated changes observed in HT-29 colon cancer cells is different from that induced by other HDAC inhibitors in many other types of cancer cells [121, 122], [133]. The present study showed that the expression of the major components of this profile e.g. proapoptotic proteins Bak and Bim specifically depends on the HDAC2 isoenzyme. Altered expression of several HDAC isoforms has been reported in different types of tumors, but the essential roles of particular HDAC isoenzymes in apoptosis have rarely been identified [109, 232, 233]. In this study a novel molecular mechanism that links the HDAC2 isoform to the regulation of the proapoptotic effector protein Bak was characterized. There are only few reports that indicated

increased expression of Bak upon HDAC inhibition and only some of them assessed the functional consequences of the induced changes for cell death [128, 130, 138, 234]. Herein, elevated expression of Bak was shown to be required for VPA-induced apoptosis in colon cancer cells. Bak overexpression alone was sufficient to induce apoptosis and Bak knockdown protected cells from VPA-induced cell death.

HDAC2 promotes intestinal tumor development in mice [94, 95]. HDAC2 is overexpressed in colon tumors and elevated HDAC2 levels are an independent marker of prognosis of gastric cancer [92, 93], [94]. HDAC2 deficiency in mice is associated with alterations of the heart and moderately affectes the embryonic development, but is compatible with a normal life span [95, 235]. Thus, selective interference with the HDAC2 isoenzyme is a particularly promising approach in cancer therapy. The results presented in this study support the design of HDAC2 selective inhibitors as a strategy to induce cell death in colon cancer cells.

It is shown in this study that VPA not only activated gene expression by interference with HDAC2, but also exerted its effects at the transcription level by repressing the expression of the transcription factor Ets2. It is reported here that Ets2 specifically regulated the expression of the prosurvival protein Bcl-XL in two different colon cancer cell lines. By this, Ets2 could be identified as an effector that mediated the VPA-induced downregulation of Bcl-XL.

5-FU-based chemotherapy regimens are the standard treatment for advanced colon carcinoma, but the response rates remain unsatisfactory, mainly due to drug resistance [164, 187, 188]. Therefore, new therapeutic strategies are required to improve the response rate in advanced colon cancer. Combining HDAC inhibitors with other anti-cancer agents is thought to be a promising approach to induce the death of cancer cells [166, 171]. In this study it was investigated if VPA can synergize with 5-FU and increase the 5-FU cytotoxicity in colorectal cancer cells. The data presented here showed that VPA changed the expression of two markers (Bcl-XL and TYMS) which are frequently overexpressed in colon cancer cells and are specifically associated with resistance to the 5-FU cytotoxic effect. VPA reduced the expression of Bcl-XL and TYMS in both 5-FU sensitive and 5-FU resistant colon cancer cells. It is reported here that VPA synergized with 5-FU to reduce the survival of DLD-1 (sensitive to 5-FU exposure) and DLD1-5-FU/R (partially resistant to 5-FU, overexpressing Bcl-XL) colon cancer cells. These results showed that combining VPA with 5-FU could be a possible therapeutic option to enhance the 5-FU cytotoxic effect in colon cancer. This data suggests that colon tumors showing 5-FU resistance due to an overexpression of Bcl-XL are likely to provide a response to the combined treatment with VPA and 5-FU. Future clinical studies should focus on testing the efficacy of a combined treatment of VPA and 5-FU in colon tumors showing this resistance phenotype.

It has been previously reported that combining HDAC inhibitors with 5-FU could overcome the 5-FU resistance by downregulating TYMS. In the present study, HDAC inhibition by VPA did not synergize with 5-FU to reduce the survival of 5F12 cells (resistant to 5-FU, overexpressing TYMS) and of their parental cells (sensitive to 5-FU). Even if VPA significantly reduced the expression levels of TYMS the amounts of TYMS still present in the HT-29p and 5F12 cells after VPA treatment might be sufficient to protect these cells against the 5-FU cytotoxic action Therefore, the efficacy of the combined therapy might be dependent not only on the ability of the HDAC inhibitors to reduce the TYMS expression level, but also on the residual levels of TYMS present in the cells upon the treatment with HDAC inhibitors. There might be a critical level of TYMS above which HDAC inhibitors could not increase the 5-FU cytotoxicity. Further studies should investigate the efficacy of HDAC inhibition in enhancing the 5-FU cytotoxic effect in colon tumors with different degrees of TYMS overexpression to identify which tumor resistant phenotypes respond better to the combined therapy.

6 ABSTRACT

Altered expression of individual histonedeacetylases (HDACs) or abnormal recruitment of HDACs to promoter regions of genes regulating cell cycle and apoptosis are involved in the pathogenesis of cancer. Previous pre-clinical studies and ongoing clinical trials of phase I to III showed that HDAC inhibitors induce cell cycle arrest and cell death in many types of cancer cells. However, several questions are currently poorly solved: i) which HDAC isoform have to be inhibited in a given tumor type; ii) is the expression of key mediators of cell death dependent on specific HDAC isoforms and iii) do HDAC inhibitors synergize with other chemotherapeutic drugs to induce the death of tumor cells?

In this study a novel molecular mechanism that links a specific HDAC isoform (HDAC2) to the alterations in the expression of Bcl-2 family members induced by HDAC inhibition was shown. HDAC inhibition by valproic acid (VPA) and genetic interference with HDAC2 induced a set of changes in HT-29 colon cancer cells which collectively promoted apoptosis. The profile of VPA-induced changes was characterized by upregulation of Bak, Bim and tBid, and downregulation of Bcl-XL expression. This profile is distinct of the frequently described HDAC inhibitors profile that involves an increase in Bax/Bcl-2 and Bax/Bcl-XL ratios. The expression of the proapoptotic proteins Bak and Bim specifically depended on the HDAC2 isoform. HDAC2 knockdown by siRNA in HT-29 cells or HDAC2 deficiency in mouse embryonic fibroblasts (MEFs) induced the expression of Bak and Bim. The expression of the antiapoptotic protein Bcl-XL was not regulated by HDAC2, but by the Ets2 transcriptor factor. The proapoptotic effector protein Bak was required for VPA-induced cell death, since Bak overexpression alone was sufficient to induce apoptosis of HT-29 cells and Bak knockdown protected cells from VPA-induced cell death. Thus, survival of colon cancer cells is associated with Bak repression specifically regulated by HDAC2 isoenzyme.

Colon tumor cells frequently acquire resistance to 5-fluorouracil (5-FU). In this study it was shown that VPA reduced the expression of two markers (Bcl-XL and TYMS), which were overexpressed in colon tumors and were specifically associated with 5-FU resistance. VPA synergized with 5-FU to inhibit the survival of DLD-1 (sensitive to 5-FU) and DLD1-5-FU/R (partially resistant to 5-FU, overexpressing Bcl-XL) cells, Thus, VPA treatment has the potential to increase the 5-FU cytotoxic effect in colon cancer. VPA has not synergized with 5-FU to reduce the survival of 5F12 cells (resistant to 5-FU, overexpressing TYMS) and of their parental cells (sensitive to 5-FU). The levels of TYMS still present in the cells after the VPA treatment might be a major limiting factor of the success of the combined therapy.

Altogether these results indicate that the VPA-induced expression profile is characterized by multiple alterations in apoptotic signaling that facilitate induction of cell death. It remains to be established which of these changes are triggered in individual cancer patients during clinical trials using VPA as a single therapeutic agent or in combinations with other anti-cancer drugs (e.g. 5-FU).

7 REFERENCES

1. Fulda, S. and K.M. Debatin, *Extrinsic versus intrinsic apoptosis pathways in anticancer chemotherapy*. Oncogene, 2006. **25**(34): p. 4798-811.
2. Kim, R., et al., *Current status of the molecular mechanisms of anticancer drug-induced apoptosis. The contribution of molecular-level analysis to cancer chemotherapy*. Cancer Chemother Pharmacol, 2002. **50**(5): p. 343-52.
3. Fesik, S.W., *Promoting apoptosis as a strategy for cancer drug discovery.* Nat Rev Cancer, 2005. **5**(11): p. 876-85.
4. Labi, V., et al., *BH3-only proteins in cell death initiation, malignant disease and anticancer therapy.* Cell Death Differ, 2006. **13**(8): p. 1325-38.
5. Kerr, J.F., A.H. Wyllie, and A.R. Currie, *Apoptosis: a basic biological phenomenon with wide-ranging implications in tissue kinetics.* Br J Cancer, 1972. **26**(4): p. 239-57.
6. Chan, S.L. and V.C. Yu, *Proteins of the bcl-2 family in apoptosis signalling: from mechanistic insights to therapeutic opportunities.* Clin Exp Pharmacol Physiol, 2004. **31**(3): p. 119-28.
7. Hengartner, M.O., *The biochemistry of apoptosis.* Nature, 2000. **407**(6805): p. 770-6.
8. Savill, J. and V. Fadok, *Corpse clearance defines the meaning of cell death.* Nature, 2000. **407**(6805): p. 784-8.
9. Erwig, L.P. and P.M. Henson, *Clearance of apoptotic cells by phagocytes.* Cell Death Differ, 2008. **15**(2): p. 243-50.
10. Riedl, S.J. and G.S. Salvesen, *The apoptosome: signalling platform of cell death.* Nat Rev Mol Cell Biol, 2007. **8**(5): p. 405-13.
11. Youle, R.J. and A. Strasser, *The BCL-2 protein family: opposing activities that mediate cell death.* Nat Rev Mol Cell Biol, 2008. **9**(1): p. 47-59.
12. Green, D.R. and G. Kroemer, *The pathophysiology of mitochondrial cell death.* Science, 2004. **305**(5684): p. 626-9.
13. Danial, N.N. and S.J. Korsmeyer, *Cell death: critical control points.* Cell, 2004. **116**(2): p. 205-19.
14. Degterev, A. and J. Yuan, *Expansion and evolution of cell death programmes.* Nat Rev Mol Cell Biol, 2008. **9**(5): p. 378-90.
15. Wei, M.C., et al., *tBID, a membrane-targeted death ligand, oligomerizes BAK to release cytochrome c.* Genes Dev, 2000. **14**(16): p. 2060-71.
16. Korsmeyer, S.J., et al., *Pro-apoptotic cascade activates BID, which oligomerizes BAK or BAX into pores that result in the release of cytochrome c.* Cell Death Differ, 2000. **7**(12): p. 1166-73.
17. Cowling, V. and J. Downward, *Caspase-6 is the direct activator of caspase-8 in the cytochrome c-induced apoptosis pathway: absolute requirement for removal of caspase-6 prodomain.* Cell Death Differ, 2002. **9**(10): p. 1046-56.
18. Zhai, D., et al., *Differential regulation of Bax and Bak by anti-apoptotic Bcl-2-family proteins, Bcl-B and Mcl-1.* J Biol Chem, 2008.
19. Dai, Y. and S. Grant, *Targeting multiple arms of the apoptotic regulatory machinery.* Cancer Res, 2007. **67**(7): p. 2908-11.
20. Kluck, R.M., et al., *The release of cytochrome c from mitochondria: a primary site for Bcl-2 regulation of apoptosis.* Science, 1997. **275**(5303): p. 1132-6.
21. Yang, J., et al., *Prevention of apoptosis by Bcl-2: release of cytochrome c from mitochondria blocked.* Science, 1997. **275**(5303): p. 1129-32.
22. Vaux, D.L. and J. Silke, *Mammalian mitochondrial IAP binding proteins.* Biochem Biophys Res Commun, 2003. **304**(3): p. 499-504.

23. Huang, Y., et al., *Requirement of both the second and third BIR domains for the relief of X-linked inhibitor of apoptosis protein (XIAP)-mediated caspase inhibition by Smac.* J Biol Chem, 2003. **278**(49): p. 49517-22.
24. Saelens, X., et al., *Toxic proteins released from mitochondria in cell death.* Oncogene, 2004. **23**(16): p. 2861-74.
25. Antignani, A. and R.J. Youle, *How do Bax and Bak lead to permeabilization of the outer mitochondrial membrane?* Curr Opin Cell Biol, 2006. **18**(6): p. 685-9.
26. Kroemer, G., L. Galluzzi, and C. Brenner, *Mitochondrial membrane permeabilization in cell death.* Physiol Rev, 2007. **87**(1): p. 99-163.
27. Tsujimoto, Y., et al., *Involvement of the bcl-2 gene in human follicular lymphoma.* Science, 1985. **228**(4706): p. 1440-3.
28. Bakhshi, A., et al., *Cloning the chromosomal breakpoint of t(14;18) human lymphomas: clustering around JH on chromosome 14 and near a transcriptional unit on 18.* Cell, 1985. **41**(3): p. 899-906.
29. Cleary, M.L., S.D. Smith, and J. Sklar, *Cloning and structural analysis of cDNAs for bcl-2 and a hybrid bcl-2/immunoglobulin transcript resulting from the t(14;18) translocation.* Cell, 1986. **47**(1): p. 19-28.
30. Vaux, D.L., S. Cory, and J.M. Adams, *Bcl-2 gene promotes haemopoietic cell survival and cooperates with c-myc to immortalize pre-B cells.* Nature, 1988. **335**(6189): p. 440-2.
31. Lalier, L., et al., *Bax activation and mitochondrial insertion during apoptosis.* Apoptosis, 2007. **12**(5): p. 887-96.
32. Shimazu, T., et al., *NBK/BIK antagonizes MCL-1 and BCL-XL and activates BAK-mediated apoptosis in response to protein synthesis inhibition.* Genes Dev, 2007. **21**(8): p. 929-41.
33. Willis, S.N., et al., *Proapoptotic Bak is sequestered by Mcl-1 and Bcl-xL, but not Bcl-2, until displaced by BH3-only proteins.* Genes Dev, 2005. **19**(11): p. 1294-305.
34. Shankar, S. and R.K. Srivastava, *Bax and Bak genes are essential for maximum apoptotic response by curcumin, a polyphenolic compound and cancer chemopreventive agent derived from turmeric, Curcuma longa.* Carcinogenesis, 2007. **28**(6): p. 1277-86.
35. Letai, A., et al., *Distinct BH3 domains either sensitize or activate mitochondrial apoptosis, serving as prototype cancer therapeutics.* Cancer Cell, 2002. **2**(3): p. 183-92.
36. Fletcher, J.I. and D.C. Huang, *BH3-only proteins: orchestrating cell death.* Cell Death Differ, 2006. **13**(8): p. 1268-71.
37. Labi, V., et al., *Targeting the Bcl-2-regulated apoptosis pathway by BH3 mimetics: a breakthrough in anticancer therapy?* Cell Death Differ, 2008. **15**(6): p. 977-87.
38. Adams, J.M. and S. Cory, *The Bcl-2 protein family: arbiters of cell survival.* Science, 1998. **281**(5381): p. 1322-6.
39. Reed, J.C., *Bcl-2 family proteins.* Oncogene, 1998. **17**(25): p. 3225-36.
40. Juin, P., et al., *Shooting at survivors: Bcl-2 family members as drug targets for cancer.* Biochim Biophys Acta, 2004. **1644**(2-3): p. 251-60.
41. Schwartz, P.S. and D.M. Hockenbery, *Bcl-2-related survival proteins.* Cell Death Differ, 2006. **13**(8): p. 1250-5.
42. Butt, A.J., et al., *A novel plant toxin, persin, with in vivo activity in the mammary gland, induces Bim-dependent apoptosis in human breast cancer cells.* Mol Cancer Ther, 2006. **5**(9): p. 2300-9.
43. Bratton, S.B. and G.M. Cohen, *Apoptotic death sensor: an organelle's alter ego?* Trends Pharmacol Sci, 2001. **22**(6): p. 306-15.

44. Puthalakath, H., et al., *The proapoptotic activity of the Bcl-2 family member Bim is regulated by interaction with the dynein motor complex.* Mol Cell, 1999. **3**(3): p. 287-96.
45. Puthalakath, H. and A. Strasser, *Keeping killers on a tight leash: transcriptional and post-translational control of the pro-apoptotic activity of BH3-only proteins.* Cell Death Differ, 2002. **9**(5): p. 505-12.
46. O'Connor, L., et al., *Bim: a novel member of the Bcl-2 family that promotes apoptosis.* Embo J, 1998. **17**(2): p. 384-95.
47. Chinnadurai, G., S. Vijayalingam, and R. Rashmi, *BIK, the founding member of the BH3-only family proteins: mechanisms of cell death and role in cancer and pathogenic processes.* Oncogene, 2008. **27 Suppl 1**: p. S20-9.
48. Nakano, K. and K.H. Vousden, *PUMA, a novel proapoptotic gene, is induced by p53.* Mol Cell, 2001. **7**(3): p. 683-94.
49. Shibue, T., et al., *Integral role of Noxa in p53-mediated apoptotic response.* Genes Dev, 2003. **17**(18): p. 2233-8.
50. Weber, A., et al., *BimS-induced apoptosis requires mitochondrial localization but not interaction with anti-apoptotic Bcl-2 proteins.* J Cell Biol, 2007. **177**(4): p. 625-36.
51. Schinzel, A., et al., *Conformational control of Bax localization and apoptotic activity by Pro168.* J Cell Biol, 2004. **164**(7): p. 1021-32.
52. Ruffolo, S.C. and G.C. Shore, *BCL-2 selectively interacts with the BID-induced open conformer of BAK, inhibiting BAK auto-oligomerization.* J Biol Chem, 2003. **278**(27): p. 25039-45.
53. Zhong, Q., et al., *Mule/ARF-BP1, a BH3-only E3 ubiquitin ligase, catalyzes the polyubiquitination of Mcl-1 and regulates apoptosis.* Cell, 2005. **121**(7): p. 1085-95.
54. Nijhawan, D., et al., *Elimination of Mcl-1 is required for the initiation of apoptosis following ultraviolet irradiation.* Genes Dev, 2003. **17**(12): p. 1475-86.
55. Chittenden, T., *BH3 domains: intracellular death-ligands critical for initiating apoptosis.* Cancer Cell, 2002. **2**(3): p. 165-6.
56. Degenhardt, K., et al., *Bax and Bak independently promote cytochrome C release from mitochondria.* J Biol Chem, 2002. **277**(16): p. 14127-34.
57. Wei, M.C., et al., *Proapoptotic BAX and BAK: a requisite gateway to mitochondrial dysfunction and death.* Science, 2001. **292**(5517): p. 727-30.
58. Cheng, E.H., et al., *BCL-2, BCL-X(L) sequester BH3 domain-only molecules preventing BAX- and BAK-mediated mitochondrial apoptosis.* Mol Cell, 2001. **8**(3): p. 705-11.
59. Zong, W.X., et al., *BH3-only proteins that bind pro-survival Bcl-2 family members fail to induce apoptosis in the absence of Bax and Bak.* Genes Dev, 2001. **15**(12): p. 1481-6.
60. Nechushtan, A., et al., *Bax and Bak coalesce into novel mitochondria-associated clusters during apoptosis.* J Cell Biol, 2001. **153**(6): p. 1265-76.
61. Youle, R.J. and M. Karbowski, *Mitochondrial fission in apoptosis.* Nat Rev Mol Cell Biol, 2005. **6**(8): p. 657-63.
62. Brooks, C., et al., *Bak regulates mitochondrial morphology and pathology during apoptosis by interacting with mitofusins.* Proc Natl Acad Sci U S A, 2007. **104**(28): p. 11649-54.
63. Wang, G.Q., et al., *A role for mitochondrial Bak in apoptotic response to anticancer drugs.* J Biol Chem, 2001. **276**(36): p. 34307-17.
64. Kirkin, V., S. Joos, and M. Zornig, *The role of Bcl-2 family members in tumorigenesis.* Biochim Biophys Acta, 2004. **1644**(2-3): p. 229-49.
65. Pommier, Y., et al., *Apoptosis defects and chemotherapy resistance: molecular interaction maps and networks.* Oncogene, 2004. **23**(16): p. 2934-49.

66. Amundson, S.A., et al., *An informatics approach identifying markers of chemosensitivity in human cancer cell lines.* Cancer Res, 2000. **60**(21): p. 6101-10.
67. Violette, S., et al., *Resistance of colon cancer cells to long-term 5-fluorouracil exposure is correlated to the relative level of Bcl-2 and Bcl-X(L) in addition to Bax and p53 status.* Int J Cancer, 2002. **98**(4): p. 498-504.
68. Degenhardt, K., et al., *BAX and BAK mediate p53-independent suppression of tumorigenesis.* Cancer Cell, 2002. **2**(3): p. 193-203.
69. Rampino, N., et al., *Somatic frameshift mutations in the BAX gene in colon cancers of the microsatellite mutator phenotype.* Science, 1997. **275**(5302): p. 967-9.
70. Kondo, S., et al., *Mutations of the bak gene in human gastric and colorectal cancers.* Cancer Res, 2000. **60**(16): p. 4328-30.
71. Krajewska, M., et al., *Elevated expression of Bcl-X and reduced Bak in primary colorectal adenocarcinomas.* Cancer Res, 1996. **56**(10): p. 2422-7.
72. Bolden, J.E., M.J. Peart, and R.W. Johnstone, *Anticancer activities of histone deacetylase inhibitors.* Nat Rev Drug Discov, 2006. **5**(9): p. 769-84.
73. Johnstone, R.W. and J.D. Licht, *Histone deacetylase inhibitors in cancer therapy: is transcription the primary target?* Cancer Cell, 2003. **4**(1): p. 13-8.
74. Glozak, M.A. and E. Seto, *Histone deacetylases and cancer.* Oncogene, 2007. **26**(37): p. 5420-32.
75. Ropero, S. and M. Esteller, *The role of histone deacetylases (HDACs) in human cancer.* Mol Oncol, 2007. **1**(1): p. 19-25.
76. Strahl, B.D. and C.D. Allis, *The language of covalent histone modifications.* Nature, 2000. **403**(6765): p. 41-5.
77. Boyle, G.M., A.C. Martyn, and P.G. Parsons, *Histone deacetylase inhibitors and malignant melanoma.* Pigment Cell Res, 2005. **18**(3): p. 160-6.
78. Kramer, O.H., M. Gottlicher, and T. Heinzel, *Histone deacetylase as a therapeutic target.* Trends Endocrinol Metab, 2001. **12**(7): p. 294-300.
79. Rosenfeld, M.G., V.V. Lunyak, and C.K. Glass, *Sensors and signals: a coactivator/corepressor/epigenetic code for integrating signal-dependent programs of transcriptional response.* Genes Dev, 2006. **20**(11): p. 1405-28.
80. Xu, W.S., R.B. Parmigiani, and P.A. Marks, *Histone deacetylase inhibitors: molecular mechanisms of action.* Oncogene, 2007. **26**(37): p. 5541-52.
81. Minucci, S. and P.G. Pelicci, *Histone deacetylase inhibitors and the promise of epigenetic (and more) treatments for cancer.* Nat Rev Cancer, 2006. **6**(1): p. 38-51.
82. Martin, M., R. Kettmann, and F. Dequiedt, *Class IIa histone deacetylases: regulating the regulators.* Oncogene, 2007. **26**(37): p. 5450-67.
83. Gregoretti, I.V., Y.M. Lee, and H.V. Goodson, *Molecular evolution of the histone deacetylase family: functional implications of phylogenetic analysis.* J Mol Biol, 2004. **338**(1): p. 17-31.
84. Verdin, E., F. Dequiedt, and H.G. Kasler, *Class II histone deacetylases: versatile regulators.* Trends Genet, 2003. **19**(5): p. 286-93.
85. Blander, G. and L. Guarente, *The Sir2 family of protein deacetylases.* Annu Rev Biochem, 2004. **73**: p. 417-35.
86. Gao, L., et al., *Cloning and functional characterization of HDAC11, a novel member of the human histone deacetylase family.* J Biol Chem, 2002. **277**(28): p. 25748-55.
87. Acharya, M.R., et al., *Rational development of histone deacetylase inhibitors as anticancer agents: a review.* Mol Pharmacol, 2005. **68**(4): p. 917-32.
88. Lin, R.J., et al., *Transcriptional regulation in acute promyelocytic leukemia.* Oncogene, 2001. **20**(49): p. 7204-15.
89. Pandolfi, P.P., *Transcription therapy for cancer.* Oncogene, 2001. **20**(24): p. 3116-27.
90. Moe-Behrens, G.H. and P.P. Pandolfi, *Targeting aberrant transcriptional repression in acute myeloid leukemia.* Rev Clin Exp Hematol, 2003. **7**(2): p. 139-59.

91. Pasqualucci, L., et al., *Molecular pathogenesis of non-Hodgkin's lymphoma: the role of Bcl-6.* Leuk Lymphoma, 2003. **44 Suppl 3**: p. S5-12.
92. Weichert, W., *HDAC expression and clinical prognosis in human malignancies.* Cancer Lett, 2009. **280**(2): p. 168-76.
93. Witt, O., et al., *HDAC family: What are the cancer relevant targets?* Cancer Lett, 2009. **277**(1): p. 8-21.
94. Zhu, P., et al., *Induction of HDAC2 expression upon loss of APC in colorectal tumorigenesis.* Cancer Cell, 2004. **5**(5): p. 455-63.
95. Zimmermann, S., et al., *Reduced body size and decreased intestinal tumor rates in HDAC2-mutant mice.* Cancer Res, 2007. **67**(19): p. 9047-54.
96. Choi, J.H., et al., *Expression profile of histone deacetylase 1 in gastric cancer tissues.* Jpn J Cancer Res, 2001. **92**(12): p. 1300-4.
97. Weichert, W., et al., *Association of patterns of class I histone deacetylase expression with patient prognosis in gastric cancer: a retrospective analysis.* Lancet Oncol, 2008. **9**(2): p. 139-48.
98. Weichert, W., et al., *Histone deacetylases 1, 2 and 3 are highly expressed in prostate cancer and HDAC2 expression is associated with shorter PSA relapse time after radical prostatectomy.* Br J Cancer, 2008. **98**(3): p. 604-10.
99. Wilson, A.J., et al., *Histone deacetylase 3 (HDAC3) and other class I HDACs regulate colon cell maturation and p21 expression and are deregulated in human colon cancer.* J Biol Chem, 2006. **281**(19): p. 13548-58.
100. Huang, B.H., et al., *Inhibition of histone deacetylase 2 increases apoptosis and p21Cip1/WAF1 expression, independent of histone deacetylase 1.* Cell Death Differ, 2005. **12**(4): p. 395-404.
101. Oehme, I., et al., *Histone deacetylase 8 in neuroblastoma tumorigenesis.* Clin Cancer Res, 2009. **15**(1): p. 91-9.
102. Ozdag, H., et al., *Differential expression of selected histone modifier genes in human solid cancers.* BMC Genomics, 2006. **7**: p. 90.
103. Bai, X., et al., *Overexpression of myocyte enhancer factor 2 and histone hyperacetylation in hepatocellular carcinoma.* J Cancer Res Clin Oncol, 2008. **134**(1): p. 83-91.
104. Sakuma, T., et al., *Aberrant expression of histone deacetylase 6 in oral squamous cell carcinoma.* Int J Oncol, 2006. **29**(1): p. 117-24.
105. Kurdistani, S.K., *Histone modifications as markers of cancer prognosis: a cellular view.* Br J Cancer, 2007. **97**(1): p. 1-5.
106. Stimson, L. and N.B. La Thangue, *Biomarkers for predicting clinical responses to HDAC inhibitors.* Cancer Lett, 2009. **280**(2): p. 177-83.
107. Hu, E., et al., *Identification of novel isoform-selective inhibitors within class I histone deacetylases.* J Pharmacol Exp Ther, 2003. **307**(2): p. 720-8.
108. Furumai, R., et al., *FK228 (depsipeptide) as a natural prodrug that inhibits class I histone deacetylases.* Cancer Res, 2002. **62**(17): p. 4916-21.
109. Haggarty, S.J., et al., *Domain-selective small-molecule inhibitor of histone deacetylase 6 (HDAC6)-mediated tubulin deacetylation.* Proc Natl Acad Sci U S A, 2003. **100**(8): p. 4389-94.
110. Gottlicher, M., et al., *Valproic acid defines a novel class of HDAC inhibitors inducing differentiation of transformed cells.* EMBO J, 2001. **20**(24): p. 6969-78.
111. Bug, G., et al., *Clinical trial of valproic acid and all-trans retinoic acid in patients with poor-risk acute myeloid leukemia.* Cancer, 2005. **104**(12): p. 2717-25.
112. Hanahan, D. and R.A. Weinberg, *The hallmarks of cancer.* Cell, 2000. **100**(1): p. 57-70.
113. Ziegler, D.S. and A.L. Kung, *Therapeutic targeting of apoptosis pathways in cancer.* Curr Opin Oncol, 2008. **20**(1): p. 97-103.

114. Batty, N., G.G. Malouf, and J.P. Issa, *Histone deacetylase inhibitors as anti-neoplastic agents.* Cancer Lett, 2009. **280**(2): p. 192-200.
115. Ungerstedt, J.S., et al., *Role of thioredoxin in the response of normal and transformed cells to histone deacetylase inhibitors.* Proc Natl Acad Sci U S A, 2005. **102**(3): p. 673-8.
116. Burgess, A., et al., *Histone deacetylase inhibitors specifically kill nonproliferating tumour cells.* Oncogene, 2004. **23**(40): p. 6693-701.
117. Insinga, A., S. Minucci, and P.G. Pelicci, *Mechanisms of selective anticancer action of histone deacetylase inhibitors.* Cell Cycle, 2005. **4**(6): p. 741-3.
118. Zhang, X.D., et al., *The histone deacetylase inhibitor suberic bishydroxamate regulates the expression of multiple apoptotic mediators and induces mitochondria-dependent apoptosis of melanoma cells.* Mol Cancer Ther, 2004. **3**(4): p. 425-35.
119. Xu, W., et al., *Intrinsic apoptotic and thioredoxin pathways in human prostate cancer cell response to histone deacetylase inhibitor.* Proc Natl Acad Sci U S A, 2006. **103**(42): p. 15540-5.
120. Shankar, S., et al., *Interactive effects of histone deacetylase inhibitors and TRAIL on apoptosis in human leukemia cells: involvement of both death receptor and mitochondrial pathways.* Int J Mol Med, 2005. **16**(6): p. 1125-38.
121. Baradari, V., et al., *Histone deacetylase inhibitor MS-275 alone or combined with bortezomib or sorafenib exhibits strong antiproliferative action in human cholangiocarcinoma cells.* World J Gastroenterol, 2007. **13**(33): p. 4458-66.
122. Mitsiades, C.S., et al., *Novel histone deacetylase inhibitors in the treatment of thyroid cancer.* Clin Cancer Res, 2005. **11**(10): p. 3958-65.
123. Sutheesophon, K., et al., *Histone deacetylase inhibitor depsipeptide (FK228) induces apoptosis in leukemic cells by facilitating mitochondrial translocation of Bax, which is enhanced by the proteasome inhibitor bortezomib.* Acta Haematol, 2006. **115**(1-2): p. 78-90.
124. Zhao, Y., et al., *Inhibitors of histone deacetylases target the Rb-E2F1 pathway for apoptosis induction through activation of proapoptotic protein Bim.* Proc Natl Acad Sci U S A, 2005. **102**(44): p. 16090-5.
125. Zhang, Y., et al., *Bmf is a possible mediator in histone deacetylase inhibitors FK228 and CBHA-induced apoptosis.* Cell Death Differ, 2006. **13**(1): p. 129-40.
126. Ruefli, A.A., et al., *The histone deacetylase inhibitor and chemotherapeutic agent suberoylanilide hydroxamic acid (SAHA) induces a cell-death pathway characterized by cleavage of Bid and production of reactive oxygen species.* Proc Natl Acad Sci U S A, 2001. **98**(19): p. 10833-8.
127. Lucas, D.M., et al., *The histone deacetylase inhibitor MS-275 induces caspase-dependent apoptosis in B-cell chronic lymphocytic leukemia cells.* Leukemia, 2004. **18**(7): p. 1207-14.
128. Singh, T.R., S. Shankar, and R.K. Srivastava, *HDAC inhibitors enhance the apoptosis-inducing potential of TRAIL in breast carcinoma.* Oncogene, 2005. **24**(29): p. 4609-23.
129. Bokelmann, I. and U. Mahlknecht, *Valproic acid sensitizes chronic lymphocytic leukemia cells to apoptosis and restores the balance between pro- and antiapoptotic proteins.* Mol Med, 2008. **14**(1-2): p. 20-7.
130. Gillespie, S., et al., *Bim plays a crucial role in synergistic induction of apoptosis by the histone deacetylase inhibitor SBHA and TRAIL in melanoma cells.* Apoptosis, 2006. **11**(12): p. 2251-65.
131. Kramer, O.H., et al., *The histone deacetylase inhibitor valproic acid selectively induces proteasomal degradation of HDAC2.* EMBO J, 2003. **22**(13): p. 3411-20.
132. Gottlicher, M., *Valproic acid: an old drug newly discovered as inhibitor of histone deacetylases.* Ann Hematol, 2004. **83 Suppl 1**: p. S91-2.

133. Armeanu, S., et al., *Apoptosis on hepatoma cells but not on primary hepatocytes by histone deacetylase inhibitors valproate and ITF2357.* J Hepatol, 2005. **42**(2): p. 210-7.
134. Valentini, A., et al., *Valproic acid induces apoptosis, p16INK4A upregulation and sensitization to chemotherapy in human melanoma cells.* Cancer Biol Ther, 2007. **6**(2): p. 185-91.
135. Facchetti, F., et al., *Modulation of pro- and anti-apoptotic factors in human melanoma cells exposed to histone deacetylase inhibitors.* Apoptosis, 2004. **9**(5): p. 573-82.
136. Catalano, M.G., et al., *Valproic acid induces apoptosis and cell cycle arrest in poorly differentiated thyroid cancer cells.* J Clin Endocrinol Metab, 2005. **90**(3): p. 1383-9.
137. Shabbeer, S., et al., *Multiple Molecular pathways explain the anti-proliferative effect of valproic acid on prostate cancer cells in vitro and in vivo.* Prostate, 2007. **67**(10): p. 1099-110.
138. Fortunati, N., et al., *Valproic acid is a selective antiproliferative agent in estrogen-sensitive breast cancer cells.* Cancer Lett, 2008. **259**(2): p. 156-64.
139. Kawagoe, R., H. Kawagoe, and K. Sano, *Valproic acid induces apoptosis in human leukemia cells by stimulating both caspase-dependent and -independent apoptotic signaling pathways.* Leuk Res, 2002. **26**(5): p. 495-502.
140. Tang, R., et al., *Valproic acid inhibits proliferation and induces apoptosis in acute myeloid leukemia cells expressing P-gp and MRP1.* Leukemia, 2004. **18**(7): p. 1246-51.
141. Takai, N., et al., *Histone deacetylase inhibitors have a profound antigrowth activity in endometrial cancer cells.* Clin Cancer Res, 2004. **10**(3): p. 1141-9.
142. Chen, J., et al., *Valproic acid and butyrate induce apoptosis in human cancer cells through inhibition of gene expression of Akt/protein kinase B.* Mol Cancer, 2006. **5**: p. 71.
143. Duenas-Gonzalez, A., et al., *Valproic acid as epigenetic cancer drug: preclinical, clinical and transcriptional effects on solid tumors.* Cancer Treat Rev, 2008. **34**(3): p. 206-22.
144. Kuendgen, A., et al., *Results of a phase 2 study of valproic acid alone or in combination with all-trans retinoic acid in 75 patients with myelodysplastic syndrome and relapsed or refractory acute myeloid leukemia.* Ann Hematol, 2005. **84 Suppl 1**: p. 61-6.
145. Kuendgen, A. and N. Gattermann, *Valproic acid for the treatment of myeloid malignancies.* Cancer, 2007. **110**(5): p. 943-54.
146. Chavez-Blanco, A., et al., *Histone acetylation and histone deacetylase activity of magnesium valproate in tumor and peripheral blood of patients with cervical cancer. A phase I study.* Mol Cancer, 2005. **4**(1): p. 22.
147. Atmaca, A., et al., *Valproic acid (VPA) in patients with refractory advanced cancer: a dose escalating phase I clinical trial.* Br J Cancer, 2007. **97**(2): p. 177-82.
148. Ricci-Vitiani, L., et al., *Colon cancer stem cells.* Gut, 2008. **57**(4): p. 538-48.
149. Longley, D.B., D.P. Harkin, and P.G. Johnston, *5-fluorouracil: mechanisms of action and clinical strategies.* Nat Rev Cancer, 2003. **3**(5): p. 330-8.
150. Goyle, S. and A. Maraveyas, *Chemotherapy for colorectal cancer.* Dig Surg, 2005. **22**(6): p. 401-14.
151. Ladner, R.D., *The role of dUTPase and uracil-DNA repair in cancer chemotherapy.* Curr Protein Pept Sci, 2001. **2**(4): p. 361-70.
152. Chu, E., et al., *Thymidylate synthase inhibitors as anticancer agents: from bench to bedside.* Cancer Chemother Pharmacol, 2003. **52 Suppl 1**: p. S80-9.
153. Formentini, A., D. Henne-Bruns, and M. Kornmann, *Thymidylate synthase expression and prognosis of patients with gastrointestinal cancers receiving adjuvant chemotherapy: a review.* Langenbecks Arch Surg, 2004. **389**(5): p. 405-13.

154. de Angelis, P.M., et al., *Molecular characterizations of derivatives of HCT116 colorectal cancer cells that are resistant to the chemotherapeutic agent 5-fluorouracil.* Int J Oncol, 2004. **24**(5): p. 1279-88.
155. De Angelis, P.M., et al., *Cellular response to 5-fluorouracil (5-FU) in 5-FU-resistant colon cancer cell lines during treatment and recovery.* Mol Cancer, 2006. **5**: p. 20.
156. Shimizu, D., et al., *Prediction of chemosensitivity of colorectal cancer to 5-fluorouracil by gene expression profiling with cDNA microarrays.* Int J Oncol, 2005. **27**(2): p. 371-6.
157. Schmidt, W.M., et al., *Dissecting progressive stages of 5-fluorouracil resistance in vitro using RNA expression profiling.* Int J Cancer, 2004. **112**(2): p. 200-12.
158. Wang, W., et al., *Mechanistic and predictive profiling of 5-Fluorouracil resistance in human cancer cells.* Cancer Res, 2004. **64**(22): p. 8167-76.
159. Peters, G.J., et al., *Induction of thymidylate synthase as a 5-fluorouracil resistance mechanism.* Biochim Biophys Acta, 2002. **1587**(2-3): p. 194-205.
160. Aschele, C., S. Lonardi, and S. Monfardini, *Thymidylate Synthase expression as a predictor of clinical response to fluoropyrimidine-based chemotherapy in advanced colorectal cancer.* Cancer Treat Rev, 2002. **28**(1): p. 27-47.
161. Johnston, P.G., et al., *Thymidylate synthase gene and protein expression correlate and are associated with response to 5-fluorouracil in human colorectal and gastric tumors.* Cancer Res, 1995. **55**(7): p. 1407-12.
162. Zhu, H., et al., *Bcl-XL small interfering RNA suppresses the proliferation of 5-fluorouracil-resistant human colon cancer cells.* Mol Cancer Ther, 2005. **4**(3): p. 451-6.
163. Oliver, L., et al., *Resistance to apoptosis is increased during metastatic dissemination of colon cancer.* Clin Exp Metastasis, 2002. **19**(2): p. 175-80.
164. Longley, D.B., W.L. Allen, and P.G. Johnston, *Drug resistance, predictive markers and pharmacogenomics in colorectal cancer.* Biochim Biophys Acta, 2006. **1766**(2): p. 184-96.
165. Zhu, H., et al., *Adenovirus-mediated small hairpin RNA targeting Bcl-XL as therapy for colon cancer.* Int J Cancer, 2007. **121**(6): p. 1366-72.
166. Frew, A.J., R.W. Johnstone, and J.E. Bolden, *Enhancing the apoptotic and therapeutic effects of HDAC inhibitors.* Cancer Lett, 2009. **280**(2): p. 125-33.
167. Ocker, M., et al., *The histone-deacetylase inhibitor SAHA potentiates proapoptotic effects of 5-fluorouracil and irinotecan in hepatoma cells.* J Cancer Res Clin Oncol, 2005. **131**(6): p. 385-94.
168. Lee, J.H., et al., *Histone deacetylase inhibitor enhances 5-fluorouracil cytotoxicity by down-regulating thymidylate synthase in human cancer cells.* Mol Cancer Ther, 2006. **5**(12): p. 3085-95.
169. Tumber, A., et al., *The histone deacetylase inhibitor PXD101 synergises with 5-fluorouracil to inhibit colon cancer cell growth in vitro and in vivo.* Cancer Chemother Pharmacol, 2007. **60**(2): p. 275-83.
170. Sung, M.W. and S. Waxman, *Combination of cytotoxic-differentiation therapy with 5-fluorouracil and phenylbutyrate in patients with advanced colorectal cancer.* Anticancer Res, 2007. **27**(2): p. 995-1001.
171. Carew, J.S., F.J. Giles, and S.T. Nawrocki, *Histone deacetylase inhibitors: mechanisms of cell death and promise in combination cancer therapy.* Cancer Lett, 2008. **269**(1): p. 7-17.
172. Leteurtre, E., et al., *Differential mucin expression in colon carcinoma HT-29 clones with variable resistance to 5-fluorouracil and methotrexate.* Biol Cell, 2004. **96**(2): p. 145-51.

173. Lesuffleur, T., et al., *Adaptation to 5-fluorouracil of the heterogeneous human colon tumor cell line HT-29 results in the selection of cells committed to differentiation.* Int J Cancer, 1991. **49**(5): p. 721-30.
174. Pfaffl, M.W., G.W. Horgan, and L. Dempfle, *Relative expression software tool (REST) for group-wise comparison and statistical analysis of relative expression results in real-time PCR.* Nucleic Acids Res, 2002. **30**(9): p. e36.
175. Gottlieb, R.A. and S. Adachi, *Nitrogen cavitation for cell disruption to obtain mitochondria from cultured cells.* Methods Enzymol, 2000. **322**: p. 213-21.
176. Chittenden, T., et al., *A conserved domain in Bak, distinct from BH1 and BH2, mediates cell death and protein binding functions.* EMBO J, 1995. **14**(22): p. 5589-96.
177. Zhu, P., et al., *Specific and redundant functions of histone deacetylases in regulation of cell cycle and apoptosis.* Cell Cycle, 2004. **3**(10): p. 1240-2.
178. Pelengaris, S., M. Khan, and G. Evan, *c-MYC: more than just a matter of life and death.* Nat Rev Cancer, 2002. **2**(10): p. 764-76.
179. Polager, S. and D. Ginsberg, *E2F - at the crossroads of life and death.* Trends Cell Biol, 2008. **18**(11): p. 528-35.
180. Sevilla, L., et al., *The Ets2 transcription factor inhibits apoptosis induced by colony-stimulating factor 1 deprivation of macrophages through a Bcl-xL-dependent mechanism.* Mol Cell Biol, 1999. **19**(4): p. 2624-34.
181. Zhang, Q., et al., *Tumor necrosis factor prevents alendronate-induced osteoclast apoptosis in vivo by stimulating Bcl-xL expression through Ets-2.* Arthritis Rheum, 2005. **52**(9): p. 2708-18.
182. Habens, F., et al., *Distinct promoters mediate constitutive and inducible Bcl-XL expression in malignant lymphocytes.* Oncogene, 2007. **26**(13): p. 1910-9.
183. Cao, X., et al., *Up-regulation of Bcl-xl by hepatocyte growth factor in human mesothelioma cells involves ETS transcription factors.* Am J Pathol, 2009. **175**(5): p. 2207-16.
184. Smith, J.L., et al., *ets-2 is a target for an akt (Protein kinase B)/jun N-terminal kinase signaling pathway in macrophages of motheaten-viable mutant mice.* Mol Cell Biol, 2000. **20**(21): p. 8026-34.
185. Yordy, J.S. and R.C. Muise-Helmericks, *Signal transduction and the Ets family of transcription factors.* Oncogene, 2000. **19**(55): p. 6503-13.
186. Yang, B.S., et al., *Ras-mediated phosphorylation of a conserved threonine residue enhances the transactivation activities of c-Ets1 and c-Ets2.* Mol Cell Biol, 1996. **16**(2): p. 538-47.
187. Van Cutsem, E. and J. Oliveira, *Primary colon cancer: ESMO clinical recommendations for diagnosis, adjuvant treatment and follow-up.* Ann Oncol, 2009. **20 Suppl 4**: p. 49-50.
188. Van Cutsem, E., B. Nordlinger, and A. Cervantes, *Advanced colorectal cancer: ESMO Clinical Practice Guidelines for treatment.* Ann Oncol, 2010. **21 Suppl 5**: p. v93-7.
189. Fazzone, W., et al., *Histone deacetylase inhibitors suppress thymidylate synthase gene expression and synergize with the fluoropyrimidines in colon cancer cells.* Int J Cancer, 2009. **125**(2): p. 463-73.
190. Salonga, D., et al., *Colorectal tumors responding to 5-fluorouracil have low gene expression levels of dihydropyrimidine dehydrogenase, thymidylate synthase, and thymidine phosphorylase.* Clin Cancer Res, 2000. **6**(4): p. 1322-7.
191. Biroccio, A., et al., *c-Myb and Bcl-x overexpression predicts poor prognosis in colorectal cancer: clinical and experimental findings.* Am J Pathol, 2001. **158**(4): p. 1289-99.
192. Glaser, K.B., et al., *Gene expression profiling of multiple histone deacetylase (HDAC) inhibitors: defining a common gene set produced by HDAC inhibition in T24 and MDA carcinoma cell lines.* Mol Cancer Ther, 2003. **2**(2): p. 151-63.

193. Peart, M.J., et al., *Identification and functional significance of genes regulated by structurally different histone deacetylase inhibitors.* Proc Natl Acad Sci U S A, 2005. **102**(10): p. 3697-702.
194. Reid, G., et al., *Multiple mechanisms induce transcriptional silencing of a subset of genes, including oestrogen receptor alpha, in response to deacetylase inhibition by valproic acid and trichostatin A.* Oncogene, 2005. **24**(31): p. 4894-907.
195. Joseph, J., et al., *Expression profiling of sodium butyrate (NaB)-treated cells: identification of regulation of genes related to cytokine signaling and cancer metastasis by NaB.* Oncogene, 2004. **23**(37): p. 6304-15.
196. Sutheesophon, K., et al., *Involvement of the tumor necrosis factor (TNF)/TNF receptor system in leukemic cell apoptosis induced by histone deacetylase inhibitor depsipeptide (FK228).* J Cell Physiol, 2005. **203**(2): p. 387-97.
197. Emanuele, S., et al., *SAHA induces apoptosis in hepatoma cells and synergistically interacts with the proteasome inhibitor Bortezomib.* Apoptosis, 2007. **12**(7): p. 1327-38.
198. Hess-Stumpp, H., et al., *MS-275, a potent orally available inhibitor of histone deacetylases--the development of an anticancer agent.* Int J Biochem Cell Biol, 2007. **39**(7-8): p. 1388-405.
199. Alao, J.P., et al., *Histone deacetylase inhibitor, trichostatin A induces ubiquitin-dependent cyclin D1 degradation in MCF-7 breast cancer cells.* Mol Cancer, 2006. **5**: p. 8.
200. Roy, S., R. Jeffrey, and M. Tenniswood, *Array-based analysis of the effects of trichostatin A and CG-1521 on cell cycle and cell death in LNCaP prostate cancer cells.* Mol Cancer Ther, 2008. **7**(7): p. 1931-9.
201. Chau, B.N., et al., *Aven, a novel inhibitor of caspase activation, binds Bcl-xL and Apaf-1.* Mol Cell, 2000. **6**(1): p. 31-40.
202. Nebbioso, A., et al., *Tumor-selective action of HDAC inhibitors involves TRAIL induction in acute myeloid leukemia cells.* Nat Med, 2005. **11**(1): p. 77-84.
203. Hemmati, P.G., et al., *Bak functionally complements for loss of Bax during p14ARF-induced mitochondrial apoptosis in human cancer cells.* Oncogene, 2006. **25**(50): p. 6582-94.
204. Catalano, M.G., et al., *Valproic acid enhances tubulin acetylation and apoptotic activity of paclitaxel on anaplastic thyroid cancer cell lines.* Endocr Relat Cancer, 2007. **14**(3): p. 839-45.
205. Castilla, C., et al., *Bcl-xL is overexpressed in hormone-resistant prostate cancer and promotes survival of LNCaP cells via interaction with proapoptotic Bak.* Endocrinology, 2006. **147**(10): p. 4960-7.
206. Simoes-Wust, A.P., et al., *Bcl-xl antisense treatment induces apoptosis in breast carcinoma cells.* Int J Cancer, 2000. **87**(4): p. 582-90.
207. Fennell, D.A., A. Chacko, and L. Mutti, *BCL-2 family regulation by the 20S proteasome inhibitor bortezomib.* Oncogene, 2008. **27**(9): p. 1189-97.
208. Almond, J.B. and G.M. Cohen, *The proteasome: a novel target for cancer chemotherapy.* Leukemia, 2002. **16**(4): p. 433-43.
209. Hur, J., et al., *Regulation of expression of BIK proapoptotic protein in human breast cancer cells: p53-dependent induction of BIK mRNA by fulvestrant and proteasomal degradation of BIK protein.* Cancer Res, 2006. **66**(20): p. 10153-61.
210. Marshansky, V., et al., *Proteasomes modulate balance among proapoptotic and antiapoptotic Bcl-2 family members and compromise functioning of the electron transport chain in leukemic cells.* J Immunol, 2001. **166**(5): p. 3130-42.
211. Zhu, H., et al., *Bik/NBK accumulation correlates with apoptosis-induction by bortezomib (PS-341, Velcade) and other proteasome inhibitors.* Oncogene, 2005. **24**(31): p. 4993-9.

212. Ying, S., et al., *Broad degradation of proapoptotic proteins with the conserved Bcl-2 homology domain 3 during infection with Chlamydia trachomatis.* Infect Immun, 2005. **73**(3): p. 1399-403.
213. Yu, J. and L. Zhang, *PUMA, a potent killer with or without p53.* Oncogene, 2008. **27 Suppl 1**: p. S71-83.
214. Concannon, C.G., et al., *Apoptosis induced by proteasome inhibition in cancer cells: predominant role of the p53/PUMA pathway.* Oncogene, 2007. **26**(12): p. 1681-92.
215. Yu, J., et al., *Differential apoptotic response to the proteasome inhibitor Bortezomib [VELCADE, PS-341] in Bax-deficient and p21-deficient colon cancer cells.* Cancer Biol Ther, 2003. **2**(6): p. 694-9.
216. Bouzar, A.B., et al., *Valproate synergizes with purine nucleoside analogues to induce apoptosis of B-chronic lymphocytic leukaemia cells.* Br J Haematol, 2009. **144**(1): p. 41-52.
217. Zhang, Y., et al., *Histone deacetylase inhibitors FK228, N-(2-aminophenyl)-4-[N-(pyridin-3-yl-methoxycarbonyl)amino- methyl]benzamide and m-carboxycinnamic acid bis-hydroxamide augment radiation-induced cell death in gastrointestinal adenocarcinoma cells.* Int J Cancer, 2004. **110**(2): p. 301-8.
218. Fritsche, P., et al., *HDAC2 mediates therapeutic resistance of pancreatic cancer cells via the BH3-only protein NOXA.* Gut, 2009. **58**(10): p. 1399-409.
219. Hsu, T., M. Trojanowska, and D.K. Watson, *Ets proteins in biological control and cancer.* J Cell Biochem, 2004. **91**(5): p. 896-903.
220. Foos, G. and C.A. Hauser, *Altered Ets transcription factor activity in prostate tumor cells inhibits anchorage-independent growth, survival, and invasiveness.* Oncogene, 2000. **19**(48): p. 5507-16.
221. Buggy, Y., et al., *Ets2 transcription factor in normal and neoplastic human breast tissue.* Eur J Cancer, 2006. **42**(4): p. 485-91.
222. de Nigris, F., et al., *Induction of ETS-1 and ETS-2 transcription factors is required for thyroid cell transformation.* Cancer Res, 2001. **61**(5): p. 2267-75.
223. Carbone, G.M., et al., *Selective inhibition of transcription of the Ets2 gene in prostate cancer cells by a triplex-forming oligonucleotide.* Nucleic Acids Res, 2003. **31**(3): p. 833-43.
224. Singh, S., et al., *ETS proteins and MMPs: partners in invasion and metastasis.* Curr Drug Targets, 2002. **3**(5): p. 359-67.
225. Hayden, M.S. and S. Ghosh, *Signaling to NF-kappaB.* Genes Dev, 2004. **18**(18): p. 2195-224.
226. Pahl, H.L., *Activators and target genes of Rel/NF-kappaB transcription factors.* Oncogene, 1999. **18**(49): p. 6853-66.
227. Wacheck, V., et al., *Bcl-x(L) antisense oligonucleotides radiosensitise colon cancer cells.* Br J Cancer, 2003. **89**(7): p. 1352-7.
228. Tsujimoto, Y. and S. Shimizu, *Bcl-2 family: life-or-death switch.* FEBS Lett, 2000. **466**(1): p. 6-10.
229. Flis, S., et al., *MS275 enhances cytotoxicity induced by 5-fluorouracil in the colorectal cancer cells.* Eur J Pharmacol. **627**(1-3): p. 26-32.
230. Voeller, D., L. Rahman, and M. Zajac-Kaye, *Elevated levels of thymidylate synthase linked to neoplastic transformation of mammalian cells.* Cell Cycle, 2004. **3**(8): p. 1005-7.
231. Popat, S., A. Matakidou, and R.S. Houlston, *Thymidylate synthase expression and prognosis in colorectal cancer: a systematic review and meta-analysis.* J Clin Oncol, 2004. **22**(3): p. 529-36.
232. Zhang, Y., et al., *HDAC-6 interacts with and deacetylates tubulin and microtubules in vivo.* EMBO J, 2003. **22**(5): p. 1168-79.

233. Hubbert, C., et al., *HDAC6 is a microtubule-associated deacetylase.* Nature, 2002. **417**(6887): p. 455-8.
234. Suzuki, T., et al., *Effect of trichostatin A on cell growth and expression of cell cycle- and apoptosis-related molecules in human gastric and oral carcinoma cell lines.* Int J Cancer, 2000. **88**(6): p. 992-7.
235. Trivedi, C.M., et al., *Hdac2 regulates the cardiac hypertrophic response by modulating Gsk3 beta activity.* Nat Med, 2007. **13**(3): p. 324-31.

8 SUPPLEMENTARY DATA

Supplementary Table 1. VPA-induced changes in the gene expression profile of HT-29 cells. VPA-induced changes in the gene expression were evaluated in HT-29 cells untreated or treated with 2 mM VPA for 24 h using Affymetrix microarray analysis. The arithmetic mean of the fluorescence signals of the 4 replicates per treatment was calculated for treated and untreated samples. The mean expression level of the VPA-treated samples was normalized against the mean expression level of the untreated samples.

Gene Name		Affymetrix probe set number	2 mM VPA / 24 h vs. 0 mM VPA
NOX1	NADPH oxidase 1	206418_at	0.08
C14orf78	Chromosome 14 open reading frame 78	212992_at	20.3
CYP1A1	Cytochrome P450, family 1, subfamily A, polypeptide 1	205749_at	20.5
ITGA7	Integrin, alpha 7	216331_at	21.4
DHRS2	Dehydrogenase/reductase (SDR family) member 2	214079_at	22.2
---	Similar to leucine rich repeat containing 10	236666_s_at	22.3
SEPP1	Selenoprotein P, plasma, 1	201427_s_at	22.4
TNNT1	Troponin T1, skeletal, slow	213201_s_at	23.1
PEG10	Paternally expressed 10	212094_at	24.1
SELM	Selenoprotein M	226051_at	26.5
COL1A1	Collagen, type I, alpha 1	1556499_s_at	27.9
ABAT	4-aminobutyrate aminotransferase	209459_s_at	29.8
B1	Parathyroid hormone-responsive B1 gene	209958_s_at	30.1
ABAT	4-aminobutyrate aminotransferase	209460_at	37.0
LGALS1	Lectin, galactoside-binding, soluble, 1 (galectin 1)	201105_at	80.6

Supplementary Table 2. Cell signaling pathways regulated by VPA in HT-29 cells. The table shows the number and the percentage of genes whose expression was changed upon treatment with VPA for 3 h and which were associated with a specific cell signaling pathway, according to KEGG and Gene Ontology (GO) pathways. The number and percentage of genes were calculated using GenFinder software.

	Map name according to pathway	Number			Percent		Z-score [4]
		Genes in pathway	Genes detected [1]	Genes changed	Genes detected [2]	Genes changed [3]	
KEGG pathways	**Androgen Receptor**	112	98	12	87.5	12.2	4.5
	Apoptosis	82	71	8	86.6	11.3	3.4
	Benzoate degradation via CoA ligation	160	115	8	71.9	7.0	2.2
	GPCRDB-Class A Rhodopsin-like	262	35	4	13.4	11.4	2.4
	Hedgehog	22	16	3	72.7	18.8	3.2
	IL-4	62	51	6	82.3	11.8	3.1
	Inositol phosphate metabolism	152	119	8	78.3	6.7	2.1
	mRNA processing	127	123	10	96.9	8.1	2.6
	Nicotinate and nicotinamide metabolism	156	111	10	71.2	9.0	3.3
	Prostaglandin synthesis regulation	31	15	4	48.4	26.7	4.7
	Sphingoglycolipid metabolism	144	118	8	81.9	6.8	2.1
	Starch and sucrose metabolism	208	119	8	57.2	6.7	2.1
	TGF-Beta signaling	52	37	7	71.2	18.9	4.9
	TGF-beta-Receptor	151	133	10	88.1	7.5	2.4
	Wnt signaling	72	49	5	68.1	10.2	2.4

(1) genes detected = the number of genes on array found to link to GO or Kegg pathway

(2) percentage of genes detected = genes detected on array / genes in pathway X 100

(3) percentage of genes changed = genes changed / genes detected on array X 100;

(4) Z score = standard statistical test under the hypergeometric distribution; Z-score of 1.96 or -1.96 correlates with a p-value of 0.05

Supplementary Table 2 (continued 1). Cell signaling pathways regulated by VPA in HT-29 cells. The table shows the number and the percentage of genes whose expression was changed upon treatment with VPA for 3 h and which were associated with a specific cell signaling pathway, according to KEGG and Gene Ontology (GO) pathways. The number and percentage of genes were calculated using GenFinder software.

	Map name according to pathway	Number			Percent		Z-score [4]
		Genes in pathway	Genes detected [1]	Genes changed	Genes detected [2]	Genes changed [3]	
GO pathways	**Acyltransferase activity**	109	74	8	67.9	10.8	3.6
	Biopolymer glycosylation	108	62	5	57.4	8.1	2.1
	Cell-cell signaling	274	76	8	27.7	10.5	3.5
	Chromatin modification	100	85	7	85.0	8.2	2.5
	Cytokine activity	203	53	5	26.1	9.4	2.5
	DNA repair	187	164	11	87.7	6.7	2.4
	Extracellular space	274	79	6	28.8	7.6	2.1
	Gametogenesis	153	60	5	39.2	8.3	2.2
	Growth factor activity	157	53	10	33.8	18.9	6.3
	Male gamete generation	125	46	4	36.8	8.7	2.0
	Negative regulation of cellular metabolism	148	106	12	71.6	11.3	4.6
	Negative regulation of nucleic acid metabolism	126	93	12	73.8	12.9	5.2
	Negative regulation of programmed cell death	103	59	6	57.3	10.2	2.9
	Negative regulation of transcription	116	85	12	73.3	14.1	5.6
	Neurogenesis	237	97	10	40.9	10.3	3.8
	Positive regulation of cell proliferation	113	58	6	51.3	10.3	3.0
	Potassium channel activity	132	33	4	25.0	12.1	2.8
	Potassium ion transport	156	39	4	25.0	10.3	2.4

(1) genes detected = the number of genes on array found to link to GO orKegg pathway

(2) percentage of genes detected = genes detected on array / genes in pathway X 100

(3) percentage of genes changed = genes changed / genes detected on array X 100;

(4) Z score = standard statistical test under the hypergeometric distribution; Z-score of 1.96 or -1.96 correlates with a p-value of 0.05

Supplementary Table 2 (continued 2). Cell signaling pathways regulated by VPA in HT-29 cells. The table shows the number and the percentage of genes whose expression was changed upon treatment with VPA for 3 h and which were associated with a specific cell signaling pathway, according to KEGG and Gene Ontology (GO) pathways. The number and percentage of genes were calculated using GenFinder software.

	Map name according to pathway	Number			Percent		Z-score [4]
		Genes in pathway	Genes detected [1]	Genes changed	Genes detected [2]	Genes changed [3]	
GO pathways	**Protein amino acid glycosylation**	105	61	5	58.1	8.2	2.1
	Response to DNA damage stimulus	206	179	12	86.9	6.7	2.5
	Response to endogenous stimulus	219	182	12	83.1	6.6	2.5
	RNA polymerase II transcription factor activity	199	131	10	65.8	7.6	2.8
	Sexual reproduction	189	73	6	38.6	8.2	2.3
	Spermatogenesis	125	46	4	36.8	8.7	2.0
	Transcription coactivator activity	130	95	7	73.1	7.4	2.2
	Transcription cofactor activity	219	163	12	74.4	7.4	2.9
	Transcription factor binding	253	187	13	73.9	7.0	2.8
	Transferase activity, transferring groups other than amino-acyl groups	109	74	8	67.9	10.8	3.6
	Voltage-gated ion channel activity	167	46	4	27.5	8.7	2.2

(1) genes detected = the number of genes on array found to link to GO or Kegg pathway

(2) percentage of genes detected = genes detected on array / genes in pathway X 100

(3) percentage of genes changed = genes changed / genes detected on array X 100;

(4) Z score = standard statistical test under the hypergeometric distribution; Z-score of 1.96 or -1.96 correlates with a p-value of 0.05

Supplementary Table 3. Cell signaling pathways regulated by VPA in HT-29 cells. The table shows the number and the percentage of genes whose expression was changed upon treatment with VPA for 24 h and which were associated with a specific cell signaling pathway, according to KEGG and Gene Ontology (GO) pathways. The number and percentage of genes were calculated using GenFinder software.

	Map name according to pathway	Number			Percent		Z-score [4]
		Genes in pathway	Genes detected [1]	Genes changed	Genes detected [2]	Genes changed [3]	
KEGG pathways	**B-Cell Receptor**	158	123	13	77.8	10.6	-2.05
	Cell Cycle-G1 to S control	67	64	33	95.5	51.6	7.2
	Cell-cycle	91	83	35	91.2	42.2	6.0
	DNA replication	42	41	29	976.0	70.7	9.0
	EGFR1	177	155	9	87.6	5.8	-3.9
	Electron Transport Chain	105	87	5	82.9	5.7	-2.9
	Focal adhesion	187	119	7	63.6	5.9	-3.4
	Glycine, serine and threonine metabolism	64	25	8	39.1	32.0	2.0
	Homologous recombination	13	12	5	923	41.7	2.2
	IL-6	100	85	6	85.0	7.1	-2.6
	Insulin signaling	159	138	13	86.8	9.4	-2.5
	Kit-Receptor	67	50	3	74.6	6.0	-2.2
	Mismatch-repair	9	9	4	100.0	44.4	2.1
	mRNA processing	127	123	47	96.9	38.2	6.1
	One carbon pool by folate	22	12	8	54.5	66.7	4.6
	Purine metabolism	181	84	23	46.4	27.4	2.6
	Pyrimidine metabolism	98	63	25	64.3	39.7	4.9
	Regulation of actin cytoskeleton	146	101	4	69.2	4.0	-3.6
	Ribosomal proteins	88	85	6	96.6	7.1	-2.6
	Valine, leucine and isoleucine biosynthesis	17	6	3	35.3	50.0	2.2

(1) genes detected = the number of genes on array found to link to GO or Kegg pathway

(2) percentage of genes detected = genes detected on array / genes in pathway X 100

(3) percentage of genes changed = genes changed / genes detected on array X 100

(4) Z score = standard statistical test under the hypergeometric distribution; Z-score of 1.96 or -1.96 correlates with a p-value of 0.05

Supplementary Table 3 (continue 1). Cell signaling pathways regulated by VPA in HT-29 cells. The table shows the number and the percentage of genes whose expression was changed upon treatment with VPA for 24 h and which were associated with a specific cell signaling pathway, according to KEGG and Gene Ontology (GO) pathways. The number and percentage of genes were calculated using GenFinder software.

	Map name according to pathway	Number			Percent		Z-score (4)
		Genes in pathway	Genes detected (1)	Genes changed	Genes detected (2)	Genes changed (3)	
GO pathways	**Actin binding**	213	129	12	60.6	9.3	-2.3
	Actin cytoskeleton	217	126	7	58.1	5.6	-3.4
	Calmodulin binding	117	54	3	46.2	5.6	-2.2
	Cell cycle	173	144	39	83.2	27.1	3.4
	Cell division	116	92	23	79.3	25.0	2.2
	Cytokinesis	116	92	23	79.3	25.0	2.2
	DNA repair	187	164	56	87.7	34.1	6.1
	DNA replication	146	116	53	79.5	45.7	8.5
	Electron transporter activity	246	174	19	70.7	10.9	-2.1
	Energy derivation by oxidation of organic compounds	143	100	9	699.0 .	9.0	-2.2
	Enzyme activator activity	220	151	14	68.6	9.3	-2.5
	Golgi apparatus	296	223	8	75.3	3.6	-5.3
	GTPase activator activity	152	114	7	75.0	6.1	-3.0
	Helicase activity	131	113	41	86.3	36.3	5.7
	Intracellular protein transport	194	153	12	78.9	7.8	-3.0
	Lipid binding	193	106	9	54.9	8.5	-2.275
	Lipid metabolism	149	100	9	67.1	9.0	-2.1
	M phase	164	137	40	83.5	29.2	4.0
	Motor activity	151	78	6	51.7	7.7	-2.1
	mRNA processing	240	189	56	78.8	29.6	4.9
	Muscle development	142	59	4	41.5	6.8	-2.1

(1) genes detected = the number of genes on array found to link to GO or Kegg pathway

(2) percentage of genes detected = genes detected on array / genes in in pathway X 100

(3) percentage of genes changed = genes changed / genes detected on array X 100

(4) Z score = standard statistical test under the hypergeometric distribution; Z-score of 1.96 or -1.96 correlates with a p-value of 0.05

Supplementary Table 3 (continue 2). Cell signaling pathways regulated by VPA in HT-29 cells. The table shows the number and the percentage of genes whose expression was changed upon treatment with VPA for 24 h and which were associated with a specific cell signaling pathway, according to KEGG and Gene Ontology (GO) pathways. The number and percentage of genes were calculated using GenFinder software.

	Map name according to pathway	Number			Percent		Z-score [4]
		Genes in pathway	Genes detected [1]	Genes changed	Genes detected [2]	Genes changed [3]	
GO pathways	**Nuclear mRNA splicing, via spliceosome**	169	137	45	81.1	32.8	5.2
	Nuclear transport	102	80	25	78.4	31.2	3.5
	Nucleocytoplasmic transport	109	87	29	79.8	33.3	4.2
	Nucleoplasm	195	153	40	78.5	26.1	3.2
	Nucleotide binding	134	93	25	69.4	26.9	2.7
	Nucleotidyltransferase activity	115	82	24	71.3	29.3	3.1
	Protein complex assembly	242	125	30	51.7	24.0	2.2
	Protein targeting	133	110	27	82.7	24.5	2.2
	Regulation of cell cycle	187	138	32	73.8	23.2	2.1
	Regulation of protein kinase activity	110	78	22	70.9	28.2	2.8
	Regulation of transcription from RNA polymerase II promoter	221	157	36	71.0	22.9	2.1

(1) genes detected = the number of genes on array found to link to GO or Kegg pathway

(2) percentage of genes detected = genes detected on array / genes in pathway X 100

(3) percentage of genes changed = genes changed / genes detected on array X 100

(4) Z score = standard statistical test under the hypergeometric distribution; Z-score of 1.96 or -1.96 correlate with a p-value of 0.05

Supplementary Table 3 (continue 3). Cell signaling pathways regulated by VPA in HT-29 cells. The table shows the number and the percentage of genes whose expression was changed upon treatment with VPA for 24 h and which were associated with a specific cell signaling pathway, according to KEGG and Gene Ontology (GO) pathways. The number and percentage of genes were calculated using GenFinder software.

	Map name according to pathway	Number			Percent		Z-score [4]
		Genes in pathway	Genes detected [1]	Genes changed	Genes detected [2]	Genes changed [3]	
GO pathways	**Regulation of transferase activity**	110	78	22	70.9	28.2	2.8
	Response to DNA damage stimulus	206	179	60	86.9	33.5	6.2
	Response to endogenous stimulus	219	182	60	83.1	33.0	6.0
	RNA splicing	197	162	52	82.2	32.1	5.4
	RNA splicing, via transesterification reactions	169	137	45	81.1	32.8	5.2
	Secretory pathway	141	107	5	75.9	4.7	-3.4
	Signal transducer activity	272	172	17	63.2	9.9	-2.4
	Small GTPase mediated signal transduction	241	165	13	68.5	7.9	-3.1
	Small GTPase regulator activity	133	92	8	69.2	8.7	-2.1
	Transcription coactivator activity	130	95	28	73.1	29.5	3.4
	Transcription cofactor activity	219	163	40	74.4	24.5	2.7
	Transcription factor binding	253	187	45	73.9	24.1	2.8

(1) genes detected = the number of genes on array found to link to GO or Kegg pathway

(2) percentage of genes detected = genes detected on array / genes in pathway X 100

(3) percentage of genes changed = genes changed / genes detected on array X 100

(4) Z score = standard statistical test under the hypergeometric distribution; Z-score of 1.96 or -1.96 correlates with a p-value of 0.05

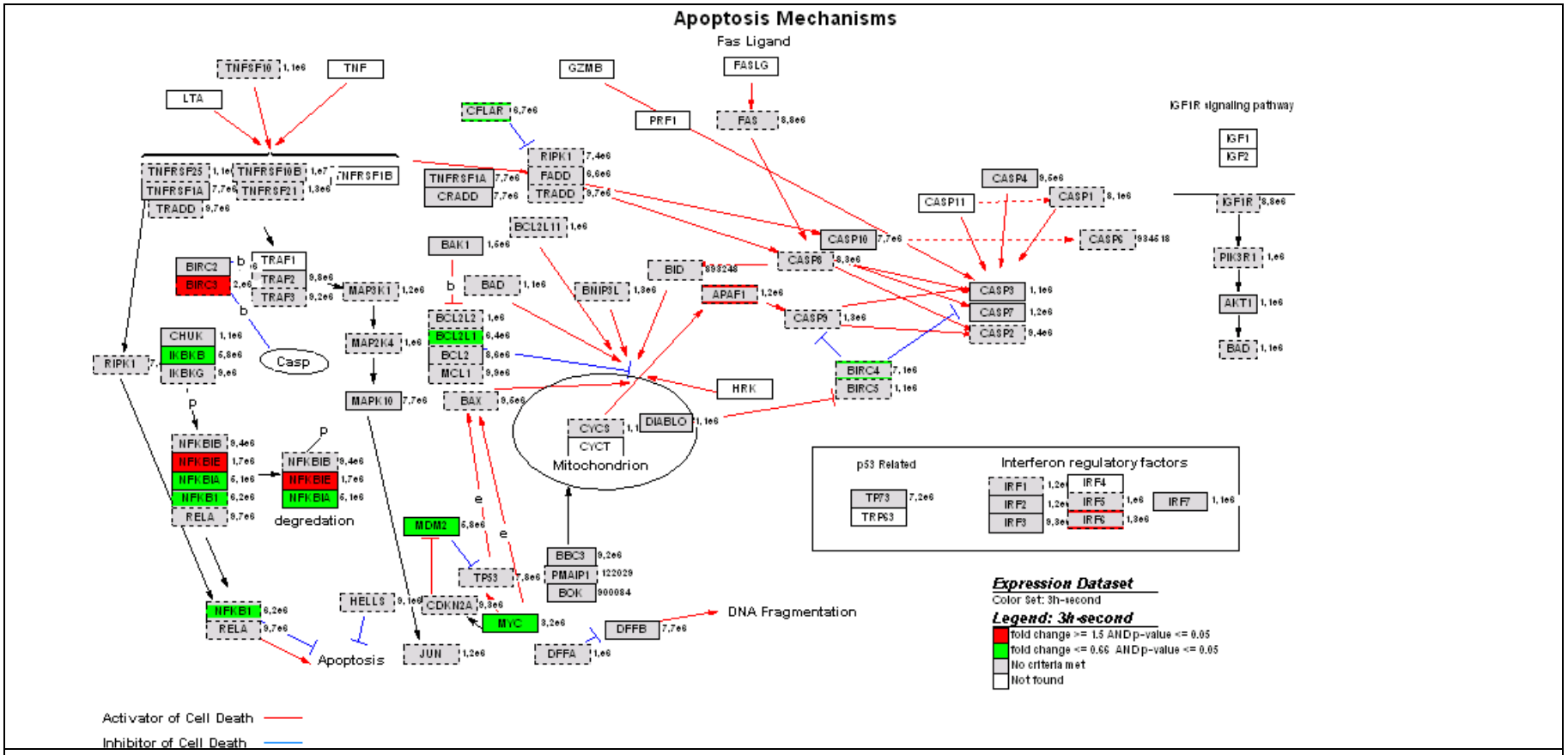

Supplementary Figure 1. The effect of VPA treatment for 3 h on the expression of genes associated with apoptosis in HT-29 cells. The effect of VPA on expression of genes involved in apoptosis, according to the KEGG pathways is shown. In red: more than 1.5 fold upregulated genes; in green: more than 1.5 fold downregulated genes; in gray: unchanged genes; in white: gene expression level lower than basal threshhold. The map was generated using GenMAPP software.

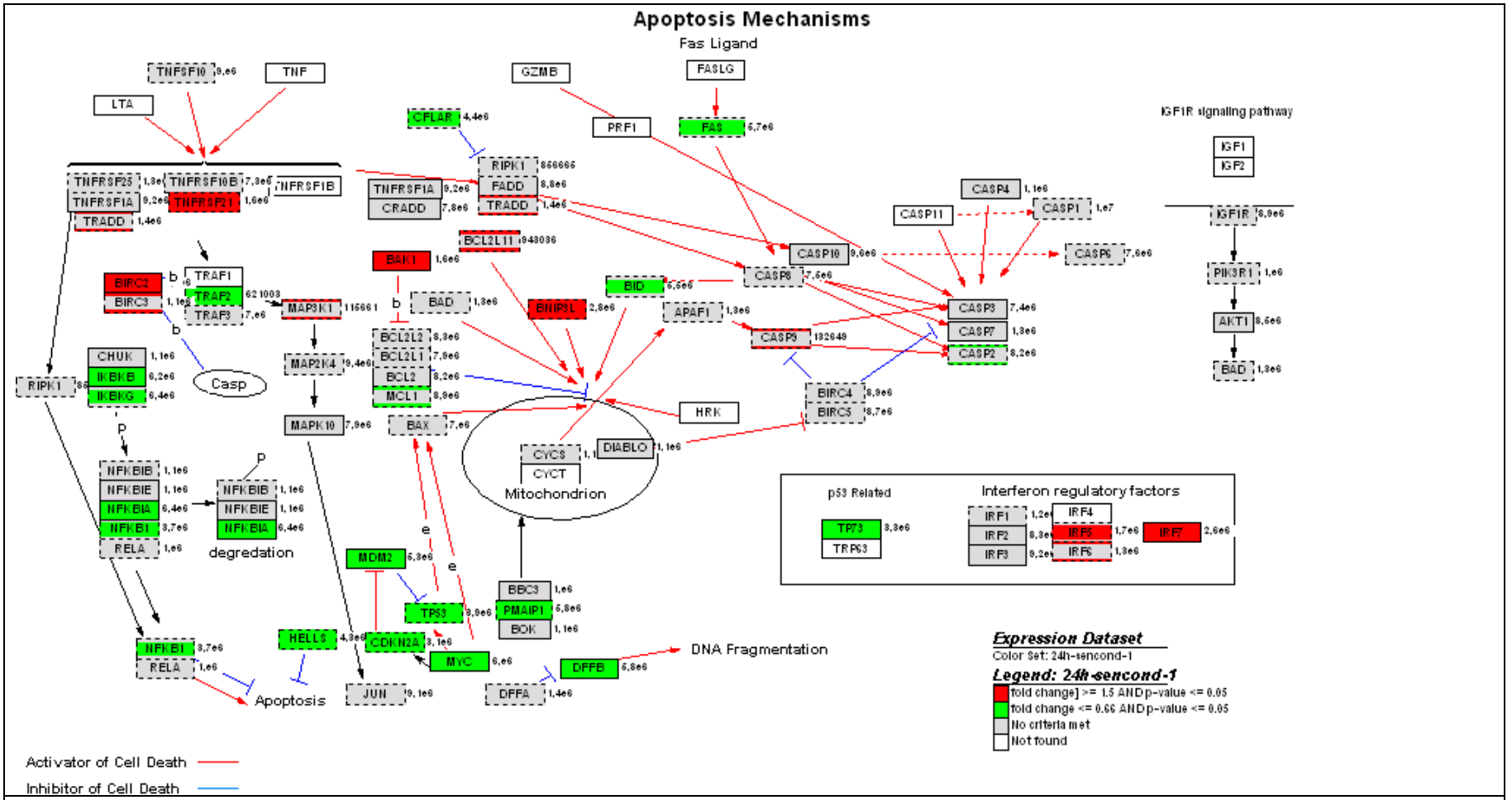

Supplementary Figure 2. The effect of the VPA treatment for 24 h on the expression of genes associated with apoptosis in HT-29 cells. The effect of VPA on expression of genes involved in apoptosis, according to the KEGG pathways is shown. In red: more than 1.5 fold upregulated genes; in green: more than 1.5 fold downregulated genes; in gray: unchanged genes; in white: gene expression level lower than basal threshhold. The map was generated using GenMAPP software.

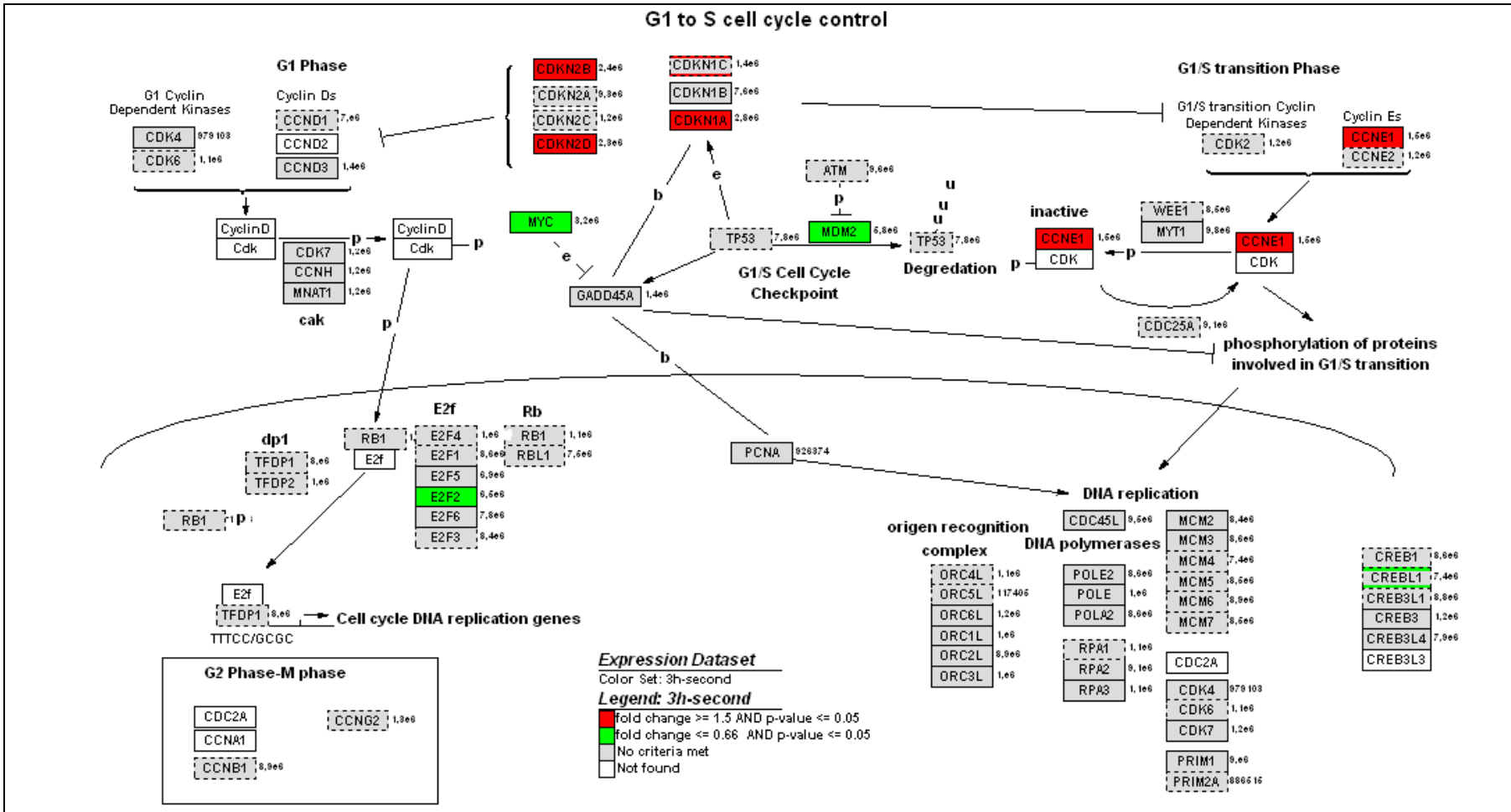

Supplementary Figure 3. The effect of VPA treatment for 3 h on the expression of genes associated with cell cycle control at the G1/S checkpoint in HT-29 cells. The effect of VPA on genes involved in the G1/S cell cycle control, according to the KEGG pathways is shown. In red: more than 1.5 fold upregulated genes; in green: more than 1.5 fold dowregulated genes; in gray: unchanged genes; in white: gene expression level lower than basal threshhold. The map was generated using GenMAPP

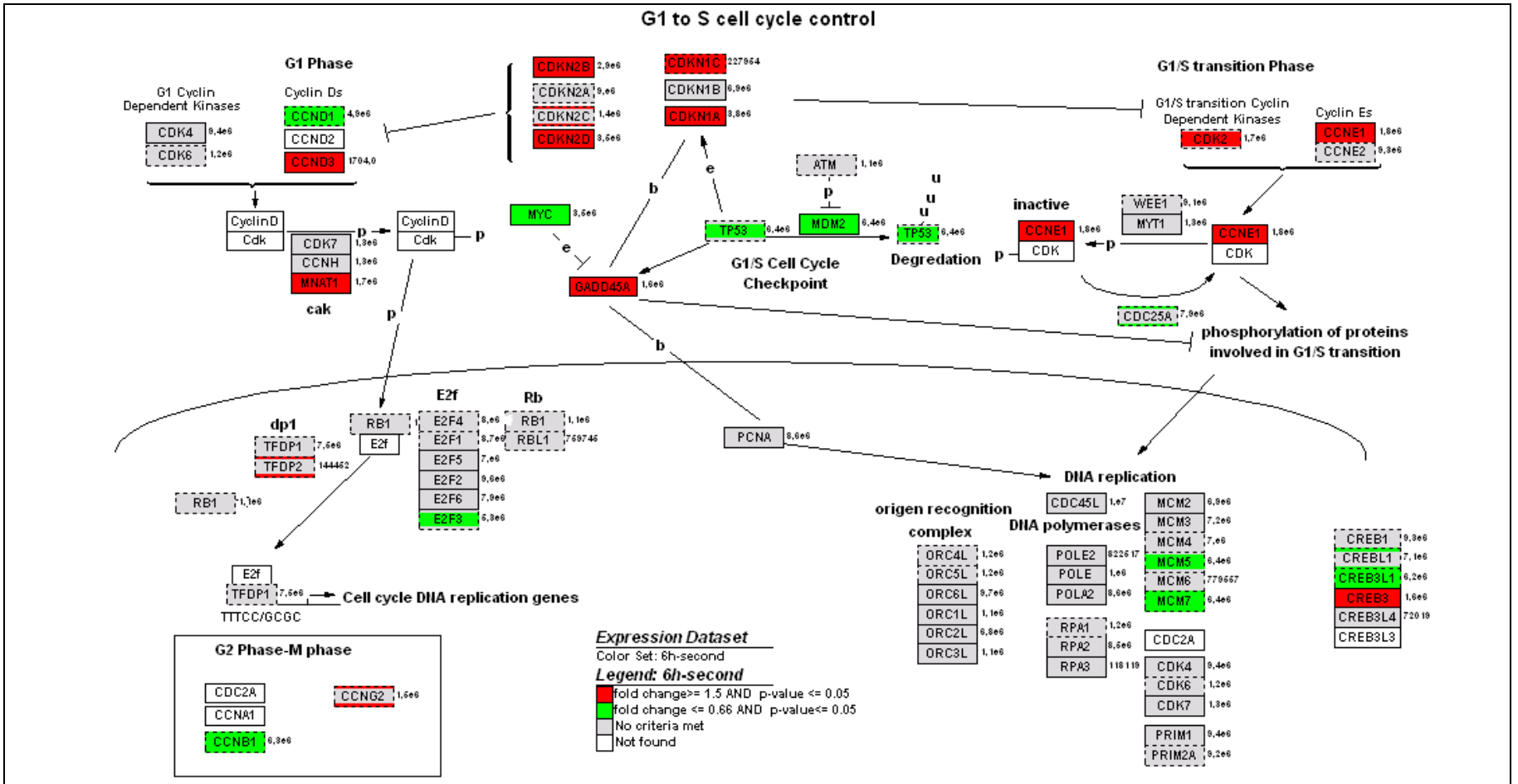

Supplementary Figure 4. The effect of VPA treatment for 6 h on the expression of genes associated with cell cycle control at the G1/S checkpoint in HT-29 cells. The effect of VPA on genes involved in the G1/S cell cycle control, according to the KEGG pathways is shown. In red: more than 1.5 fold upregulated genes; in green: more than 1.5 fold dowregulated genes; in gray: unchanged genes; in white: gene expression level lower than basal threshhold. The map was generated using GenMAPP software.

Supplementary Table 4. The effect of the VPA treatment on the mRNA expression of Aven in HT-29 cells. VPA-induced changes in the gene expression of Aven were evaluated in HT-29 cells untreated or treated with 2 mM VPA for 24 h using Affymetrix microarray analysis (described in the paragraph 3.1.1).

Gene Name	**Affymetrix probe set number**	**2 mM VPA vs. 0 mM VPA**		
		3 h VPA	**6 h VPA**	**24 h VPA**
AVEN	219366_at	0.9 ± 0.06 (p = 0.04)	0.61 ± 0.07 (p = 0.0001)	0.14 ± 0.03 (p = 0.000002)
β-actin	200801_x_at	1.0 ± 0.08 (p = 0.2)	1.0 ± 0.04 (p = 0.6)	1.0 ± 0.03 (p = 0.1)

Supplementary Table 5. **The effect of the VPA treatment on the mRNA expresion of Mcl-1 in HT-29 cells.**VPA-induced changes in the gene expression of Mcl-1 were evaluated in HT-29 cells untreated or treated with 2 mM VPA for 3, 6 and 24 h using Affymetrix microarray analysis (described in the paragraph 3.1.1).

Gene Name	**Affymetrix probe set number**	**2 mM VPA vs. 0 mM VPA**		
		3 h VPA	**6 h VPA**	**24 h VPA**
Mcl-1	200797_s_at	1.1 ± 0.07 (p = 0.07)	1.1 ± 0.02 (p = 0.1)	1.1 ± 0.05 (p = 0.2)
β-actin	200801_x_at	1.0 ± 0.08 (p = 0.2)	1.0 ± 0.04 (p = 0.6)	1.0 ± 0.03 (p = 0.1)

Supplementary Figure 6. The effect of the VPA treatment on the protein expresion of Bmf in HT-29 cells. HT-29 cells were treated with 2 mM VPA for the indicated time periods before harvesting. The expression of Bmf was evaluated in whole cell lysates by Western Blot analysis. Actin was used as loading control.

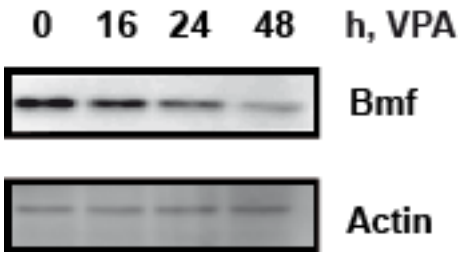

Supplementary Table 7. **The effect of the VPA treatment on the mRNA expresion of E2F1 transcription factor in HT-29 cells.**VPA-induced changes in the gene expression of E2F1 were evaluated in HT-29 cells untreated or treated with 2 mM VPA for 3, 6 and 24 h using Affymetrix microarray analysis (described in the paragraph 3.1.1).

Gene Name	**Affymetrix probe set number**	**2 mM VPA vs. 0 mM VPA**		
		3 h VPA	**6 h VPA**	**24 h VPA**
E2F1	204947_at	0.8 ± 0.1 (p = 0.1)	0.9 ± 0.1 (p = 0.5)	0.4 ± 0.1 (p = 0.003)
β-actin	200801_x_at	1.0 ± 0.08 (p = 0.2)	1.0 ± 0.04 (p = 0.6)	1.0 ± 0.03 (p = 0.1)

Supplementary Table 8. **The effect of VPA treatment on the mRNA expresion of STAT transcription factors involved in activation of Bcl-XL expression.** VPA-induced changes in the gene expression of STAT transcription factors were evaluated in HT-29 cells untreated or treated with 2 mM VPA for 3, 6 and 24 h using Affymetrix microarray analysis (described in the paragraph 3.1.1).

Gene Name	**Affymetrix probe set number**	**2 mM VPA vs. 0 mM VPA**		
		3 h VPA	**6 h VPA**	**24 h VPA**
STAT5A	203010_at	0.7 ± 0.2 (p = 0.4)	0.8 ± 0.03 (p = 0.3)	0.5 ± 0.7 (p = 0.1)
STAT5B	212549_at	0.9 ± 0.2 (p = 0.5)	1.1 ± 0.1 (p = 0.2)	0.8 ± 0.06 (p = 0.04)
STAT3	225289_at	1.3 ± 0.7 (p = 0.006)	1.5 ± 0.1 (p = 0.003)	1.6 ± 0.2 (p = 0.01)
STAT6	201331_s_at	0.9 ± 0.03 (p = 0.01)	0.7 ± 0.03 (p = 0.0001)	0.7 ± 0.04 (p = 0.001)
β-actin	200801_x_at	1.0± 0.08 (p = 0.2)	1.0 ± 0.04 (p = 0.6)	1.0 ± 0.03 (p = 0.1)

Supplementary Table 9. **The effect of VPA treatment on the mRNA expresion of Rel/NFkB transcription factors and their target genes in HT-29 colon tumor cells**. VPA-induced changes in the gene expression of Rel/NFkB transcription factors and their targets were evaluated in HT-29 cells untreated or treated with 2 mM VPA for 3, 6 and 24 h using Affymetrix microarray analysis (described in the paragraph 3.1.1).

	Gene Name	**Affymetrix probe set number**	**2mM VPA vs. 0mM VPA**		
			3 h VPA	**6 h VPA**	**24 h VPA**
Rel/NFkB transcription factors	RELA	201783_s_at	1.0 ± 0.1 (p = 0.7)	1.0 ± 0.06 (p = 0.2)	1.0 ± 0.04 (p = 0.9)
	RELB	205205_at	0.9 ± 0.1 (p = 0.1)	0.8 ± 0.1 (p = 0.06)	0.7 ± 0.2 (p = 0.07)
	NFKB1	209239_at	0.6 ± 0.07 (p = 0.03)	0.4 ± 0.02 (p = 0.006)	0.4 ± 0.02 (p = 0.005)
	NFKB2	207535_s_at	1.3 ± 0.2 (p = 0.1)	1.8 ± 0.1 (p = 0.002)	1.2 ± 0.1 (p = 0.02)
Rel/NFkB targets	VEGF	210512_s_at	1.1 ± 0.2 (p = 0.08)	1.1 ± 0.1 (p = 0.1)	1.1 ± 0.1 (p = 0.05)
	c-IAP1	202076_at	1.2 ± 0.01 (p = 0.02)	1.6 ± 0.1 (p = 0.001)	1.6 ± 0.1 (p = 0.0005)
	IRF1	202531_at	1.2 ± 0.2 (p = 0.1)	1.2 ± 0.04 (p = 0.01)	1.1 ± 0.07 (p = 0.01)
β-actin		200801_x_at	1.0 ± 0.08 (p = 0.2)	1.0 ± 0.04 (p = 0.6)	1.0 ± 0.03 (p = 0.1)

Supplementary Table 10. **The effect of VPA on the expression of transcription factors involved in the repression of Bcl-XL expression.** VPA-induced changes in the gene expression of STAT1, ETV6/TEL and TP53 were evaluated in HT-29 cells untreated or treated with 2 mM VPA for 3, 6 and 24 h using Affymetrix microarray analysis (described in the paragraph 3.1.1).

Gene Name	**Affymetrix probe set number**	**2 mM VPA vs. 0 mM VPA**		
		3 h VPA	**6 h VPA**	**24 h VPA**
STAT1	200887_s_at	1.0 ± 0.06 (p = 0.6)	1.1 ± 0.04 (p = 0.1)	1.1 ± 0.08 (p = 0.03)
ETV6/TEL	235056_at	1.0 ± 0.05 (p = 0.6)	1.0 ± 0.03 (p = 0.7)	0.9 ± 0.03 (p = 0.3)
TP53	201746_at	0.8 ± 0.04 (p = 0.01)	0.7 ± 0.1 (p = 0.03)	0.4 ± 0.01 (p = 0.001)
β-actin	200801_x_at	1.0± 0.08 (p = 0.2)	1.0 ± 0.04 (p = 0.6)	1.0 ± 0.03 (p = 0.1)

9 ACKNOWLEDGEMENTS

I would like to thank Dr. Evamaria Huber (now Stütz) (Institute of Toxicology, Helmholtz Center Munich) for the countless helpful discussions and support.

Equally, I would like to thank Prof. Martin Göttlicher for giving me the possibility to work in his lab and for supervision.

I would also like to thank Dr. Martin Irmler (Institute of Developmental Genetics, Helmholtz Center Munich) and Dr. Michael Mader (Institute of Bioinformatics, Helmholtz Center Munich) for the technical support with the microarray analysis.

I would like to thank Prof. Wolfgang Wurst, Prof. Michael Schemann and Dr. Klaus-Peter Janssen for agreeing to take part in the examination commission.

Special thanks to Dr. Thomas Meindl, Dr. Mark Wormke, Dr. Natascha Bachmann, Dr. Hans Zischka, Dr. Felix Dulich and to all colleagues from the Institute of Toxicology, Helmholtz Center Munich.